LÉA RITA PESTANA FERREIRA MELLO

VALORIZAÇÃO DO BAGAÇO DE MALTE:

APLICAÇÃO COMO BIOADSORVENTE E ESTUDO DE PRÉ-TRATAMENTOS PARA A OBTENÇÃO DE AÇÚCARES FERMENTESCÍVEIS

Londrina
2019

LÉA RITA PESTANA FERREIRA MELLO

VALORIZAÇÃO DO BAGAÇO DE MALTE:

APLICAÇÃO COMO BIOADSORVENTE E ESTUDO DE PRÉ-TRATAMENTOS PARA A OBTENÇÃO DE AÇÚCARES FERMENTESCÍVEIS

Tese apresentada ao Programa de Pós Graduação em Biotecnologia do Departamento de Bioquímica e Biotecnologia da Universidade Estadual de Londrina como requisito parcial à obtenção do título de Doutor em Biotecnologia.

Orientador: Profa. Dra. Suzana Mali de Oliveira
Co-orientador: Profa. DraMaria Josefa Santos Yabe

Londrina
2019

Ficha de identificação da obra elaborada pelo autor, através do Programa de Geração Automática do Sistema de Bibliotecas da UEL

Mello, Léa Rita Pestana Ferreira .
Valorização do bagaço de malte: aplicação como bioadsorvente e estudo de pré-tratamentos para a obtenção de açúcares fermentescíveis / Léa Rita Pestana Ferreira Mello. - Londrina, 2019.
104 f. : il.

Orientador: Suzana Mali de Oliveira.
Coorientador: Maria Josefa Santos Yabe.
Tese (Doutorado em Biotecnologia) - Universidade Estadual de Londrina, Centro de Ciências Exatas, , 2019. Inclui bibliografia.

1. Adsorção de chumbo - Tese. 2. Pré-tratamentos para fibras lignocelulósicas - Tese. 3. Bioadsorvente para metais pesados - Tese. 4. Aproveitamento de resíduos da agroindústria - Tese. I. Mali de Oliveira, Suzana . II. Santos Yabe, Maria Josefa . III. Universidade Estadual de Londrina. Centro de Ciências Exatas. . IV. Título.

LÉA RITA PESTANA FERREIRA MELLO

VALORIZAÇÃO DO BAGAÇO DE MALTE:
APLICAÇÃO COMO BIOADSORVENTE E ESTUDO DE PRÉ-TRATAMENTOS PARA A OBTENÇÃO DE AÇÚCARES FERMENTESCÍVEIS

Tese apresentada ao Programa de Pós-Graduação em Biotecnologia do Departamento de Bioquímica e Biotecnologia da Universidade Estadual de Londrina como requisito parcial à obtenção do título de Doutor em Biotecnologia.

BANCA EXAMINADORA

_____
Profa. Dra. Suzana Mali de Oliveira
Universidade Estadual de Londrina – UEL

_____
Profa. Dra Ana Elisa Stefani Vercelheze
Serviço Nacional de Aprendizagem Industrial – SENAI

_____
Prof. Dr Doumit Camilios Neto
Universidade Estadual de Londrina – UEL

_____
Prof. Dr Fábio Yamashita
Universidade Estadual de Londrina – UEL

_____
Profa. Dra Maria Victória Eiras Grossmann
Universidade Estadual de Londrina – UEL

Londrina, 22 de março de 2019.

Dedico este trabalho aos meus pais Adalberto e Elidia, meu esposo Cristiano e minha filha Lívia.

AGRADECIMENTOS

Agradeço à minha orientadora Profa. Dra Suzana Mali de Oliveira pela constante orientação e grande dedicação a este trabalho, por todos os ensinamentos e conselhos, pela confiança e inestimável amizade.

À minha co - orientadora Profa. Dra Maria Josefa Santos Yabe pela oportunidade de vislumbrar novos caminhos, apoio e parceria.

A todos os professores que participaram na minha formação acadêmica e contribuiram na minha formação de vida.

Ao Nelson Janeiro, técnico do laboratório de pesquisa, por toda a sua ajuda na realização dos expeimentos e a todos os funcionários do Departamento de Bioquímica e Biotecnologia.

Aos colegas e estagiários que participaram da realização deste trabalho.

À CAPES pela concessão da bolsa de estudo e apoio a pesquisa.

“A vida é para quem é corajoso o suficiente para se arriscar e humilde o bastante para aprender.”

Clarice Lispector

APRESENTAÇÃO

Este trabalho apresenta a parte de Material e Métodos, e Resultados e Discussão, na forma de artigos científicos. O artigo I (Capítulo 4) está escrito nas Normas da ABNT e os artigos II e III (Capítulos 5 e 6, respectivamente) estão escritos nas normas da revista 3 BIOTECH.

MELLO, Léa Rita Pestana Ferreira. **Valorização do bagaço de malte:** aplicação como bioadsorvente e estudo de pré-tratamentos para a obtenção de açúcares fermentescíveis. 2019. 104 f. Tese (Doutorado em Biotecnologia) – Universidade Estadual de Londrina, Londrina, 2019.

RESUMO

Os resíduos agroindustriais lignocelulósicos são matérias-primas de fontes renováveis e podem ser empregados na produção de biocombustíveis, energia, produtos químicos e novos materiais. Novas e promissoras tecnologias têm sido amplamente estudadas para melhorar a eficiência da conversão da biomassa lignocelulósica em produtos de maior valor. O bagaço de malte é um resíduo lignocelulósico gerado em abundância pela indústria cervejeira, rico em fibras, lipídios e proteínas, tendo como principal destino o uso como ração animal, e devido a esta complexa composição, pode ser empregado com matéria-prima para obtenção de produtos de maior valor agregado. Neste contexto, este trabalho teve como objetivo valorizar o bagaço de malte através do estudo da sua aplicação como bioadsorvente para o tratamento de efluentes contaminados com chumbo e do estudo de pré-tratamentos para a obtenção de açúcares fermentescíveis. O bagaço de malte foi avaliado quanto sua capacidade de sorção de chumbo em soluções aquosas. A modelagem matemática foi utilizada para prever o comportamento de sorção e dessorção de chumbo no bagaço e os parâmetros do modelo duplo de Langmuir-Freundlich foram utilizados para entender os mecanismos de interação entre sorvente e sorvato. A rápida e alta eficiência na sorção (> 90 %) e o baixo fator de mobilização (< 5 %) indicaram que o bagaço de malte é um material com potencial de aplicação para ser utilizado como bioadsorvente na remoção de chumbo, além de ser de baixo custo e ecologicamente correto. Para o estudo do pré-tratamento através da ultrassonicação em meio ácido diluído, o bagaço de malte foi submetido a diferentes valores de pH (3, 4 e 5), tempos de ultrassonicação (10, 35 e 60 min) e conteúdo de biomassa (6, 8 e 10 %). Em geral, as amostras pré-tratadas demonstraram maior índice de cristalinidade e estabilidade térmica do que o bagaço de malte *in natura*. O tempo foi a variável mais importante, maiores tempos resultaram em maior liberação de açúcares e maiores mudanças na fração sólida residual recuperada após o pré-tratamento. A amostra processada em pH 5 por 60 min com concentração de biomassa de 8 % resultou no maior teor de celulose, menor teor de lignina e maior remoção de outros componentes, como proteínas e lipídios. A combinação do ultrassom em meio alcalino foi realizada através de um planejamento fatorial completo (32), que foi empregado para avaliar os efeitos do pH (9, 10 e 11) e do tempo de ultrassonicação (10, 35 e 60 min) no bagaço de malte. As amostras pré-tratadas apresentaram maiores índices de cristalinidade e estabilidade térmica que o bagaço de malte *in natura*. O tempo foi a variável mais importante, maiores tempos de processo resultaram em maior liberação de açúcares e maiores alterações na fração sólida residual recuperada após o pré-tratamento. A condição que resultou na amostra com maior conteúdo de celulose e remoção de conteúdo de lignina obtida em pH 9 por 60 min. A ultrassonicação em meio alcalino resultou nos melhores resultados para a liberação de açúcares do bagaço de malte, com rendimentos duas vezes maiores para açúcares redutores em comparação com o pré-tratamento ácido, demonstrando maior eficiência na sacarificação do bagaço de malte.

Palavras-chave: Resíduos lignocelulósicos. Adsorvente. Ultrassonicação. Sacarificação.

MELLO, Léa Rita Pestana Ferreira. **Valorization of malt bagasse:** application as bioadsorbent and study of pretreatments to obtain fermentable sugars. 2019. 104 p. Thesis (Doctorate's degree in Biotechnology) – Universidade Estadual de Londrina, 2019.

ABSTRACT

The lignocellulosic agroindustrial residues are renewable sources raw materials that can be used for the production of biofuels, energy, chemicals and new materials. New and promising technologies have been extensively studied to improve the efficiency of the conversion of lignocellulosic biomass to higher value products. Malt bagasse is a lignocellulosic residue generated in abundance by the brewing industry, rich in fiber, lipids and proteins, and its main destination is for animal feed, and due to this complex composition, can be used as raw material for the obtainment of high value-added products. In this context, the objective of this work was to valorize the malt bagasse through the study of its application as a bioadsorbent for the treatment of effluents contaminated with lead and the study of pre-treatments to obtain fermentable sugars. Malt bagasse was evaluated for its sorption capacity of lead in aqueous solutions. Mathematical modeling was used to predict the sorption and desorption behavior of lead in the malt bagasse and the parameters of the Langmuir-Freundlich dual model were applied to understand the mechanisms of interaction between sorbent and sorbate. The rapid and high sorption efficiency (> 90 %) and the low mobilization factor (< 5 %) indicated that malt bagasse is a material with potential application to be used as a bioadsorbent in the removal of lead, besides being of low-cost and environmentally friendly. For the study ultrasonication in diluted acid medium as pretreatment, malt bagasse was submitted to different pH values (3, 4 and 5), ultrasonication times (10, 35 and 60 min) and biomass contents (6, 8 and 10 %). In general, the pretreated samples demonstrated a higher crystallinity index and thermal stability than raw malt bagasse. Considering the experimental conditions used in this study, time was the most important variable; more time resulted in higher sugar release and greater changes in the residual solid fraction recovered after pretreatment. The sample processed at pH 5 for 60 min with a biomass concentration of 8 % resulted in the highest cellulose content, lowest lignin content, and greatest removal of other components, such as proteins and lipids. The combination of ultrasonication in alkaline medium was performed using a factorial experimental design (3^2) that was employed to evaluate the effects of pH (9, 10 and 11) and time of ultrasonication (10, 35 and 60 min) on malt bagasse. The pretreated samples had higher crystallinity indexes and thermal stability than raw malt bagasse. The time was the most important variable, higher processing times resulted in higher sugars release and greater changes in the residual solid fraction recovered after pretreatment. The condition that resulted in the sample with the highest cellulose content and lignin content removal was that employing pH 9 for 60 min. Ultrasonication in alkaline medium resulted in better results for sugars release from malt bagasse, with yields two times higher for reducing sugars compared to acid pretreatment, demonstrating greater efficiency in saccharification of malt bagasse.

Keywords: Lignocellulosic residues. Adsorbent. Ultrasonication. Saccharification.

LISTA DE ILUSTRAÇÕES

LISTA DE TABELAS

LISTA DE ABREVIATURAS E SIGLAS

EDS	Energy dispersive spectrometry
EDXRF	Energy dispersive X-ray fluorescence
FAAS	Flame atomic absorption spectroscopy
FT-IR	Fourier transform-infrared spectroscopy
HI	Hysteresis index
MF	Mobilization factor
SEM	Scanning electron microscopy
TGA	Thermogravimetric analysis
XRD	X-ray diffraction

SUMÁRIO

1 INTRODUÇÃO

Nos últimos anos, vários grupos de pesquisa vêm atuando no desenvolvimento de processos biotecnológicos para o aproveitamento de resíduos agroindustriais como fonte de matéria-prima para a obtenção de produtos de maior valor agregado (MUSSATTO; ROBERTO, 2005; MUSSATTO et al., 2006; SILVA et al., 2009; ALVIRA et al., 2010; GÍRIO et al., 2010; CANILHA et al., 2012; MOOD et al., 2013; DUQUE et al., 2014; LIYAKATHALI et al. 2016; BHOWMICK et al., 2018).

Uma das possibilidades de aplicação para os resíduos agroindustriais que tem despertado grande interesse para os pesquisadores é a capacidade da biomassa lignocelulósica adsorver metais pesados, podendo ser utilizada como matéria-prima para a produção de bioadsorventes bastante eficientes (DEMIRBAS, 2008; SUD; MAHAJA; KAUR, 2008; LESMANA et al., 2009; KUMAR et al., 2011; NGUYEN et al., 2013).

O desenvolvimento industrial e tecnológico das últimas décadas tem sido um dos principais responsáveis pela contaminação do meio ambiente, por negligência do tratamento dos efluentes ou por contaminações acidentais (PINO et al., 2006; SAMPAIO et al., 2010). Os metais pesados são considerados poluentes perigosos, devido à sua mobilidade, persistência no ambiente e nocividade para os organismos vivos. Águas residuais de processos industriais, como galvanização, operações de mineração, refino de minérios, curtumes, baterias, tintas e pigmentos, fundições, ligas, pilhas, pesticidas e têxteis, trazem grandes preocupações ambientais devido à sua toxicidade, mesmo em baixas concentrações. Dentre os metais mais poluentes estão: Pb, Cr, Hg, U, Se, Zn, As, Cd, Au, Ag, Cu e Ni (FERNANDES, 1997; KADIRVELU et al., 2001; FLOREA; BÜSSELBERG, 2005, 2006).

A composição química dos resíduos agroindustriais, em sua maioria, compostos de celulose, hemicelulose e lignina, são reconhecidamente associados à remoção de metais pesados. A sorção de metais pesados por estes materiais é atribuída, principalmente, aos grupos funcionais destes compostos, tais como hidroxilas, carboxilas e grupos aminas, que são capazes de se ligar aos íons metálicos, atuando como sítios de ligação ou sítios de troca iônica para os metais pesados (CHOI; YUN, 2006; OFOMAJA ; HO, 2007; SUD; MAHAJAN; KAUR, 2008; LESMANA et al., 2009; NGUYEN et al., 2013).

Outra possibilidade de aplicação dos resíduos lignocelulósicos é a sua sacarificação, com a obtenção de açúcares fermentescíveis para emprego como substrato em diferentes processos fermentativos. Tanto a celulose (homopolissacarídeo formado por moléculas de glicose ligadas através de ligações β-1,4-glicosídicas), como a hemicelulose (heteropolissacarídeo ramificado formado principalmente por xilose, arabinose, galactose, glicose e manose, ligados por ligações glicosídicas β-1,4, ácidos urônicos e galacturônicos), podem ser convertidos em substratos para fermentação, de forma seletiva, através do uso de enzimas. No entanto, para que a sacarificação enzimática destes materiais seja eficiente, um pré-tratamento, ou a combinação de pré-tratamentos, se fazem necessários, para separar a matriz de lignina, reduzir a cristalinidade da celulose e aumentar a área de superfície e porosidade das fibras, em outras palavras, deixar as cadeias de celulose e hemicelulose mais disponíveis para que as enzimas tenham amplo acesso ao substrato, atingindo um maior rendimento (MOSIER et al., 2005; CARVALHEIRO; DUARTE; GÍRIO, 2008; OGEDA et al., 2010; CANILHA et al., 2010).

Novos processos para a desconstrução da fibra lignocelulósica têm sido amplamente estudados. A combinação de pré-tratamentos térmicos, físicos e químicos, combinados à ação biocatalítica da hidrólise enzimática, tem alcançado elevados rendimentos na obtenção de açúcares fermentescíveis utilizados como fonte para a produção de etanol, produtos químicos, materiais poliméricos e outros produtos derivados de maior valor agregado (CARVALHEIRO; DUARTE; GÍRIO, 2008; ALVIRA et al., 2010; MENON; RAO, 2012; DUQUE et al., 2014).

A ultrassonicação é um processo físico que pode ser empregado como pré-tratamento em fibras lignocelulósicas ainda pouco explorado, mas que tem demostrado resultados satisfatórios em estudos de extração de hemicelulose, celulose e lignina e na aceleração da sacarificação da biomassa lignocelulósica (VINATORU, 2001; SUN; TOMKINSON, 2002; YACHMENEV et al., 2009; SINDHU et al., 2017; BUNDHOO; MOHEE, 2018; HASSAN et al., 2018). Os mecanismos de extração por irradiação ultrassônica são atribuídos ao fenômeno da cavitação, onde o impacto produzido pelo colapso de bolhas de cavitação proporciona um importante benefício de abertura da superfície de fibras lignocelulósicas (MASON, 2002; GOGATE; KABADI, 2009; PILLI et al., 2011).

Portanto, a proposta deste trabalho foi avaliar o potencial de aplicação do bagaço de malte como bioadsorvente de chumbo em soluções aquosas e estudar os

efeitos de pré-tratamentos neste resíduo, combinando a ultrassonicação em meios ácido e básico para a obtenção de açúcares fermentescíveis, além de uma fração sólida residual mais susceptível à hidrólise enzimática.

2 OBJETIVOS

2.1 OBJETIVO GERAL

Valorizar o bagaço de malte através do estudo da sua aplicação como bioadsorvente para o tratamento de efluentes contaminados com chumbo e do estudo de pré-tratamentos para a obtenção de açúcares fermentescíveis.

2.2 OBJETIVOS ESPECÍFICOS

- Avaliar o potencial do bagaço de malte na remoção de chumbo em soluções aquosas, visando a aplicação deste resíduo como bioadsorvente.

- Estudar o emprego da ultrassonicação em meio ácido diluído e em meio básico como pré-tratamentos na sacarificação do bagaço de malte.

- Determinar as melhores condições dentre os pré-tratamentos empregados que resultem na maior liberação de açúcares fermentescíveis e na obtenção de fração sólida residual que seja mais acessível à hidrólise enzimática.

3 REVISÃO DE LITERATURA

3.1 RESÍDUOS AGROINDUSTRIAIS

O Brasil é um dos maiores produtores agrícolas do mundo, o que gera quantidades significativas de biomassa lignocelulósica. Os resíduos agrícolas têm origem na fase de cultivo e colheita de determinadas espécies, como cana de açúcar, soja, milho, arroz, algodão, entre outros, enquanto os resíduos agroindustriais resultam do processamento industrial da biomassa (MAPA, 2018).

Os resíduos agroindustriais como casca de arroz, casca de aveia, bagaço de cana de açúcar, bagaço de malte, entre outros, são considerados materiais lignocelulósicos, ricos em fibras. A utilização adequada destes resíduos pode amenizar os problemas ambientais e gerar produtos com relevantes aplicações na indústria (MUSSATTO et al., 2006; ASCHERI et al., 2007; SILVA et al., 2009; GÍRIO et al., 2010; CANILHA et al., 2012). No entanto, para que o aproveitamento destes resíduos seja efetivo, novas tecnologias têm sido desenvolvidas com o objetivo de utilizar estes materiais como matéria-prima para a obtenção de produtos de maior valor agregado, contribuir com o meio ambiente e promover a sustentabilidade dos processos industriais (SUN; CHENG, 2002; MUSSATTO; ROBERTO, 2005; CARVALHEIRO; DUARTE; GÍRIO, 2008; PENG et al., 2012; LUO et al., 2014).

3.1.1 Bagaço de Malte

O Brasil produziu 427,4 mil toneladas de cevada em 2018, sendo 60 % deste total colhidas no Paraná (251,9 mil toneladas), seguido do Rio Grande do Sul (157,8 mil toneladas), São Paulo (12,5 mil toneladas) e Santa Catarina (5,2 mil toneladas) (IBGE, 2019). No Paraná também está a maior maltaria da América Latina (Cooperativa Agrária - Guarapuava), que produz anualmente cerca de 350 mil toneladas de malte, volume destinado, integralmente, à indústria cervejeira, o que representa 30 % da demanda do mercado brasileiro (AGRARIA, 2019).

A indústria cervejeira produz grandes quantidades de subprodutos e resíduos; o bagaço de malte, o bagaço de lúpulo e as leveduras são os mais comuns e são gerados principalmente nas etapas de filtragem, envase e tratamento de água e efluentes. O malte utilizado na fabricação de cerveja é o produto resultante da

germinação e posterior dessecação do grão de cevada (*Hordeum sativum*) ou de outros cereais. O produto é designado simplesmente "malte" quando obtido da cevada; quando obtido de outro cereal, é designado pela palavra "malte" seguido do nome do cereal de origem. Por exemplo, "malte de trigo" (ANVISA, 1978).

O bagaço de malte é obtido dos grãos da cevada e consiste nas camadas externas, (casca, testa e pericarpo) e resíduos do endosperma do grão de cevada maltada que permanece após o processo de moagem do grão (KUNZE, 1996). É o principal resíduo sólido, representando 85 % do total dos subprodutos gerados no processo cervejeiro (Figura 1), que se inicia com a moagem do malte seguida de adição de água e então fervido em caldeiras de mostura, processo este denominado de brassagem, após a fervura ocorre a filtração do mosto, e a fração residual sólida retida na peneira, constitui o resíduo sólido de cervejaria ou bagaço de malte (SANTOS; RIBEIRO, 2005; OLAJIRE, 2012).

Figura 1 - Representação esquemática do processo para obtenção do bagaço de malte na indústria cervejeira

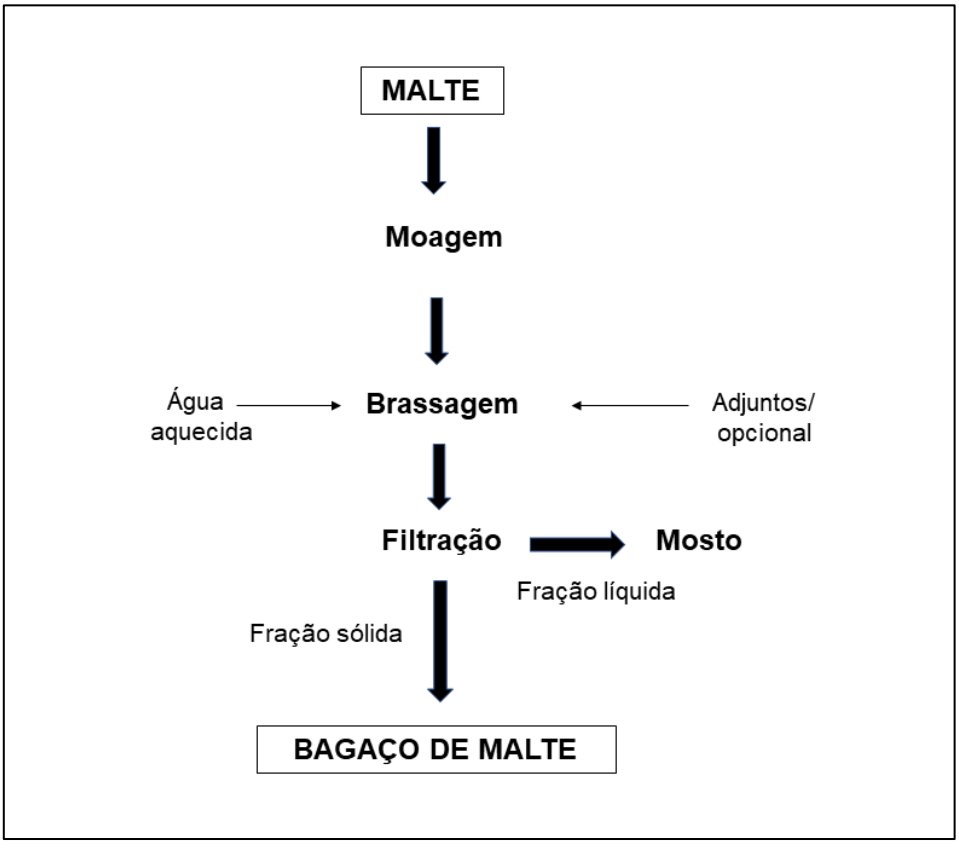

Fonte: o próprio autor

Para cada 100 kg de grãos de malte processados, são gerados 120 a 130 kg de bagaço úmido com cerca de 80 % de umidade, correspondentes a 20 kg de bagaço de malte para cada hectolitro de cerveja de produzida, o que confirma o setor cervejeiro como um grande gerador de resíduos e a importância do descarte ou destinação adequadas para este resíduo, que tem como destino principal a alimentação animal (FILLAUDEAU et al., 2006; OLAJIRE, 2012).

O bagaço de malte é um resíduo lignocelulósico, rico em proteínas (14 %) e carboidratos (74 %), os quais são compostos por 62 % de fibras insolúveis, que incluem 12 % de celulose, 23 % de hemicelulose, principalmente arabinoxilanos, e 28 % de lignina. Do ponto de vista biotecnológico, os açúcares contidos nas frações celulósica (glicose) e hemicelulósica (xilose, arabinose, glicose, manose e galactose) representam os substratos que podem ser utilizados para a produção de etanol e outros produtos de maior importância nas indústrias de alimentos e farmacêutica (MUSSATO et al., 2006; MELLO; MALI, 2014; DASGUPTA et al., 2017).

3.2 BIOMASSA LIGNOCELULÓSICA

A biomassa lignocelulósica constitui a maior fonte renovável de carboidratos no mundo, representando cerca de 90 % da massa seca de uma célula vegetal e é constituída por três principais frações poliméricas: celulose, hemicelulose e lignina. A parede celular vegetal é composta por diferentes camadas, que diferem quanto à estrutura e composição química (Figura 2).

Figura 2 - Estrutura de uma parede celular vegetal e seus principais componentes

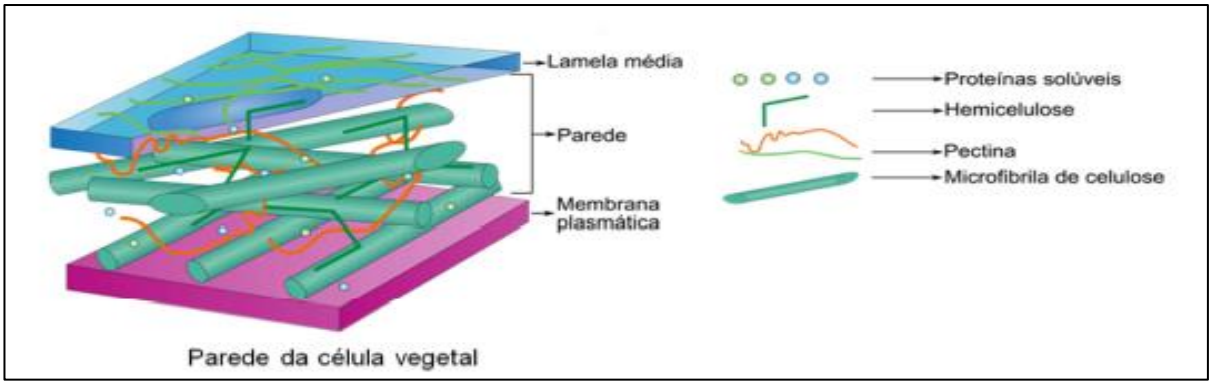

Fonte: (STICKLEN, 2008)

A fração celulósica é formada por fibras de celulose e encontram-se disposta em espirais, de forma a conferir força e flexibilidade ao material. Esta fração está associada à lignina, polímero aromático heterogêneo, que atua como agente enrijecedor no interior das fibras, aumentando a resistência da estrutura a ataques químicos e enzimáticos e a fração hemicelulósica, atua como um elo químico entre a celulose e a lignina. A força de adesão entre as fibras de celulose e a lignina é ampliada pela existência de ligações covalentes entre as cadeias de lignina e os constituintes da celulose e da hemicelulose (SILVA et al., 2009; CASTRO; PEREIRA JUNIOR, 2010).

A composição química da biomassa lignocelulósica varia entre 35-50 % de celulose, seguido de 20-35 % de hemicelulose, 10-25 % de lignina, pectina, pequenas quantidades de ceras e ácidos graxos (SANTOS et al., 2012). Esta composição química depende do tipo de vegetal, condições de crescimento e parte da planta colhida conforme mostrado na Tabela 1.

Tabela 1- Composição química de diferentes biomassas lignocelulósicas

Biomassa Lignocelulósica	% Celulose	% Hemicelulose	% Lignina
Bagaço de cana	32-48	19-24	23-32
Madeira dura	43-47	25-35	16-24
Espiga de milho	45	35	15
Algodão	95	2	0,3
Palha de trigo	30	50	15
Sisal	73,1	14,2	11
Palha de arroz	43,3	26,4	16,3
Fibra de coco	36-43	0,15-0,25	41-45
Fibra de bananeira	60-65	6-8	5-10
Palha de cevada	31-45	27-38	14-19

Fonte: (SANTOS et al., 2012)

A celulose é um polímero linear com ligações glicosídicas β-1,4 entre unidades de D-glicopiranose (Figura 3), e a junção de duas moléculas de glicose forma o dissacarídeo celobiose. As cadeias de celulose em parede celular primária de plantas têm graus de polimerização na faixa de 2.000 a 7.500, na madeira o grau de polimerização é em torno 10.000, e na de celulose de algodão é de 15.000. Apresenta três grupos hidroxila por unidade de anidroglucose (AGU), e os grupos hidroxilas em ambos os finais da cadeia de celulose exibem diferentes comportamentos, o carbono 1 (C-1) tem propriedades redutoras, enquanto o grupo hidroxila no carbono 4 (C-4) livre é dito não redutor. Os grupamentos hidroxila estabelecem ligações de hidrogênio intra e intermoleculares que contribuem para a formação de regiões altamente ordenadas, chamadas de regiões cristalinas, que compreendem de 50 a 70 % do total, entrecortadas por regiões menos ordenadas, as regiões amorfas, e este elevado grau de interações confere insolubilidade em água e na maioria dos solventes orgânicos à celulose (OGUEDA; PETRI, 2010).

Figura 3 - Representação esquemática da celulose

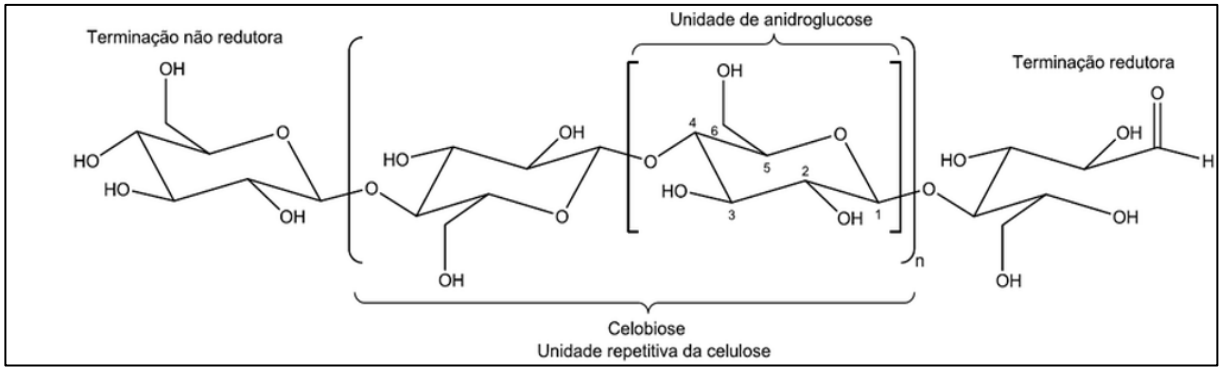

Fonte: (SANTOS et al., 2012)

As hemiceluloses, também designadas de polioses, são uma classe heterogênea de polímeros que representam cerca de 15-35 % da biomassa vegetal. Podem conter pentoses (β D-xilose, α L-arabinose), hexoses (β D-manose, β D-glucose, α D-galactose) e / ou ácidos urônicos (α D-glicorônico, α D-4-metil-O galacturônico e ácidos α D-galacturônico) (Figura 4). Outros açúcares como a α L-ramnose e α L-fucose também podem estar presentes em pequenas quantidades. Os homopolímeros de xilose, chamados homoxilanas só ocorrem em algas vermelhas e verdes. As hemiceluloses mais relevantes são as xilanas e glucomananas, sendo as xilanas as mais abundantes (GÍRIO et al., 2010).

De acordo com os seus monômeros, as hemiceluloses podem ser classificadas como xilanas, mananas, arabinoxilanas, arabinogalactanas e arabinanas (OGEDA; PETRI, 2010). A natureza química das hemiceluloses varia, nas plantas, em relação ao tipo de tecido vegetal e à espécie a que pertencem. Em geral, as hemiceluloses estão presentes nas madeiras em 20 a 30 % da composição total, enquanto, nas gramíneas, estes valores podem chegar a 50 % (EBRINGEROVA; HROMADKOVA, 2005).

Figura 4 - Representação esquemática da hemicelulose

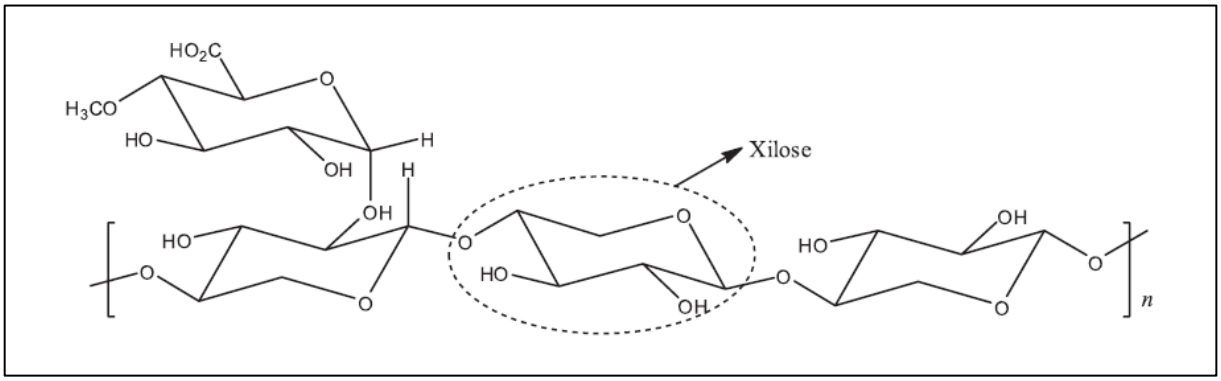

Fonte: (SANTOS et al., 2012)

A hemicelulose heteropolissacarídica pode ser extraída por hidrólise ácida quase que integralmente do complexo lignocelulósico, por processos que utilizam tratamento térmico na presença de ácido inorgânico como catalisador em pequenas concentrações. Este processo pode ser seguido ou não de rápida descompressão, e deste modo, promove um desarranjo na estrutura física do material, facilitando a extração de um licor, composto principalmente de xilose com pequeno grau de polimerização (BETANCUR; PEREIRA JUNIOR, 2010).

A lignina é um heteropolímero amorfo que consiste em três diferentes unidades de fenilpropanos: álcool *p*-cumarílico, álcool coferílico e álcool sinapílico. Depois da celulose, a lignina é a macromolécula mais abundante dentre as biomassas lignocelulósicas (Figura 5). A composição e a organização destes monômeros varia entre as espécies vegetais, e sua função biológica é fornecer suporte estrutural à parede celular, impermeabilidade e resistência contra o ataque microbiano.

No processo de hidrólise enzimática dos resíduos lignocelulósicos, a lignina atua como uma barreira física para as enzimas, que podem ser irreversivelmente capturadas pela lignina, assim, aumentando a quantidade de enzima necessária para

a hidrólise, e podendo dificultar a recuperação da enzima. O teor e distribuição da lignina são os fatores responsáveis pela recalcitrância nos materiais lignocelulósicos, limitando a acessibilidade das enzimas, sendo então necessários o emprego de pré-tratamentos para que a hidrólise enzimática seja eficiente (TAHERZADEH; KARIMI, 2007; SILVA et al., 2012).

Figura 5 – Representação estrutural da lignina de eucalipto

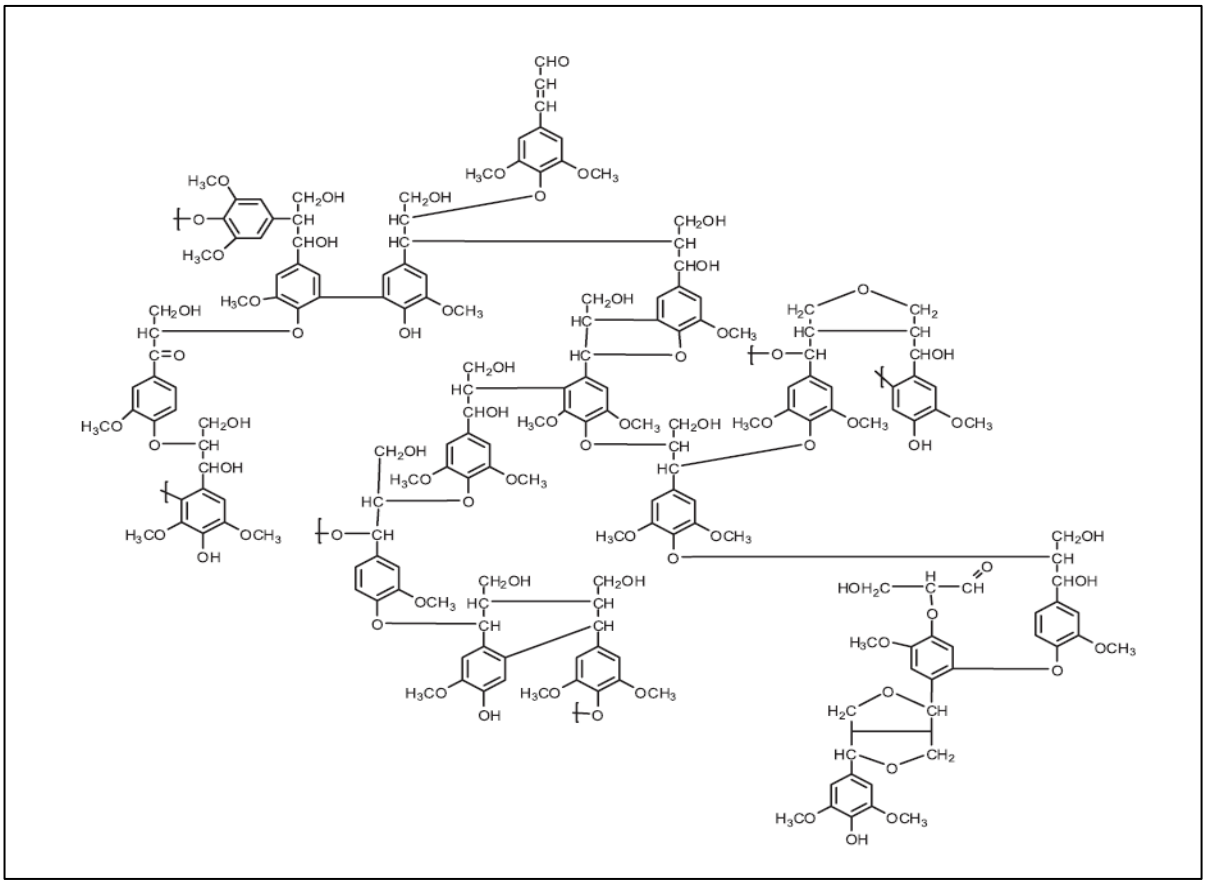

Fonte: (SANTOS et al., 2012)

As principais características químicas e estruturais celulose e da hemicelulose estão apresentadas na Tabela 2. A compreensão destas características é de fundamental importância para o desenvolvimento de estratégias de aproveitamento destas biomassas.

Tabela 2 – Principais diferenças entre celulose e hemicelulose

Características	Celulose	Hemicelulose
Unidades monoméricas	Unidades de glicose ligadas entre si	Várias unidades de pentoses e hexoses ligadas entre si
Grau de polimerização	Alto (1000 a 15000 monômeros)	Baixo (50 a 300monômeros)
Arranjo espacial	Forma arranjo fibroso	Não forma arranjo fibroso
Regiões cristalinas	Apresenta regiões cristalinas e amorfas	Apresenta somente regiões amorfas
Hidrólise ácida	Degradada lentamente por ácido diluído a quente	Degradada rapidamente por ácido diluído a quente
Solubilidade em álcalis	Insolúvel	Solúvel

Fonte: (Adaptado de BON et al., 2008)

3.3 Aplicação de Biomassa Lignocelulósica como Bioadsorvente de Chumbo

A remoção de metais pesados das águas contaminadas pode ser conseguida por várias técnicas, como precipitação química, floculação, filtração por membrana, troca iônica e adsorção. Apesar da disponibilidade de inúmeras técnicas para o tratamento de efluentes com metais pesados, a adsorção é constantemente vista como uma técnica altamente eficaz para este fim, especialmente em soluções de baixa concentração de metal (LESMANA et al., 2009).

Águas residuais de fundição de chumbo, fabricantes de bateria, indústria de papel e celulose e indústria de munição contém chumbo. Os íons de chumbo são tóxicos e mesmo em baixas concentrações, podem afetar quase todos os órgãos e sistemas do organismo, trazendo sérios riscos à saúde humana, ao meio ambiente e todos os organismos vivos (WADANAMBI; DUBEY; TOWNSEND, 2008).

Considerável atenção tem sido voltada para o emprego de biomassa ou resíduos lignocelulósicos, como materiais adsorventes nos processos de biossorção do chumbo e de outros metais pesados, sendo denominados bioadsorventes (SUD;

MAHAJAN; KAUR, 2008; DERMIBAS, 2008; KUMAR et al., 2011; NGUYEN et al., 2013).

Dentre alguns resíduos empregados como bioadsorventes podemos citar o farelo de arroz (Wang et al., 2006), cascas de café (Oliveira et al., 2008), resíduo de casca de manga (Iqbal; Saeed; Kalim, 2009) e pó de serragem (Naiya et al., 2009; Akunwa; Muhammad; Akunna, 2014), bagaço de malte (Li; Chai; Qin, 2012), borra de café (Dutta et al., 2015), resíduos de chá (Abdolali et al., 2016), biomassa de girassol (Jain et al., 2016).

Particularmente, para a remoção de íons de chumbo, vários trabalhos são encontrados na literatura como: cascas de banana e laranja (Annadurai et al., 2003), farelo de arroz (Montanher et al., 2005), resíduos de moagem de grão-de-bico (Saeed et al., 2005), casca de arroz (Zulkali et al., 2006), fibras de coco (Conrad; Hansen, 2007), folhas de Rosa Canina (Ghasemi et al., 2014), resíduos de biomassa de casca de avelã e amêndoa (Pehlivan et al., 2009a), palha de cevada (Pehlivan et al., 2009b), casca de pepino (Basu et al., 2017), resíduos da indústria de azeite (Pretella et al., 2018), serragem de pinheiro-de-alepo (Semerjian et al., 2018), casca de coco, casca de café, casca de eucalipto (Correia et al., 2018). Li et al., (2009a; 2009b) relataram o uso de bagaço de malte modificado para remover o chumbo da solução aquosa. Não foram encontrados trabalhos na literatura consultada, que relatem o potencial do bagaço de malte *in natura* como adsorvente de chumbo em efluentes contaminados.

3.3.1 Processo e Mecanismos de Biossorção

A biomassa lignocelulósica é composta, majoritariamente, por celulose, hemicelulose e lignina, e outros compostos, como extrativos: lipídios, proteínas, amido, açúcares simples, cinzas e água, com uma variedade de grupos funcionais, que incluem álcoois, aldeídos, cetonas, fenóis e éteres, aos quais é atribuído o processo de biossorção, sendo então, essencial identificar os grupos funcionais responsáveis pela ligação com o metal, a fim de se compreender o mecanismo pelo qual os metais ligam-se à biomassa (LESMANA et al., 2009; KUMAR et al., 2011).

A biossorção de metais pesados em soluções aquosas é um processo relativamente novo e promissor, principalmente, quando os adsorventes são resíduos lignocelulósicos, por apresentarem vantagens como: (1) alta eficiência, mesmo em baixas concentrações; (2) grande disponibilidade; (3) baixo custo; (4) fonte renovável

e (5) sem efeitos prejudiciais ao meio ambiente. Os mecanismos envolvidos no processo de biossorção, embora ainda pouco elucidados incluem: quimissorção, complexação e quelação, troca iônica, adsorção em superfície e difusão através de poros. A capacidade de sorção da biomassa lignocelulósica para íons metálicos é geralmente descrito como adsorção. (DEMIRBAS, 2008; SUD; MAHAJAN; KAUR, 2008; NGUYEN et al., 2013). A biossorção é um processo rápido, eficiente e pode ser reversível, que ocorre em diferentes etapas: adsorção, separação sólido-líquido e regeneração (dessorção) ou destruição da biomassa, apresentadas na Figura 6.

Figura 6 - Fluxograma esquemático de um processo de biossorção

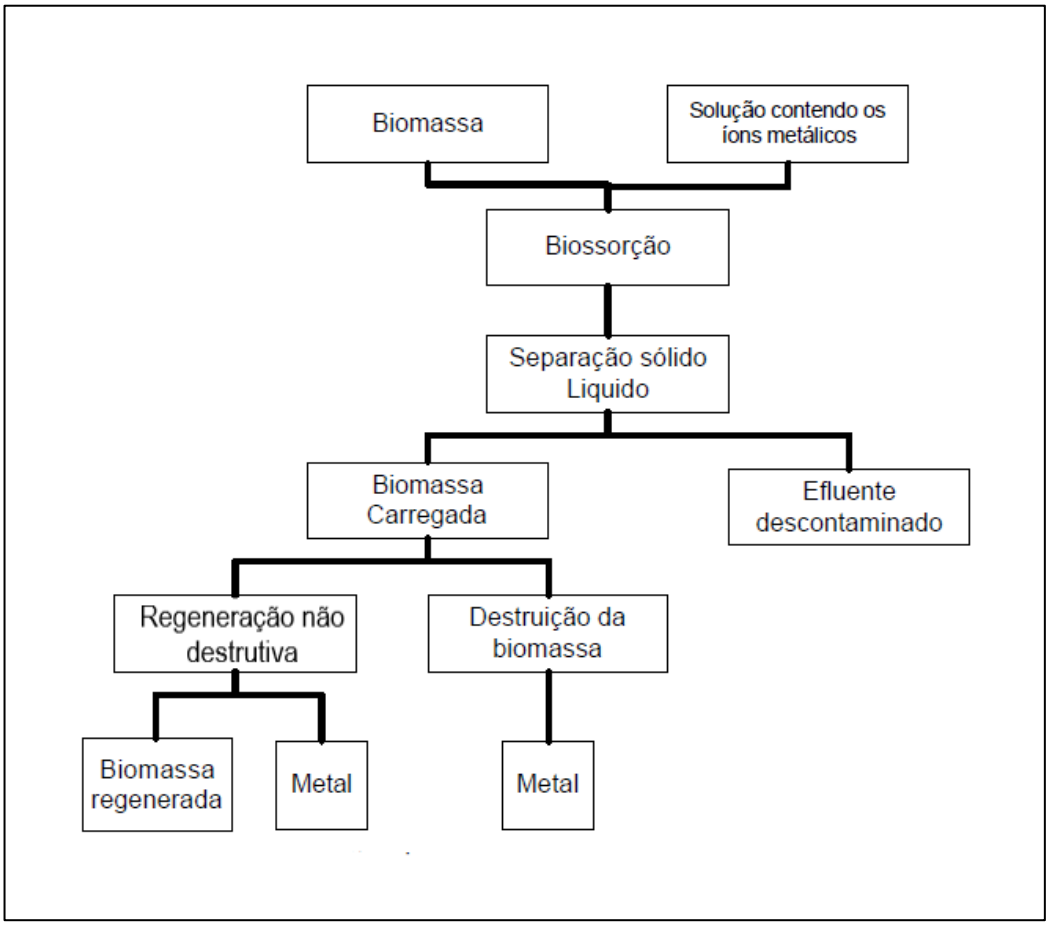

Fonte: (BENVINDO et al., 2002)

3.3.2 Adsorção

A adsorção é o processo físico-químico mais importante na retenção de substâncias orgânicas e inorgânicas. Pode ser definido como o acúmulo de uma substância em uma interface e pode ocorrer nos sistemas líquido-gás, líquido-líquido,

sólido-líquido e sólido-gás. A adsorção ocorre na superfície ou interface do adsorvente, enquanto que na absorção, esse mecanismo ocorre pela penetração de um sorvato em outra fase, implicando no acúmulo da substância absorvida em todo o volume do absorvente. A adsorção e a absorção podem ocorrer simultaneamente, e quando não podem ser distinguidas, o termo sorção é utilizado (DĄBROWSKI, 2001).

O processo de adsorção envolve uma fase sólida (adsorvente) e uma fase líquida onde se encontram as espécies dissolvidas que serão sorvidas (adsorvato, por exemplo, os íons metálicos). O adsorvato é atraído pelo adsorvente por diferentes mecanismos, dependendo da composição química do material e continua até atingir o equilíbrio entre os íons capturados e os íons dissolvidos. O processo inverso à adsorção é a dessorção (VOLESKY, 2004).

De forma geral, existem dois tipos de adsorção: adsorção física (fisissorção) e a adsorção química (quimissorção). A adsorção física é resultante das interações de Van der Waals entre o adsorvente e o adsorvato envolvendo forças intermoleculares fracas e baixas energias, é um processo reversível, de baixa especificidade, o equilíbrio é atingido rapidamente e é de fácil dessorção. A adsorção química envolve a formação de uma ligação química (covalente) entre o adsorvato e o adsorvente, caracterizando-se por altas energias de adsorção. As interações são relativamente superiores, quando comparadas às forças observadas na adsorção física, tornando a dessorção mais difícil. É um processo de especificidade elevada, mais lento e frequentemente irreversível (DĄBROWSKI, 2001). Na adsorção física pode ocorrer a formação de múltiplas camadas, a força de adsorção diminui à medida que se aumenta o número de camadas, enquanto na adsorção química, ocorre a formação de uma monocamada de adsorvato (GORELOV et al., 1994).

3.3.3 Isotermas de Adsorção e Modelos Matemáticos

A adsorção pode ser avaliada quantitativamente através das isotermas de adsorção. As isotermas são equações matemáticas que expressam a relação entre a quantidade de determinado íon adsorvido por unidade de massa do adsorvente e a sua concentração em solução no equilíbrio à temperatura constante. Quando o equilíbrio da adsorção é atingido, temos a concentração final do adsorvato na fase líquida em equilíbrio (C_{eq}) e a concentração do adsorvato na fase sólida em equilíbrio (C_{sorb}). C_{eq} pode ser determinada por técnicas analíticas (tais como cromatografia

gasosa ou líquida, espectrofotometria no ultravioleta ou visível, espectrometria de absorção ou emissão ou outros meios adequados) e C_{sorb} (mg/g) é calculado de acordo com a Equação 1.

$$\mathrm{C_{sorb}} = C_i - C_{eq}) \frac{V}{m} \quad (1)$$

Onde C_{sorb} é a concentração de adsorvato em equilíbrio (mg/g); C_i é a concentração inicial do adsorvato; C_{eq} é a concentração de adsorvato na fase líquida em equilíbrio (mg/L); *V (*L) é o volume da solução; *m* (g) é a massa do adsorvente. É importante mencionar que as unidades para cada variável ficam a critério do pesquisador. Após as determinações de C_{sorb} e C_{eq}, pode-se construir um gráfico (C_{sorb} na ordenada e C_{eq} na abscissa, o qual tem-se como resultado o gráfico de uma isoterma de adsorção (VOLESKY, 2004; NASCIMENTO et al., 2014).

A forma que a isoterma adquire é uma ferramenta experimental que fornece informações importantes sobre o mecanismo de adsorção. De acordo com Mccabe et al. (1993) elas mostram os tipos de interações que podem ocorrer entre o adsorvente e o adsorvato (Figura 7):

- Isoterma Linear: a massa de adsorvato retida por unidade de massa do adsorvente é proporcional à concentração de equilíbrio do adsorvato na fase fluida;
- Isoterma Favorável: a massa do adsorvato retida por unidade de massa do adsorvente é alta para uma baixa concentração de equilíbrio do adsorvato na fase fluida;
- Isoterma Irreversível: a massa de adsorvato retida por unidade de massa do adsorvente independe da concentração de equilíbrio do adsorvato na fase fluida;
- Isoterma Desfavorável: a massa do adsorvato retida por unidade de massa do adsorvente é baixa mesmo para uma alta concentração de equilíbrio do adsorvato na fase fluida.

Figura 7 – Formas de isotermas de adsorção mais comuns: *q* é a concentração do adsorvato na fase sólida e C_e a concentração do adsorvato na fase líquida

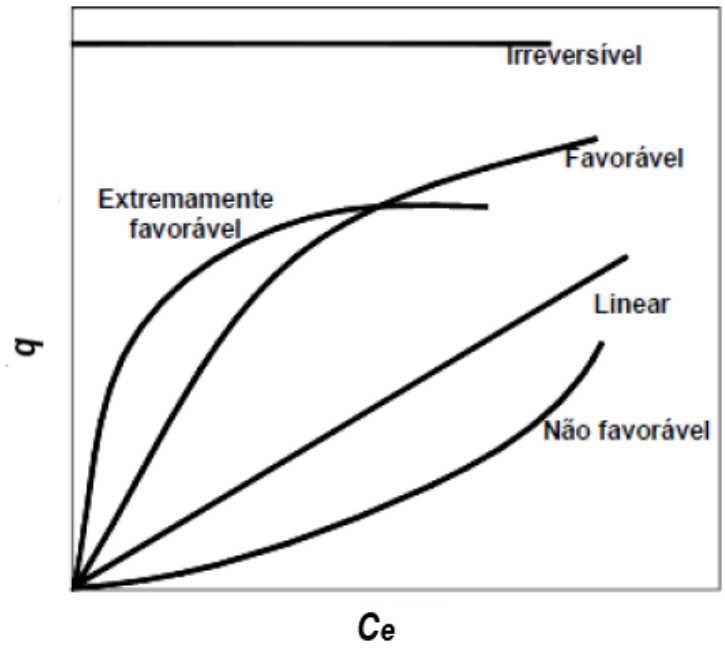

Fonte: (McCABE et al., 1993)

Giles et al., (1974) classificaram as isotermas de adsorção baseando-se na inclinação inicial em quatro classes e estas divididas em subgrupos, baseados na presença de platôs e pontos de inflexão (Figuras 8 e 9). As quatro classes foram nomeadas de S - Spherical, L - Langmuir, H - High Affinity e C - Constant Partition e estão descritas a seguir (HINZ, 2011):

- A isoterma do tipo S é côncava e mostra que a adsorção inicial é baixa e aumenta com o número de moléculas adsorvidas. Isto indica que ocorreu associação entre moléculas adsorvidas, chamada de adsorção cooperativa. Neste tipo de isoterma a afinidade entre adsorvente e soluto é baixa;

- A isoterma do tipo L convexa. Há alta afinidade entre o adsorvente pelo soluto a baixas concentrações. Ocorre a diminuição da disponibilidade dos sítios de adsorção com o aumento da concentração da solução;

- A isoterma do tipo H é convexa. É um caso especial de curva do tipo L e pode ser obtida em sistemas em que a superfície do adsorvente possui alta afinidade pelo soluto adsorvido;

- A isoterma do tipo C representa uma partição constante do soluto entre a solução e o adsorvente resultando em uma curva de aspecto linear. As condições que

favorecem as curvas do tipo C são sólidos porosos flexíveis e regiões de diferentes graus de solubilidade para o soluto.

Figura 8 - Tipos de isotermas de adsorção baseadas nas inclinações das curvas: (a) L - Langmuir, (b) H - High affinity, S – Spherical, C - Constant partition

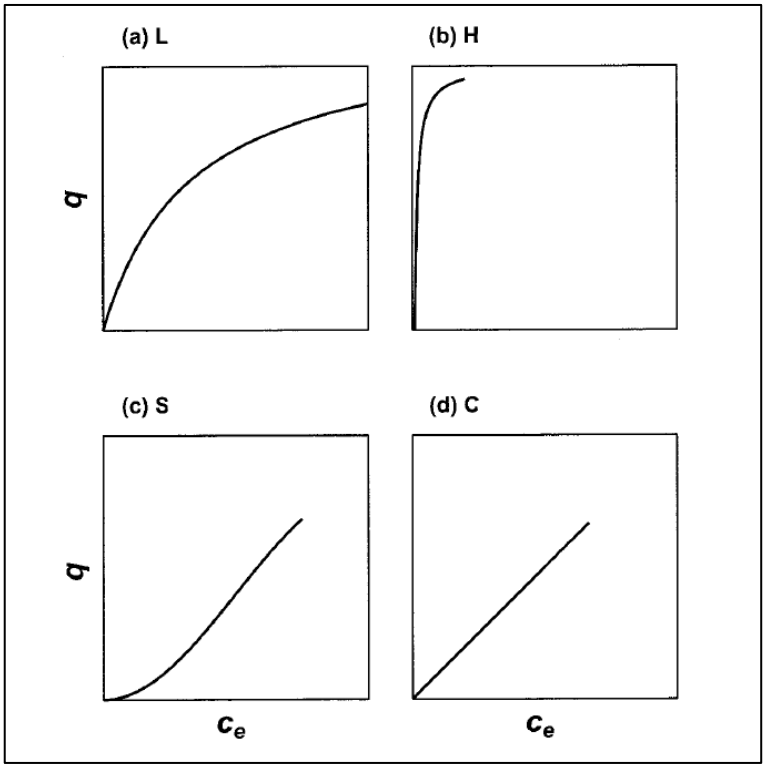

Fonte: (GILES et al., 1974)

Os subgrupos são definidos pelo comportamento de sorção em altas concentrações. O subgrupo 1 não apresenta platôs, o subgrupo 2 caracteriza-se por apresentar um platô, o subgrupo 3 tem um ponto de inflexão devido à mudança de para a forma côncava. Dois platôs são característicos do subgrupo 4 e o subgrupo *max* que é definido pela existência de um máximo (não mostrado na Figura 9). Esta classificação é baseada na observação pura e não revela a ligação entre o processo e a forma da isoterma (Figura 9) (GILES et al., 1974).

Há também a classificação para as isotermas de adsorção dos sistemas gás/sólido descrita por Sing (1985) aceita pela União Internacional de Química Pura e Aplicada (IUPAC) que utiliza a numeração romana de I a VI. É uma classificação específica para a adsorção física entre gás e sólido poroso, enquanto que a

classificação de Giles é mais apropriada para uma descrição geral das isotermas de adsorção, especialmente quando o processo de retenção não é conhecido.

Figura 9 - Classificação das isotermas de acordo com Giles et al., (1974). Onde *q* é a quantidade de material adsorvido e C_e a concentração de equilíbrio em solução

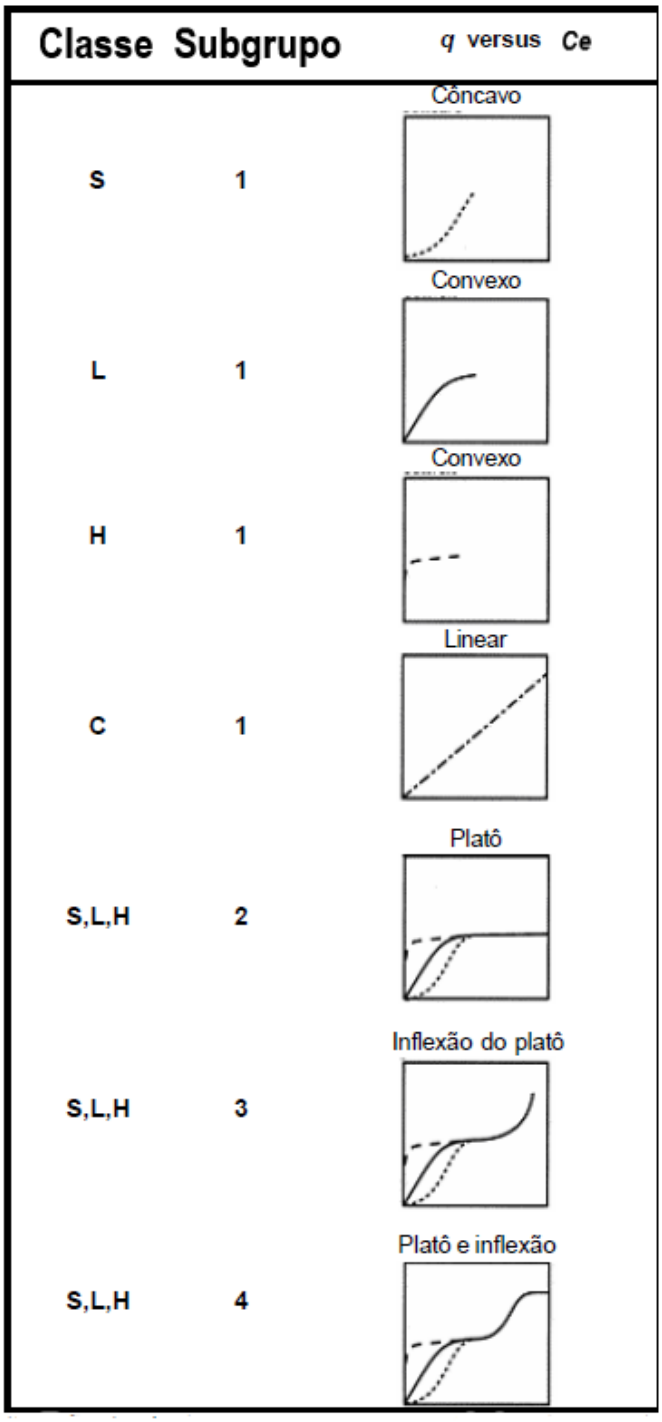

Fonte: (GILES et al., 1974)

3.3.3.1 Isotermas de Langmuir

O modelo de isoterma de Langmuir (Langmuir, 1916) é um dos mais utilizados para a representação de processos de adsorção. Ele pressupõe que a adsorção ocorre em um número definido de sítios e que cada sítio pode comportar apenas uma molécula adsorvida. Os sítios têm energia equivalente e as moléculas adsorvidas não interagem umas com as outras. A adsorção ocorre em monocamada. O modelo é representado pela Equação (2).

$$C_{sorb} = \frac{bKC_{eq}}{1+KC_{eq}} \quad (2)$$

Onde C_{sorb} é a concentração de adsorvato em equilíbrio (mg/g); C_{eq} é a concentração de adsorvato na fase líquida em equilíbrio (mg/L); *b* é a capacidade máxima de sorção determinada pelo número de sítios de adsorção reativa e *K* uma constante relacionada à afinidade de adsorção.

3.3.3.2 Isotermas de Freundlich

O modelo de Freundlich (Freundlich, 1906) é uma equação empírica que considera a adsorção em multicamada sem considerar a saturação máxima do metal e a saturação do sítio de adsorção. O modelo afirma que os primeiros sítios ocupados são aqueles com maior energia de interação, com diminuição exponencial na energia de interação até que o processo de adsorção esteja completo. Este modelo pode ser aplicado a sistemas não ideais e superfícies heterogêneas (Equação 3).

$$C_{sorb} = K\,(C_{eq})^{n} \quad (3)$$

Onde C_{sorb} representa a quantidade de adsorvato no equilíbrio (mg/g); C_{eq} é a concentração de adsorvato na fase líquida em equilíbrio (mg/L); *K* é a constante de Freundlich referente à capacidade da adsorção (L/mg); n é a constante que informa sobre a heterogeneidade dos sítios de adsorção (adimensional). Se $0 < n < 1$, a adsorção é benéfica: a heterogeneidade do local diminui e, correspondentemente, a homogeneidade do aumenta à medida que *n* se aproxima 1. Um maior valor de *n*

significa que o sistema é mais heterogêneo, o que geralmente resulta em não linearidade a isoterma de adsorção (FREUNDLICH, 1906; LIMOUSIN, 2007).

3.3.3.3 Modelo duplo de Langmuir-Freundlich

O modelo duplo Langmuir-Freundlich (Sips, 1950) combina os modelos de Freundlich e Langmuir para prever a adsorção em sistemas heterogêneos. Em baixas concentrações de adsorvato, Sips se reduz ao modelo de Freundlich, enquanto em altas concentrações, prediz uma capacidade de adsorção em monocamada, característica do modelo de Langmuir (Equação 4).

$$\mathrm{C_{sorb}} = \frac{b_1(k_1 Ceq)^{n1}}{1+(k_1 Ceq)^{n1}} + \frac{b_2(k_2 Ceq)^{n2}}{1+(k_2 Ceq)^{n2}} \quad (4)$$

Onde K_1 e K_2 são as energias de ligação associadas com uma constante de equilíbrio dependente do pH (L/mg); b_1 e b_2 são a capacidade máxima de adsorção determinada pelos sítios de superfície reativa em um sistema de monocamada ideal (mg/g); n_1 e n_2 são parâmetros adimensionais e informam sobre a heterogeneidade dos sítios de adsorção; os índices 1 e 2 representam dois tipos diferentes de sítios de adsorção (GALUNIN et al., 2004).

3.4 PRÉ-TRATAMENTOS DE RESÍDUOS LIGNOCELULÓSICOS

Nas últimas duas décadas, vários pesquisadores têm despendido grande esforço nos estudos para o aproveitamento de subprodutos e resíduos gerados pelas industrias agrícolas e de alimentos como fontes de energia e novos produtos, de forma a contribuir para a sustentabilidade destes setores. Neste conceito, as biorrefinarias englobam um sistema integrado e planta de processamento diversificada, onde as matérias-primas oriundas das biomassas lignocelulósicas são convertidas em uma ampla gama de produtos de maior valor agregado, de modo que se tenha cadeias de valor similares aos derivados do petróleo, porém, com redução de impactos negativos ao meio ambiente e uma abordagem de desperdício zero (CARVALHEIRO; DUARTE; GÍRIO, 2008; ALVIRA et al., 2010; GÍRIO et al., 2010; MENON; RAO, 2012; DUQUE

et al., 2014; BHOWMICK et al., 2018). Biorrefinaria pode ser considerada como uma evolução dos conceitos, "Química Verde" ou Quimurgia (KAMM et al., 2006).

Várias tecnologias de pré-tratamentos (empregados separadamente ou em combinação) têm sido propostas na literatura. Em termos gerais, os pré-tratamentos podem ser categorizados em 4 tipos: físicos, físico-químicos, químicos e biológicos (ALVIRA et al., 2010). O objetivo do pré-tratamento das fibras lignocelulósicas é desorganizar a estrutura cristalina das macro e microfibrilas a fim de liberar as cadeias poliméricas de celulose e hemicelulose (Figura 10), além de aumentar a porosidade destes materiais, para que as enzimas tenham amplo acesso ao substrato no processo de hidrólise enzimática, tornado a sacarificação mais eficiente (MOOD et al., 2013).

Figura 10 – Esquema genérico da ação dos pré-tratamentos na organização das fibras lignocelulósicas

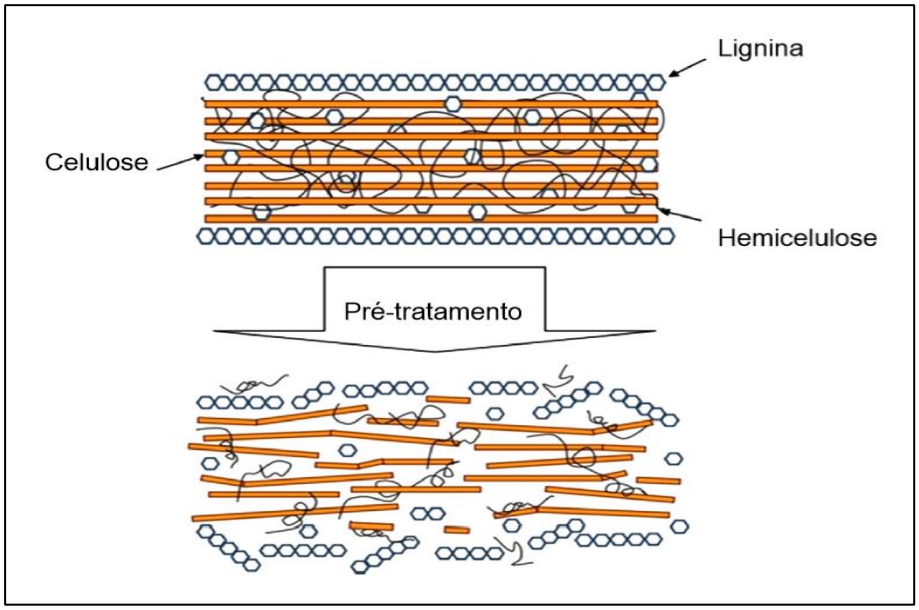

Fonte: (MOOD et al., 2013)

O pré-tratamento deve atender os seguintes requisitos para ser eficaz por: (1) favorecer o acesso aos carboidratos ou habilitar estes carboidratos para a hidrólise enzimática; (2) evitar a degradação ou perda de carboidrato; (3) evitar a formação de subprodutos inibitórios para a subsequente hidrólise e fermentação e (4) ser rentável (SUN; CHENG, 2002). Vários métodos de pré-tratamentos e seus efeitos sobre a biomassa lignocelulósica foram revisados nos últimos anos e estão apresentados na Tabela 3 (TAHERZADEH; KARIMI, 2008; KUMAR et al.; 2011; ALVIRA et al., 2010;

CANILHA et al., 2012; MENON; RAO, 2012; MOOD et al., 2013; KARIMI et al., 2014; BHOWMICK et al., 2018).

Tabela 3 - Efeito de diferentes métodos de pré-tratamento na composição e estrutura química da biomassa lignocelulósica, suas vantagens e limitações

Pré-tratamentos	**Vantagens**	**Limitações**
Trituração mecânica	Reduz a cristalinidade da celulose	Alto consumo de energia
Explosão a vapor	Causa transformação da lignina e solubilização da hemicelulose; baixo custo	Degradação da xilana como produto inibitório
Explosão com amônia (AFEX)	Aumenta a área de superfície acessível; remove lignina e hemicelulose não produz inibidores	Não é eficiente para biomassa com alto teor de lignina
Explosão com CO_2	Aumenta a área de superfície acessível; não produz inibidores; baixo custo	Não modifica lignina e hemiceluloses
Ozonólise	Reduz o teor de lignina; não produz resíduos tóxicos	Requer grandes quantidades de ozônio; custo elevado
Hidrólise ácida	Hidrolisa hemicelulose a xilose e outros açúcares; altera a estrutura da lignina	Custo elevado, corrosão de equipamentos, formação de substâncias tóxicas
Hidrólise alcalina	Remove hemicelulose e lignina; aumenta a área de superfície acessível	Requer longo tempo; sais formados irrecuperáveis incorporados na biomassa
Organosolv	Hidrolisa lignina e hemicelulose	Alto custo; os solventes precisam ser drenados do reator, evaporado, condensado e reciclado
Pirólise	Produz gás e líquidos	Temperatura alta; produção de cinzas
Biológico	Degrada a lignina e hemiceluloses; baixo consumo de energia	Taxa de hidrólise é muito baixa
Ultrassonicação	Aumenta a área de superfície acessível; ruptura da célula vegetal; não produz inibidores	Processo anda em estudo

Fonte: Adaptado de KARIMI et al., 2014; BHOWMICK et al., 2018

3.5 Ultrassonicação como Pré-Tratamento de Resíduos Lignocelulósicos

A ultrassonicação é uma tecnologia emergente para o pré-tratamento da biomassa lignocelulósica, que vem despertando cada vez mais interesse por ser uma alternativa viável aos métodos convencionais de pré-tratamentos. É um processo físico que apresenta resultados satisfatórios na extração de hemicelulose, celulose e lignina e na aceleração da sacarificação da biomassa lignocelulósica (SINDHU et al., 2017; BUNDHOO; MOHEE, 2018; HASSAN et al., 2018). O ultrassom é uma onda acústica mecânica dividido em três regiões: ultrassom de baixa frequência (20–100 kHz), ultrassom de alta frequência (100 kHz–1MHz) e ultrassonografia diagnóstica (1–500 MHz) (MASON, 2002; KARIMI et al., 2014).

A maioria das pesquisas tem usado uma variação de frequência entre 10 kHz a 100 kHz para pré-tratamentos onde mudanças físicas são desejadas, como a ruptura das células vegetais e degradação polimérica em biomassa lignocelulósica (REHMAN et al., 2013; LIYAKATHALI et al., 2016). À medida em que as ondas se movem pelas áreas de baixa pressão (rarefações), bolhas de gás e vapor são formadas e, subsequentemente, aumentam em tamanho até um diâmetro crítico quando implodem, criando um fenômeno conhecido como cavitação (Figura 11) (MASON, 2002). A cavitação induzida que ocorre durante a ultrassonicação resulta no colapso violento e repentino de grande número de microbolhas, o que gera uma poderosa força de cisalhamento hidromecânico no meio líquido no qual a biomassa está sendo ultrassonicada (GOGATE; KABADI, 2009; PILLI et al., 2011).

A frequência ultrassônica influencia o comportamento das bolhas de cavitação através da alteração no tempo de duração do ciclo acústico, que é curto em frequências relativamente altas (por exemplo, 2 µs para 500 kHz) e longo para baixas frequências (por exemplo, 50 µs par 20 kHz). A alta frequência não favorece a ocorrência de cavitação ativa como o tempo para o crescimento, o movimento radial e o colapso das bolhas podem ser insuficientes. Isto também leva ao rápido decaimento da energia acústica no meio líquido LUO et al., 2014).

Figura 11 – Esquema do desenvolvimento e colapso das bolhas de cavitação

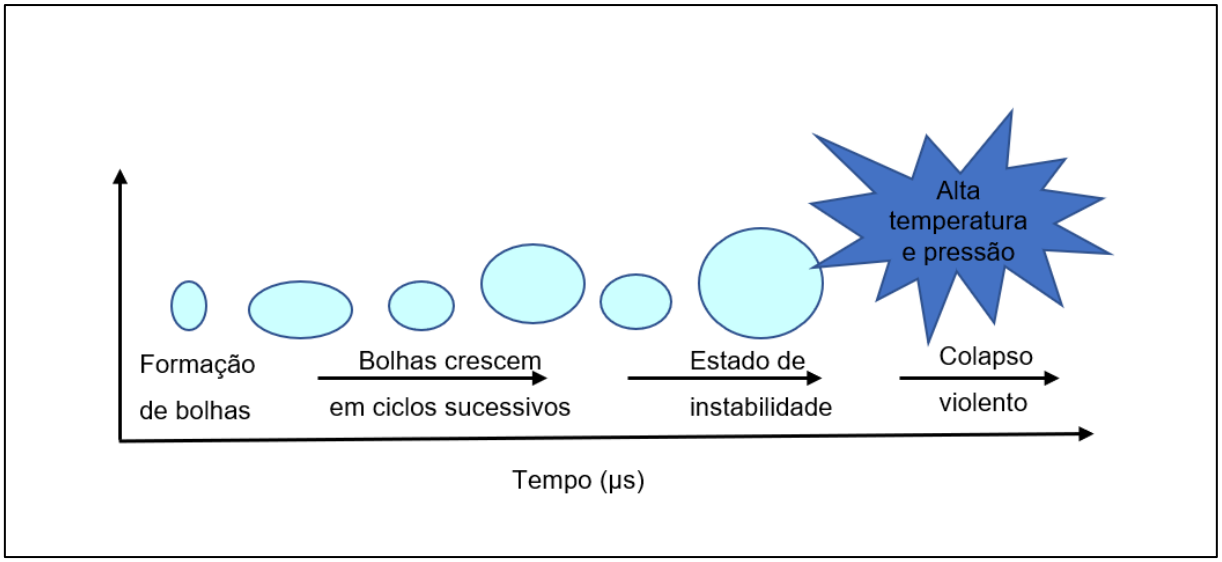

Fonte: (PILLI et al., 2011)

A ultrassonicação empregada como pré-tratamento provoca efeitos sobre a integridade estrutural das fibras lignocelulósicas, como a remoção de cera e corpos de sílica presentes em sua superfície, redução no tamanho da partícula, erosão na superfície da biomassa devido ao efeito da cavitação. Quando a energia ultrassônica é associada à reagentes ácidos ou alcalinos, pode-se potencializar a deslignificação e fracionamento da hemicelulose de materiais lignocelulósicos e destruir a cristalinidade da celulose, facilitando da sacarificação destes materiais (LUO et al., 2014).

Nos últimos anos, os métodos de pré-tratamento por hidrólise ácida ou hidrólise alcalina combinados à ultrassonicação receberam considerável atenção de grupos de pesquisadores, pois podem reduzir significativamente o tempo de pré-tratamento, facilitando a hidrólise enzimática de vários tipos de biomassa lignocelulósica, como bagaço de cana de açúcar, palha de trigo, sabugo de milho, resíduos de madeira (pó de serra) (VELMURUGAN; MUTHUKUMAR, 2011, 2012; SINGH et al., 2014; SINDHU et al., 2016, 2017; SOONTORNCHAIBOON et al., 2016; SUBHEDAR; GOGATE, 2014, 2018; WANG et al., 2018; WU et al., 2017; LUFT et al. 2018; WANG et al., 2019), no entanto, não há estudos publicados empregando a ultrassonicação combinada à hidrólise química e o bagaço de malte.

4 ARTIGO I

Potential of malt bagasse to remove lead from aqueous solution

Abstract

The agroindustrial residues have become a very promising alternative in the removal of metals from water solutions. Malt bagasse is a fibrous residue composed mainly of cellulose, hemicellulose and lignin, and its functional groups are attributed the sorption capacity of heavy metals. The objective of this study was to evaluate the potential of malt bagasse application as a bioadsorbent in the removal of Pb(II). The sorption and desorption studies were performed in batch equilibrium and the isotherm were fitted by dual-mode Langmuir–Freundlich model. The effect of contact time on the adsorption of lead by malt bagasse was also evaluated. The maximum sorption capacity obtained for malt bagasse was 19.90 mg g^{-1}. The scanning electron microscopy (SEM), energy dispersive spectrometry (EDS) and energy dispersive X-ray fluorescence (EDXRF) analyzes confirm the adsorption of lead in the malt bagasse. Low mobilization factors and high sorption efficiency (MF < 5 %, SE ≈ 95 %) indicated that malt bagasse is an interesting material to be used as a lead bioadsorbent.

Keywords: Bioadsorbent. Lignocellulosic material. Sorption. Desorption.

Introduction

Malt bagasse or brewer spent grain is a by-product of the brewing industry and it is obtained from barley and consists in the outer pericarp seed coat layer of the malted barley grain that remains after the mashing process. Malt bagasse represents 85 % of all byproducts generated by the brewing industry, being considered a lignocellulosic material, containing approximately 62 % insoluble fibers, which include 12 % cellulose, 23 % hemicellulose and 26 % lignin. Additionally, this raw material presents around 14 % proteins, and because of this it is generally used as low value animal feed (Mussatto et al., 2006; Li et al., 2009a; 2009b; Mello and Mali, 2014; Ravindran et al., 2018). However, considering its composition it can be used for industrial exploitation resulting in higher value-added products.

According to De Corato et al. (2018), it is a great challenge the transformation of complex, heterogeneous and disposable biomasses into valuable and marketable high-value added products rather than fossil sources alone, which encompasses the biorefinery concept. The main idea is to transform a disposable biomass into a wide range of marketable bio-based products and commodities using different feedstock by integrated biotechnology.

Mussatto and Roberto (2005), Mussatto et al. (2008) and Ravindran et al. (2018) reported the use of malt bagasse to obtain xylose from hemicellulose hydrolysis. Mello and Mali (2014) reported the use of malt bagasse as reinforcement agent to obtain biodegradable trays employed as food packaging. Fontana et al. (2016) investigated the potential of malt bagasse as biosorbent for the removal of textile dye from aqueous solution. Li et al. (2009a; 2009b) reported the use of modified malt bagasse to remove lead from aqueous solution.

Lignocellulosic materials are interesting materials to be used as bioadsorbent for heavy metals removal because they are inexpensive and abundantly available. In the last few years several works reported the lead removal using lignocellulosic residues, such as banana and orange peels (Annadurai et al., 2003), rice bran (Montanher et al., 2005), crop milling waste (Saeed et al., 2005), rice husk (Zulkali et al.,2006), *Rosa Canina-L* leaves (Ghasemi et al., 2014), waste biomass of hazelnut and almond shell (Pehlivan et al., 2009a), barley straw (Pehlivan et al., 2009b), cucumber peel (Basu et al., 2017), olive oil industry waste (Pretella et al., 2018), *Pinus halepensis* sawdust (Semerjian et al., 2018), coconut shell, banana peel, spent coffee grounds, eucalyptus bark (Correia et al., 2018).

The use of bioadsorbents based on lignocellulosic materials can be a relevant alternative used in heavy metals removal from aqueous media. The adsorption of toxic metals by these materials may be related to the presence of functional groups with metal-binding capacity, such

as carboxylic and hydroxylic groups in lignin and hemicellulose. Such functional groups act as binding sites or ion exchange sites for pollutants. During the extraction, electrostatic attraction between charged pollutants and functional groups of the adsorbent in the solution plays a significant role in the extraction of pollutants (Mallampati et al.; 2015; Correia et al., 2018). Considering this, pH exerts an important role in adsorption process. At pH between 5 and 6, the number of negatively charged groups on the adsorbent matrix probably increases and enhances the removal of cationic species from aqueous solutions, while in low pH values, the overall surface charge on the particles becomes positive and disfavors the approach of positively charged metal cations (Montanher et al., 2005; Ghasemi et al., 2014; Correia et al., 2018).

The objective of this study was to evaluate the potential of malt bagasse in the removal of lead from aqueous solutions aiming the application of this lignocellulosic residue as bioadsorbent. The malt bagasse was chosen because it is a biodegradable and abundant material and there are very few works reporting the use of this raw material as to its biosorption capacity for the removal of lead from aqueous solutions.

Materials and methods

Malt bagasse preparation

The malt bagasse was kindly provided by Microcervejaria Fábrica 1 (Londrina-Paraná, Brazil) and it was dried (60 °C) in an air circulation oven (Marconi MA 035 – São Paulo, Brazil) for 48 h, and milled to yield particles with 0.20 - 0.30 mm and stored. For the biosorption experiments, the material was washed with distilled water three times and dried again for 24 h at 60 °C.

Chemical composition and physico-chemical properties of malt bagasse

The chemical composition of the residue (proteins, lipids, moisture and ash) was determined according to the Association of Official Analytical Chemists (AOAC) method (2003), and the total amount of carbohydrates was determined by calculating the difference. All samples were run in triplicate. Total dietary fiber and soluble and insoluble fractions were determined according to the American Association of Cereal Chemists method (AACC method 32-07, 1990). Cellulose and hemicellulose contents were determined by the Van Soest method (1967) and lignin content was determined by the Technical Association of the Pulp and Paper

Industry method (TAPPI T222 om-88 method, 1999). Bulk density of malt bagasse was determined according to Toshiguki and Yukata (2003) and pH according to Brasil (2005).

Chemicals and metal solution preparation

All chemicals used were of analytical reagent grade (purity > 99 %). Lead nitrate II ($Pb(NO_3)_2$), sodium nitrate $NaNO_3$ and calcium nitrate $Ca(NO_3)_2$ were purchased from Merk (Darmstadt-Germany). Stock solution of Pb(II) (1000 mg L^{-1}) was prepared with Milli-Q ultrapure water (Millipore, Bedford, MA-USA) and used for further dilutions. All glassware used in the experiments was soaked in a 10 % nitric acid solution (J.T. Baker, Phillipsburg, NJ, USA) for 24 h, rinsed with Milli-Q ultrapure water (Millipore, Bedford, MA, USA) and then dry-cleaned.

Sorption and desorption experiments of lead by malt bagasse

The sorption experiments were carried out in batch with 10 mL of Pb(II) solution ranging from 20 to 200 mg L^{-1} prepared by dilution of the stock solutions, in addition to 0.1 g of malt bagasse and 0.0025 mol L^{-1} $NaNO_3$, employed as background electrolyte. Samples were shaken at 30 rpm for 24 h and 25 °C (Novatecnica, Brazil), and the pH was measured before and after sorption equilibration. After sorption equilibrium suspensions were centrifuged at 4000 rpm for 10 min and filtered through 0.22 µm cellulose ester membranes (Millipore, USA). All the experiments were performed in triplicate and the results expressed as average values. Then, the supernatant was collected into polyethylene vials and the residual solid was dried at 40 °C for further characterization. Lead ion concentration was determined using flame atomic absorption spectroscopy – FAAS (AA-140 Varian, CA, USA). The AA-140 was equipped with a deuterium lamp background correction and a multielement hollow cathode lamp (Al/Ca) operating at 10.0 mA and 427.7 nm for lead analysis. The flow rate was 4.50 and 3.50 L min^{-1} for acetylene and N_2O, respectively. The solid fractions were dried at 105 °C and analyzed by Energy dispersive X-Ray fluorescence (EDXRF), Fourier transform-infrared spectroscopy (FT-IR), Scanning electron microscopy (SEM) and energy dispersive spectrometry (EDS).

Desorption tests were carried out from the highest initial sorption concentration (200 mg L^{-1}) in ten sequential dilutions and 24 h for equilibrium. At each desorption step (N) the 5.0 mL taken from the liquid phase, for lead ion quantitation and pH measurement, were exchanged

by the same volume of 0.1 mol L^{-1} $Ca(NO_3)_2$ (Merck, Darmstadt, Germany). The other experimental conditions and procedures were similar to those described for the sorption case.

Calculating sorption-desorption adjustable parameters

The initial concentration (C_i, mg L^{-1}) and equilibrium concentration (Ceq, mg L^{-1}) were quantified by FAAS (AA-140 Varian, CA, USA). The sorbed concentration ($C_{sorb,}$ mg g^{-1}) was calculated considering sorbent mass (m in g) and volume (V in L), according to Equation (1):

$$C_{sorb} = (C_i - C_{eq})\frac{V}{m} \quad (1)$$

The sorption distribution coefficient (K_d, L mg^{-1}) and sorption efficiency indicate the capability of a material to retain a solute and the extent of solute movement to the liquid phase, and can be calculated by the ratio C_{sorb}:C_{eq} (Equation 2) and the relation by difference between initial and equilibrium concentration, respectively:

$$K_d = \frac{C_{sorb}}{C_{eq}} \quad (2)$$

The lead ion remaining in the samples after N desorption steps ($C_{sorb,\ D(N)}$) was determined according to Equation (3), as shown by Galunin et al. (2014).

$$C_{sorb,D(N)} = C_{i,D(N-1)} - C_{i,D(N)} - C_{eq,D(N)})\frac{V}{m} \quad (3)$$

where $C_{i,D(N)}$= 0.5 $C_{i,D(N-1)}$ and $C_{i,D(N-1)}$ are the sorbate initial concentration in the solution at each step N and previous step N − 1, respectively; $C_{eq,D(N)}$ (mg L^{-1}) is the equilibrium concentration at each step N (mg L^{-1}).

The Langmuir-Freundlich dual isotherm model (Sips, 1950) was employed to predict adsorption and desorption behavior (Equation 4).

$$C_{sorb} = \frac{b_1(k_1 Ceq)^{n1}}{1+(k_1 Ceq)^{n1}} + \frac{b_2(k_2 Ceq)^{n2}}{1+(k_2 Ceq)^{n2}} \quad (4)$$

where K_1 and K_2 are the bonding energies associated with a pH-dependent equilibrium constant (L mg^{-1}); b_1 and b_2 are the maximum sorption capacity determined by the reactive surface sites in an ideal monolayer system (mg g^{-1}); n_1 and n_2 are dimensionless parameters and inform on the heterogeneity of sorption sites; the indices 1 and 2 stand for two different types of sorption sites (Galunin et al., 2004).

Hysteresis index (HI) and mobilization factor (MF)

After the biosorbent have achieved its maximum sorption capacity, the solid phase can continue to hold the sorbed metal or release it back to the liquid phase by desorption process. Non-coincidence of sorption and desorption isotherms as a result of the difference between forces involved in these processes is called hysteresis (Essington, 2004). However, the use of such sorption parameters just leads to interpretation of the mean or even point values instead of carrying out integrated evaluation. The HI varies from 0 to 1, from minimum to maximum desorption, or from 0 to1, from minimum to maximum sorption capacity, depending on whether desorption isotherm is below or above the respective sorption isotherm. To assess the lead mobility or the sorption reversibility, the Hysteresis Index (HI) was determined by Equation (5) (Galunin et al. 2014), considering the areas of the sorption (A) and desorption (A_D) isotherms constructed by applying the Langmuir–Freundlich dual model.

$$HI = \frac{A - A_D}{A_D} \tag{5}$$

Mobilization factor (MF) is a parameter to indicate the sorbate mobilization from the solid to the liquid phase. The parameter estimated by Equation (6) is related to the hysteresis index (HI) and the normalization factor (B), which considers an ideal desorption area A_{Di}, presented in Equation (7) (Constantino et al., 2017).

$$MF = (1 - HI).B \tag{6}$$

$$B = abs(1 - A_D/A_{Di}) \tag{7}$$

Effect of contact time on sorption of lead by malt bagasse

The kinetics experiments were performed using 10.0 mL of 20 mg L^{-1} Pb(II) prepared by dilution of the stock solutions; 0.1 g of malt bagasse and 0.0025 mol L^{-1} $NaNO_3$ were employed as background electrolyte. Samples were shaken at 30 rpm and 25 °C (Novatecnica, Brazil), collected at different contact times, centrifuged at 4000 rpm for 10 min and filtered through 0.22 µm cellulose ester membranes (Millipore, USA). The pH was measured before and after the sorption experiment. All the experiments were performed in triplicate and the results expressed as mean values. Lead concentration was determined by AA-140 FAAS (Varian, CA, USA).

Energy dispersive X-Ray fluorescence (EDXRF)

EDXRF analysis were carried out in an EDX-720 spectrometer (Shimadzu, Kyoto, Japan), with Rh anode X-Ray tube and Si(Li) detector. The measures were performed ranging from sodium to uranium, using two channels: Ti–U at 50 kV, 13 µA and Na–Sc at 15 kV, 202 µA for100 s, with collimation incident beam of 10 mm, using sample supports of polyester thin-film 2.5" and 63.5 mm diameter (Chemplex, Palm City, USA).

Fourier transform-infrared spectroscopy (FT-IR)

For this analysis, the samples were finely powdered (particles < 0.18 mm) and mixed with potassium bromide and compressed into tablets. The FT-IR analyses were carried out in a Shimadzu FT-IR-8300 (Japan), with spectral resolution of 4 cm^{-1} and spectral range of 4000-500 cm^{-1}.

Scanning electron microscopy (SEM) and energy dispersive spectrometry (EDS)

SEM/EDS analyses were performed with a FEI Quanta 200 microscope (Oregon, USA). The dried samples were mounted for visualization on bronze stubs using double-sided tape. The surfaces were then coated with a thin gold layer (40–50 nm). All samples were examined using an accelerating voltage of 30 kV. The EDS analyses were performed before and after sorption experiments in order to identify the presence of lead onto malt bagasse surface.

Data analysis

The sorption and desorption isotherm data were obtained by implementing the *cftool* (Interactive Environment for Fitting Curves to One-Dimensional Data) from MatLab 9.1™ (The MathWorks, Inc., R2016b) software. Fitting coefficients were constrained by positive values of ≥ 95 % confidence limits and calculated by the non-linear least square method using the Trust-region algorithm. The kinetics was analyzed using analysis of variance (ANOVA) and Tukey's mean comparison test ($p \leq 0.05$) were performed with Statistica software version 7.0 (Statsoft, Oklahoma, USA).

Results and Discussion

Chemical composition and physico-chemical properties of malt bagasse

The chemical composition of malt bagasse used in this study is presented in Table 1. The results were very close to the results reported by Mello and Mali (2014), who determined a composition of 12.29 % cellulose, 23.41 % hemicellulose and 26.41 % lignin. Ravindran et al. (2018) reported that malt bagasse contains approximately 19.21 % cellulose, 26.94 % hemicellulose and 30.48 % lignin, values that were in accordance with our results, except for cellulose, which herein presented a lower content.

Considering its composition, malt bagasse can be considered a raw material with great potential to be used as bioadsorbent. Its high hemicelluloses and lignin content are interesting characteristics, because the metal sorption mechanism of lignocellulosic materials are mainly related to the presence of carboxyl and hydroxyl groups in lignin and hemicellulose, which can act as binding sites or ion exchange sites for heavy metals.

Table 1 – Chemical composition, pH, apparent density and particle size of malt bagasse

Component/Property	Result
Moisture (g/100 g)	4.04 ± 0.49
Ash (g/100 g)	4.11 ± 0.49
Lipid (g/100 g)	9.10 ± 0.35
Protein (g/100 g)	20.60 ± 0.0.84
Carbohydrates	62.14 ± 0.34
Total dietary fiber	61.80 ± 0.60
Soluble dietary fiber	1.01 ± 0.10
Insoluble dietary fiber	60.80 ± 0.32
Cellulose	8.66 ± 1.02
Hemicellulose	26.76 ± 1.89
Lignin	25.38 ± 3.15
pH	6.05 ± 0.05
Apparent density (g/cm^3)	0.478 ± 0.002
Particle size (mm)	0.20 – 0.30

Lead sorption and desorption isotherm fitting by Langmuir–Freundlich dual model

In this study the pH values during sorption tests ranged from 4.79 (lead concentration of 200 mg L^{-1}) to 5.88 (lead concentration of 20 mg L^{-1}), and it ranged from 5.47 to 6.27 (lead concentration of 200 mg L^{-1}) during desorption tests. pH governs heavy metals sorption phenomenon by influencing surface charge of the sorbent besides controlling other factors like metal speciation, sequestration and mobility (Basu et al., 2017). Several authors working with lignocellulosic biomass as adsorbents for lead reported biomass surface charge progressively more negative with pH increasing, as a result of deprotonation of functional groups of the biomass, such as carboxyl and hydroxyl groups on the adsorbent surface; the deprotonated groups act as easily accessible binding sites to metal ions in sorption. Thus, the adsorption of lead in the acidic medium is low, and studies revealed that optimized value for biosorption of lead in lignocellulosic biomass materials is found around pH 5 - 6 (Montanher et al., 2005; Saeed et al., 2005; Zulkali et al., 2006; Pehluvan et al., 2009a; Ghasemi et al., 2014; Abbaszadeh

et al., 2016; Basu et al., 2017). Thus, in our work the pH remained in a range close to the optimum for sorption of lead.

The study of metal ions adsorption process on the adsorbents is a very important protocol to understand their adsorption mechanism, including the understanding of how the adsorbed ions were distributed at the adsorbent interfaces (Negm et al., 2018). Lead sorption and desorption isotherms are presented in Figure 1. The sorption isotherm presented concave shape and two plateaus and can be classified as type S4 according to Giles et al. (1974) indicating that the initial sorption is low and increases with the number of sorbed molecules and suggests the existence of at least two sorts of sorption sites for malt bagasse.

Figure 1 – Lead sorption and desorption isotherms by Langmuir–Freundlich dual model

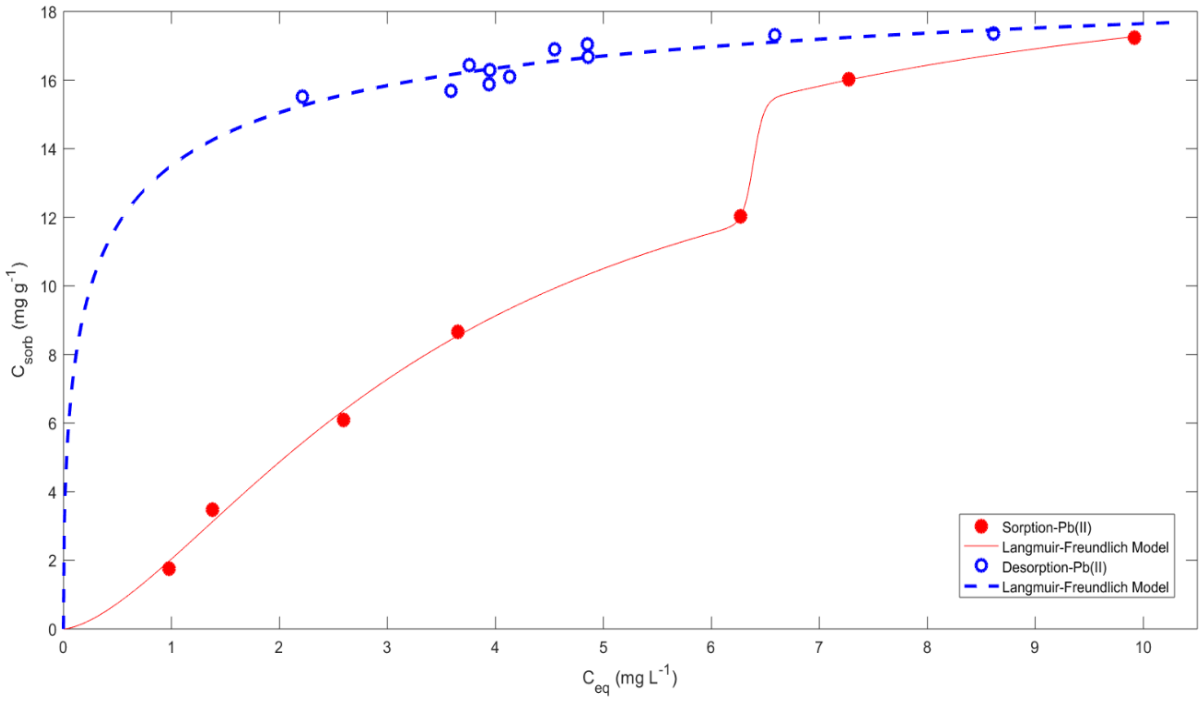

To achieve a better understand of the adsorption process, it was necessary to correlate the equilibrium adsorption data to an isotherm model. Among the employed models to heavy metal sorption studies, Langmuir and Freundlich models have been widely employed. The Langmuir isotherm is the simplest theoretical model that can be used to describe monolayer adsorption. In its derivation, Langmuir isotherm refers to homogeneous adsorption, in which all sites possess equal affinity for the adsorbate. It is an empirical model and assumes that adsorption can only occur at a finite number of definite localized sites, which are identical and equivalent, with no transmigration of adsorbate in the plane surface. Considering Langmuir

model, once a site is filled, no further sorption can take place at that site, indicating that its surface reached to a saturation point (Langmuir, 1916; 1918).

The Freundlich isotherm model is based on adsorption on a heterogeneous surface, not restricted to the formation of monolayer. This model considers multilayer sorption, with non-uniform distribution of sorption heat and affinities over the heterogeneous surface (Freundlich, 1906). Recently, Freundlich isotherm was criticized because it is suitable for use with heterogeneous surfaces but can describe adsorption data over a restricted range only, especially at high and intermediate concentrations, and it may provide a poor fit to data at low concentrations (Ng et al., 2002; Foo; Hameed, 2010).

The Langmuir-Freundlich dual isotherm model can predict adsorption in heterogeneous systems circumventing limitations of Langmuir and Freundlich isotherm models. At low adsorbate concentrations, it reduces to Freundlich isotherm; while at high concentrations, it predicts a monolayer adsorption capacity characteristic of the Langmuir isotherm (Foo and Hameed, 2010). It can describe sorption binding interactions among sorbing compounds considering sorption sites with different affinities (Galunin et al., 2014; Constantino et al., 2017).

Considering the complex composition and structural arrangement of malt bagasse in our study, the dual mode Langmuir-Freundlich model was employed to fit the isotherms experimental data, and the adjustable parameters are presented in Table 2. It can be observed that the correlation coefficient (R^2) was 0.9988, demonstrating the validity of the employed adsorption model in explaining the adsorption process mechanism studied in this work. According Huang and Li (2013), when the dual mode Langmuir-Freundlich model fit to the equilibrium experimental data this is an indicating that both physical and chemical adsorption took place simultaneously. This model was useful to discriminate 2 types of sorption sites, which can be associated with high and low-affinity sites, respectively.

K_1 and K_2 are the bonding energies associated with a pH-dependent equilibrium constant, and the indices 1 and 2 are related to the two types of sorption sites. According to Galunin et al. (2014), low K_1 and K_2 values are indicative of a low-energy character for all the sorption sites, and in our work both K_1 and K_2 values were low (Table 2), confirming the low-energy character for all the sorption sites. K_2 value (0.2888) was higher than K_1 (0.1565), indicating that the higher value was related to a higher-affinity between this group of sorption sites with the sorbate.

The parameters b_1 and b_2 are the maximum sorption capacity determined by the reactive surface sites in an ideal monolayer system, and the sum of b_1 and b_2 (19.90 mg g^{-1}) indicate the maximum sorption capacity of malt bagasse (Table 2).

Table 2 - Isotherm parameters for the adsorption and desorption of Pb(II) on malt bagasse calculated from Langmuir–Freundlich dual model, determination coefficient of the model *(R^2);* root mean square error *(RMSE),* hysteresis index *(HI)* and mobilization factor *(MF)*

Parameter	Adsorption	Parameter	Desorption
K_1 (L mg^{-1})	0.1565	K_{1d} (L mg^{-1})	3.018
K_2 (L mg^{-1})	0.2888	K_{2d} (L mg^{-1})	406.1
b_1 (mg g^{-1})	3.50	b_{1d} (mg g^{-1})	18.61
b_2 (mg g^{-1})	16.40	b_{2d} (mg g^{-1})	1.47
n_1	134.2	n_{1d}	0.557
n_2	1.572	n_{2d}	0.558
R^2	0.9988	R^2	0.8815
RMSE	0.5198	*RMSE*	0.4367
MF	0.0498		
HI	0.3552		

K_i (L mg^{-1}): constants related to the sorbate-sorbent affinity parameter; b_i (mg g^{-1}): sorption capacity; n_i: heterogeneity of the sorption sites

The parameters n_1 and n_2 inform on the heterogeneity of sorption sites (Galunin et al., 2014). The value of n can be used as an empirical coefficient, representing the type and extent of cooperativity present in the binding interaction, and also indicating the degree of nonlinearity between solution concentration and adsorption; if $n = 1$, then adsorption is linear, but when $n > 1$, positive cooperativity is suggested, while when $0 < n < 1$ negative cooperativity in the binding process is indicated (Praus; Turicová, 2007; Dada et al., 2012; Desta, 2013). In our work n_1 and n_2 were 134.2 and 1.572, respectively (Table 2), and for both adsorption sites it can be supposed that they exhibited positive cooperativity for the lead sorption process. According to Galunin et al. (2014), the greater n value generally corresponds to the lower sorption capacity, and the lower one to the higher capacity, and considering our results, it can be inferred that sorption

sites corresponding to n_2 had a more favorable sorption process, which are consistent to the higher K_2 and b_2 values compared to K_1 and b_1, respectively, confirming that the sorption sites corresponding to b_2 had higher affinity for lead (Table 2). The sorption efficiencies were shown in Table 3, and it can be observed that while sorption efficiency (SE) ranged from 94.73 to 94.55 % for the minimum and maximum lead concentration.

The low value found for the mobilization factor (0.0498 %) and the positive *HI* value (0.3552), suggest very low lead desorption from malt bagasse (Table 2). The poor recovery may be related to the pH range (5.47 to 6.27) during desorption tests, which not favored the desorption of lead from malt bagasse surface; in this pH range, the functional groups were deprotonated and the bound metal ions found it difficult to be released from the bioadsorbent.

Table 3 – Sorption efficiencies at different lead concentrations

Lead concentration (mg L^{-1})	Sorption efficiency (*SE*) (%)
20	94.73
40	96.18
80	95.91
100	95.96
140	95.04
180	95.66
200	94.55

Effect of contact time on adsorption of lead by malt bagasse

According to Ghasemi et al. (2014), the equilibrium time is a very important parameter on the development of wastewater treatment systems. The effect of contact time on the adsorption of lead is presented in Figure 2, and it can be observed that after 30 min 90 % of lead was adsorbed and the equilibrium was established after 60 min. According to Ghasemi et al. (2014), the fast adsorption of lead at the initial stages possibly occurs because the availability of the uncovered surface and active sites on the surface of adsorbents, and with increasing time, the number of free adsorption sites decreases and the adsorption became slow.

Figure 2 – Effect of contact time on adsorption of lead by malt bagasse

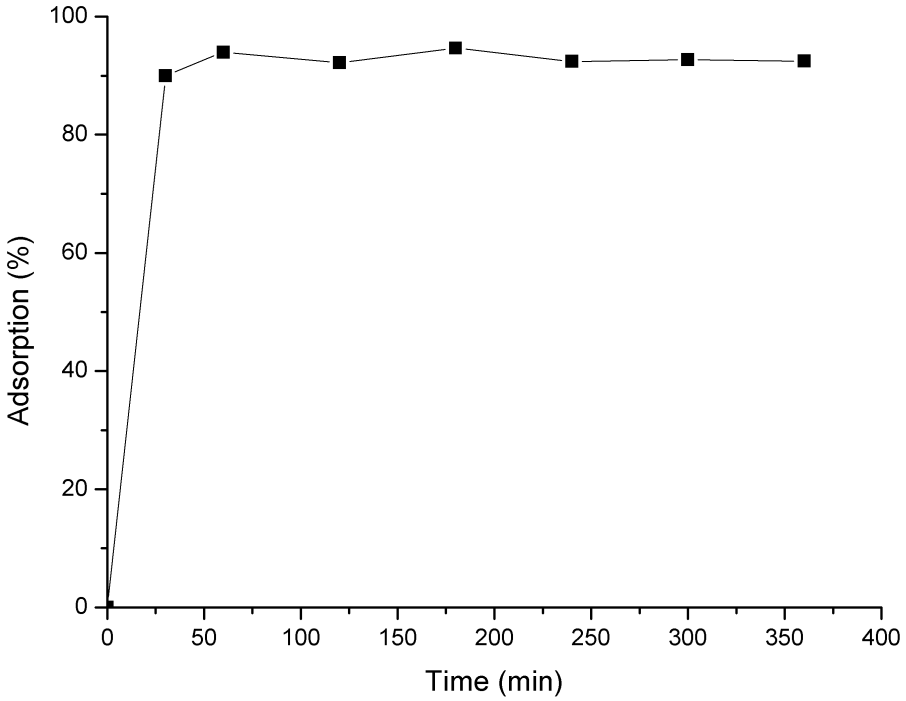

Energy dispersive X-Ray fluorescence (EDXRF)

In Figure 3 it can be observed the EDXRF spectra for raw malt bagasse and malt bagasse after being submitted to sorption and desorption tests. Samples of malt bagasse submitted to sorption tests showed significant lead emission peaks at 10.52 and 12.61 kVe (Ayawei et al., 2015), while after desorption tests the peaks decreased but remained present in the sample, confirming the lower desorption efficiency of malt bagasse observed in desorption tests.

Figure 3 – EDXRF of raw malt bagasse and malt bagasse after being submitted to sorption and desorption tests with 200 mg L^{-1} Pb(II)

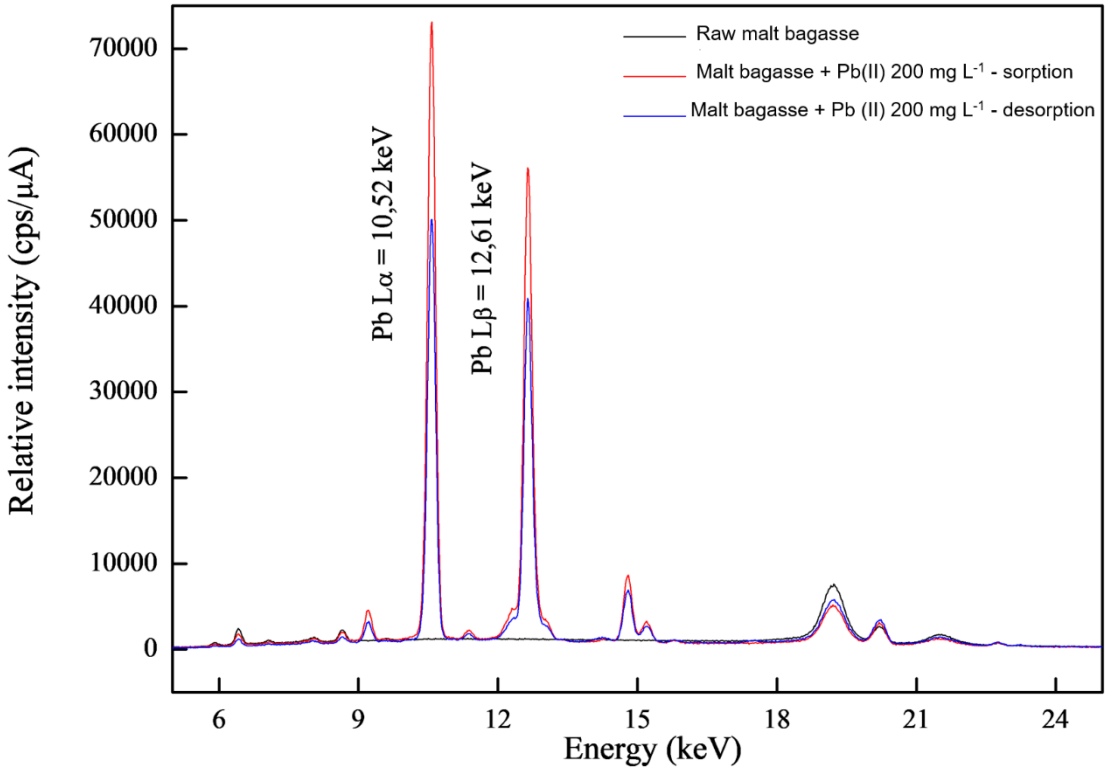

Fourier transform-infrared spectroscopy (FT-IR)

In Figure 4 it can be observed the FTIR spectra for raw malt bagasse and malt bagasse after being submitted to sorption tests with 20 and 200 mg L^{-1} of lead. All spectra showed wide absorption bands at approximately 3600-3250 cm^{-1}, corresponding to axial deformations of the OH functional groups and the vibrations of H bound to the OH groups. This band was reallocated after lead adsorption, indicating the participation of hydroxyl and amino groups in the metal sorption process.

Figure 4 – FTIR of raw malt bagasse and malt bagasse after being submitted to sorption tests with 20 and 200 mg L^{-1} Pb(II)

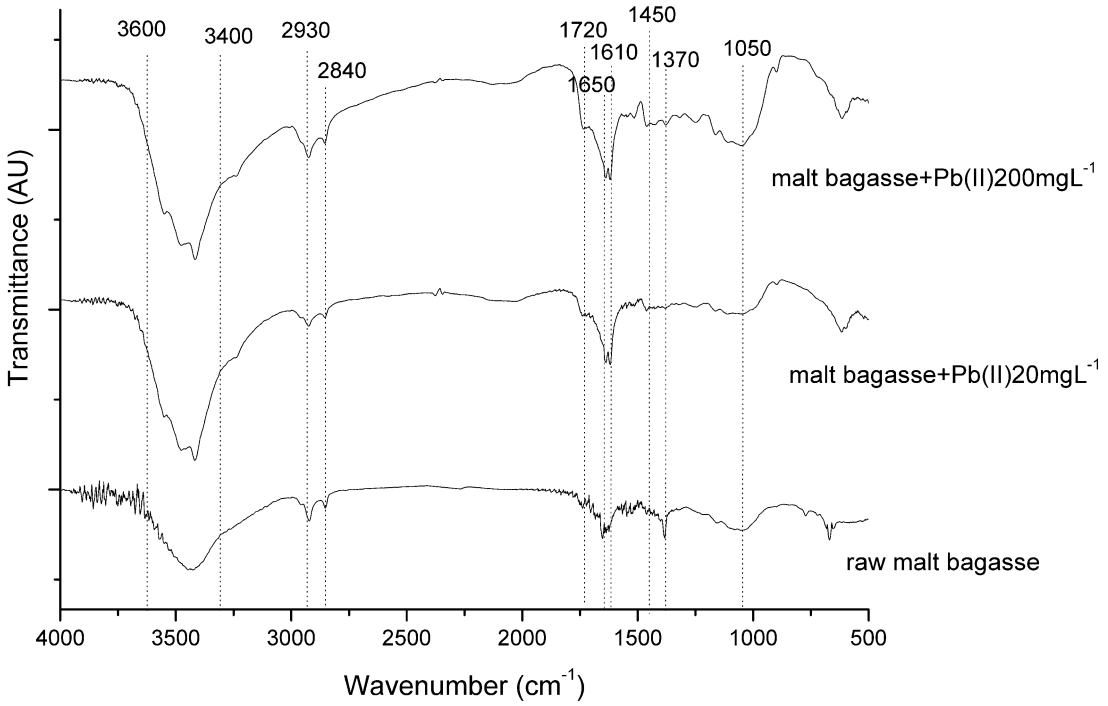

The bands observed at 2930 cm^{-1} and 2480 cm^{-1} were attributed to –C-H stretching, H-C-H and –C-O-H-conjugated bending vibrations and appeared in all spectra (Figure 4). In all spectra a small band at 1720 cm^{-1} appeared corresponding to deformation of the carbonyl functional of C=O bond in carboxyl acids, present in hemicelluloses and lignin (Correia et al., 2018; Montanher et al., 2005).

Two small bands were observed at approximately 1610 and 1650 cm^{-1} for all samples, and these values are associated with the angular O–H bending of water molecules. Sun et al. (2004) reported that bands at approximately 1600-1650 cm^{-1} may result from water, but it could also be attributed to the aromatic C=C stretch of the aromatic ring in the lignin.

Small bands observed around 1450 cm^{-1} and 1370 cm^{-1} (Figure 4) can be attributed to carboxylate groups (Montanher et al., 2005) and to both C-O stretching and O-H deformation of carboxylic acids (Basu et al., 2017), respectively. All spectra presented bands around 1050 cm^{-1} corresponding to the linear and branched (1→4)-β-xylans, which are characteristic of hemicelluloses (Kakurácová et al., 2000). According to Montanher et al. (2005) bands at around

1030 cm^{-1} the can be assigned to phosphate and silicate groups, which appeared in EDS analysis of raw malt bagasse before and after sorption tests (Figure 5e and 5f).

The FTIR spectra obtained for malt bagasse in this work agreed with reports of other authors studying malt bagasse (Jacometti et al., 2015) and other lignocellulosic residues (Monthanher et al., 2005; Basu et al., 2017). In all FTIR spectra it was possible to identify some ionisable functional groups of malt bagasse, and it is important because the adsorption of toxic metals by lignocellulosic biomass is related to the presence of functional groups with metal-binding capacity, such as carboxylic and hydroxylic groups (Montanher et al., 2005; ; Ghasemi et al., 2014; Correia et al., 2018).

Scanning electron microscopy (SEM) and energy dispersive spectrometry (EDS)

SEM is widely used to study the morphological and surface characteristics of the adsorbent materials. Figures 4a and 4b show SEM micrographs of the raw malt bagasse in comparison with malt bagasse after being submitted to sorption tests with 200 mg L^{-1} lead (Figures 5 c and 5d). Raw malt bagasse showed a typical morphology of lignocellulosic materials, with the original fibers bundled with the nonfibrous components (hemicellulose and lignin), which formed a compact structure with an outer layer covering the material surface (Figure 5a). According to Fung et al. (2010), lignocellulosic materials in their native state contain waxes and other encrusting substances such as hemicellulose, lignin, and pectin that form a thick and smooth outer layer. In Figure 5b it can be seen an image from the cross-section of raw malt bagasse, and several pores and cavities were observed, and they can increase the contact area and facilitate pore diffusion during adsorption (Li et al., 2009a; Tay et al., 2009; Anirudhan; Sreekumari, 2011).

Figure 5 – SEM image of raw malt bagasse (a) surface and (b) cross-section; (c) and (d) malt bagasse surface after being submitted to sorption tests with 200 mg L^{-1} Pb(II); (e) EDS pattern of raw malt bagasse and (f) EDS pattern of malt bagasse after being submitted to sorption tests with 200 mg L^{-1} Pb(II)

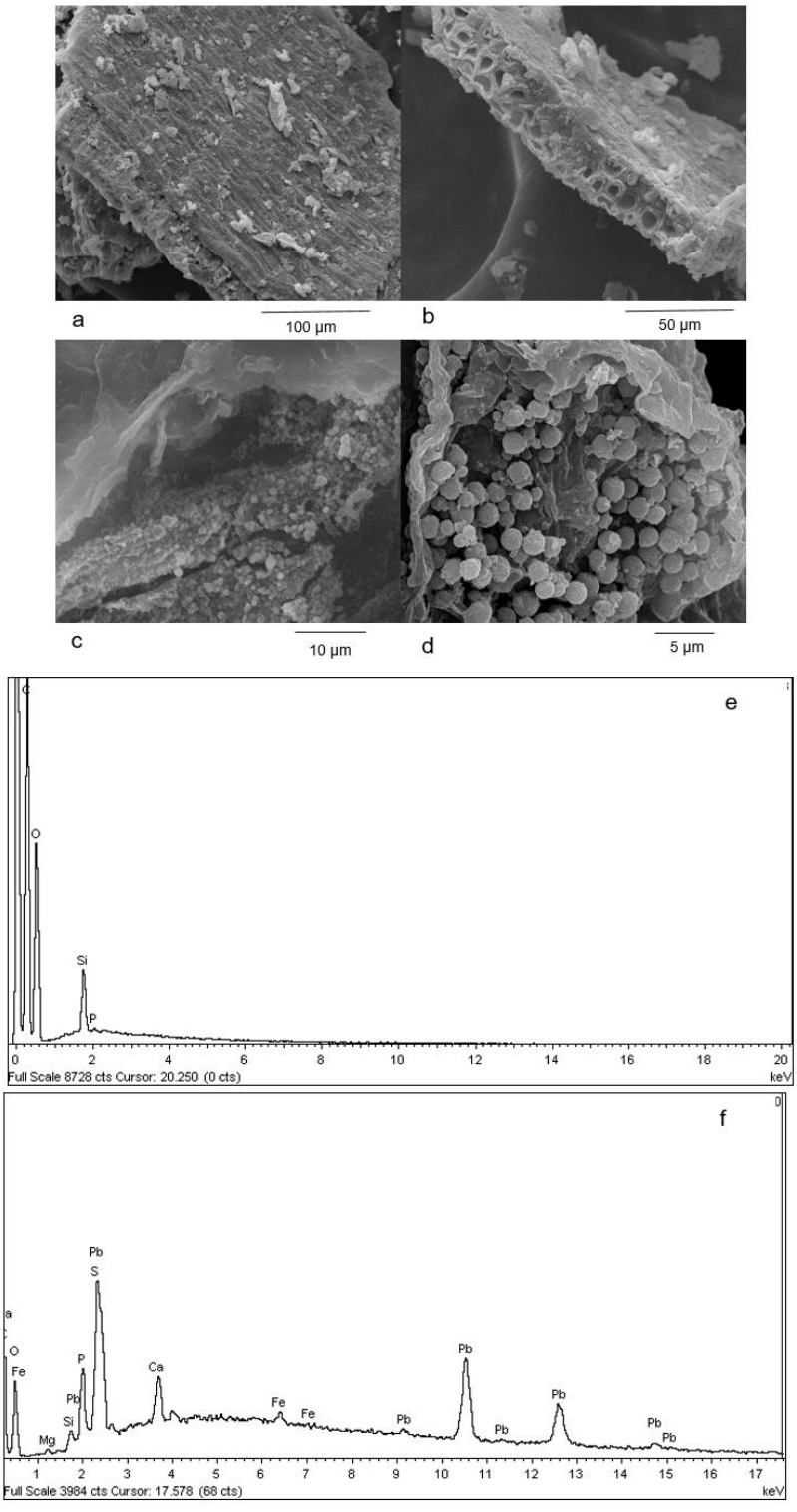

In Figure 5c and 5d a large amount of spherical particles with diameters ranging from 0.5 to 1.5 μm appear adhered to the malt bagasse surface, due to the material heterogeneity. In EDS pattern (Figure 5e and 5f) of malt bagasse before and after being submitted to sorption tests, the successful lead adsorption onto malt bagasse is marked.

Conclusions

This lignocellulosic residue was able to successfully sorb lead ions from aqueous solutions up to 90 % of lead removal after 30 min and equilibrium after 60 min. Langmuir-Freundlich dual model was successfully employed to fit the isotherms indicating high and low-affinity sites. Malt bagasse can be considered an effective and environmental-friendly material to be used as bioadsorbent for lead removal.

Reference

AACC e American Association of Cereal Chemists. (1990). Approved methods of the American association of cereal chemists. St. Paul MN: AACC.

Abbaszadeh, S., Alwi, S. R. W., Webb, C., Ghasemi, N., Muhamad, I. I. (2016). Treatment of lead-contaminated water using activated carbon adsorbent from locally available papaya peel biowaste. Journal of Cleaner Production, 118, 210-222.

Anirudhan, T. S., & Sreekumari, S. S. (2011). Adsorptive removal of heavy metal ions from industrial effluents using activated carbon derived from waste coconut buttons. Journal of Environmental Sciences, 23(12), 1989-1998.

Annadurai, G., Juang, R. S., & Lee, D. J. (2003). Adsorption of heavy metals from water using banana and orange peels. Water Science and Technology, 47(1), 185-190.

AOAC (2003). Official Methods of Analysis. 14th ed. Washington, USA: Ass. Off. Analytical Chemistry.

Ayawei, N., Ekubo, A. T., Wankasi, D., & Dikio, E. D. (2015). Equilibrium, Thermodynamic and Kinetic Studies of the Adsorption of Lead (II) on Ni/Fe Layered Double Hydroxide. Asian Journal of Applied Sciences (ISSN: 2321–0893), 3(02), 207-217.

Basu, M., Guha, A. K., Ray, L. (2017). Adsorption of lead on cucumber peel. Journal of cleaner production, 151, 603-615.

Brasil (2005) Leis, decretos, etc. Instrução Normativa nº 13 de 29 de junho de 2005. Diário Oficial da União. Brasília.

Chen, X., & Chen, B. (2015). Macroscopic and spectroscopic investigations of the adsorption of nitroaromatic compounds on graphene oxide, reduced graphene oxide, and graphene nanosheets. Environmental science & technology, 49(10), 6181-6189.

Constantino, L. V., Quirino, J. N., Monteiro, A. M., Abrão, T., Parreira, P. S., Urbano, A., Santos, M. J. (2017). Sorption and desorption of silver ions by bentonite clays. Environmental Science and Pollution Research, 24(12), 11349-11359.

Correia, I. K.S., Santos, P. F., Santana, C. S., Neris, J. B., Luzardo, F. H.Velasco, F. G. (2018). Application of coconut shell, banana peel, spent coffee grounds, eucalyptus bark, piassava (*Attalea funifera*) and water hyacinth (*Eichornia crassipes*) in the adsorption of Pb^{2+} and Ni^{2+} ions in water. Journal of Environmental Chemical Engineering, 6(2), 2319-2334.

Dada, A. O., Olalekan, A. P., Olatunya, A. M., Dada, O. (2012). Langmuir, Freundlich, Temkin and Dubinin–Radushkevich isotherms studies of equilibrium sorption of Zn^{2+} unto phosphoric acid modified rice husk. IOSR Journal of Applied Chemistry, 3(1), 38-45.

De Corato, U., De Bari, I., Viola, E., Pugliese, M. (2018). Assessing the main opportunities of integrated biorefining from agro-bioenergy co/by-products and agroindustrial residues into high-value added products associated to some emerging markets: A review. Renewable and Sustainable Energy Reviews, 88, 326-346.

Desta, M. B. (2013). Batch sorption experiments: Langmuir and Freundlich isotherm studies for the adsorption of textile metal ions onto teff straw (Eragrostis tef) agricultural waste. Journal of thermodynamics, 2013.

Essington, M.E., (2004). Soil and Water Chemistry: an Integrative Approach. CRC Press, Berlin.

Fontana, K. B., Chaves, E. S., Sanchez, J. D., Watanabe, E. R., Pietrobelli, J. M., & Lenzi, G. G. (2016). Textile dye removal from aqueous solutions by malt bagasse: isotherm, kinetic and thermodynamic studies. Ecotoxicology and environmental safety, 124, 329-336.

Foo, K. Y., & Hameed, B. H. (2010). Insights into the modeling of adsorption isotherm systems. Chemical engineering journal, 156(1), 2-10.

Freundlich HMF. Over the adsorption in solution. J Phys Chem. (1906) 57:385-471.

Fung, W. Y., Yuen, K. H., & Liong, M. T. (2010). Characterization of fibrous residues from agrowastes and the production of nanofibers. Journal of agricultural and food chemistry, 58(13), 8077-8084.

Galunin, E., Ferreti, J., Zapelini, I., Vieira, I., Tarley, C. R. T., Abrão, T., Santos, M. J. (2014). Cadmium mobility in sediments and soils from a coal mining area on Tibagi River watershed: Environmental risk assessment. Journal of hazardous materials, 265, 280-287.

Ghasemi, M., Naushad, M., Ghasemi, N., Khosravi-Fard, Y. (2014). Adsorption of Pb (II) from aqueous solution using new adsorbents prepared from agricultural waste: adsorption isotherm and kinetic studies. Journal of Industrial and Engineering Chemistry, 20(4), 2193-2199.

Giles, C.H., Smith, D., Huitson, A. (1974). A general treatment and classification of the solute adsorption isotherm. I: Theoretical. J. Colloid Interface Sci. 47, 755–765.

Huang, W., Liu, Z. M. (2013). Biosorption of Cd (II)/Pb (II) from aqueous solution by biosurfactant-producing bacteria: isotherm kinetic characteristic and mechanism studies. Colloids and Surfaces B: Biointerfaces, 105, 113-119.

Jacometti, G. A., Mello, L. R., Nascimento, P. H., Sueiro, A. C., Yamashita, F., & Mali, S. (2015). The physicochemical properties of fibrous residues from the agro industry. LWT-Food Science and Technology, 62(1), 138-143.

Kacurakova, M., Capek, P., Sasinkova, V., Wellner, N., & Ebringerova, A. (2000). FT-IR study of plant cell wall model compounds: pectic polysaccharides and hemicelluloses. Carbohydrate polymers, 43(2), 195-203.

Li, Q. Z., Chai, L. Y., Jing, Z. H. A. O., Yang, Z. H., & Wang, Q. W. (2009a). Lead desorption from modified spent grain. Transactions of Nonferrous Metals Society of China, 19(5), 1371-1376.

Li, Q., Chai, L., Yang, Z., & Wang, Q. (2009b). Kinetics and thermodynamics of Pb(II) adsorption onto modified spent grain from aqueous solutions. Applied surface science, 255(7), 4298-4303.

Langmuir I. The constitution and fundamental properties of solids and liquids. J Am Chem Soc. (1916). 38(11):2221-2295.

Langmuir I. The adsorption of gases on planes of glassmica andplatinium. J Am Chem Soc. (1918). 40:1361-1403.

Mallampati, R., Xuanjun, L., Adin, A., & Valiyaveettil, S. (2015). Fruit peels as efficient renewable adsorbents for removal of dissolved heavy metals and dyes from water. ACS Sustainable Chemistry & Engineering, 3(6), 1117-1124.

Mello, L. R., Mali, S. (2014). Use of malt bagasse to produce biodegradable baked foams made from cassava starch. Industrial Crops and Products, 55, 187-193.

Montanher, S. F., Oliveira, E. A., & Rollemberg, M. C. (2005). Removal of metal ions from aqueous solutions by sorption onto rice bran. Journal of Hazardous Materials, 117(2-3), 207-211.

Mussatto, S. I., Roberto, I. C. (2005). Acid hydrolysis and fermentation of brewer's spent grain to produce xylitol. Journal of the Science of Food and Agriculture, 85(14), 2453-2460.

Mussatto, S. I., Fernandes, M., Milagres, A. M., & Roberto, I. C. (2008). Effect of hemicellulose and lignin on enzymatic hydrolysis of cellulose from brewer's spent grain. Enzyme and Microbial Technology, 43(2), 124-129.

Negm, N. A., El Wahed, M. G. A., Hassan, A. R. A., & Kana, M. T. A. (2018). Feasibility of metal adsorption using brown algae and fungi: Effect of biosorbents structure on adsorption isotherm and kinetics. Journal of Molecular Liquids, 264, 292-305.

Ng, C., Losso, J. N., Marshall, W. E., & Rao, R. M. (2002). Freundlich adsorption isotherms of agricultural by-product-based powdered activated carbons in a geosmin–water system. Bioresource technology, 85(2), 131-135.

Pehlivan, E., Altun, T., Cetin, S., & Bhanger, M. I. (2009a). Lead sorption by waste biomass of hazelnut and almond shell. Journal of hazardous materials, 167(1-3), 1203-1208.

Pehlivan, E., Altun, T., & Parlayıcı, S. (2009b). Utilization of barley straws as biosorbents for Cu2+ and Pb2+ ions. Journal of hazardous materials, 164(2-3), 982-986.

Praus, P., Turicová, M. (2007). A physico-chemical study of the cationic surfactants adsorption on montmorillonite. Journal of the Brazilian Chemical Society, 18(2), 378-383.

Petrella, A., Spasiano, D., Acquafredda, P., De Vietro, N., Ranieri, E., Cosma, P., ... & Petruzzelli, D. (2018). Heavy metals retention (Pb (II), Cd (II), Ni (II)) from single and multimetal solutions by natural biosorbents from the olive oil milling operations. Process Safety and Environmental Protection, 114, 79-90.

Ravindran, R., Jaiswal, S., Abu-Ghannam, N., Jaiswal, A. K. (2018). A comparative analysis of pretreatment strategies on the properties and hydrolysis of brewers' spent grain. Bioresource technology, 248, 272-279.

Saeed, A., Iqbal, M., Akhtar, M. W. (2005). Removal and recovery of lead (II) from single and multimetal (Cd, Cu, Ni, Zn) solutions by crop milling waste (black gram husk). Journal of Hazardous Materials, 117(1), 65-73.

Semerjian, L. (2018). Removal of heavy metals (Cu, Pb) from aqueous solutions using pine (Pinus halepensis) sawdust: Equilibrium, kinetic, and thermodynamic studies. Environmental Technology & Innovation, 12, 91-103.

Sips R. (1950). On the structure of a catalyst surface. J Chem Phys. 16:490-495.

TAPPI Test Method T222 om-88. (1999). Acid-insoluble lignin in wood and pulp. In Tappi test methods. Atlanta: Tappi Press.

Tay, T., Ucar, S., & Karagöz, S. (2009). Preparation and characterization of activated carbon from waste biomass. Journal of Hazardous Materials, 165(1-3), 481-485.

Toshiguki S. and Yukata K. (2003). Pyrolysis of Plant, Animal and Human Wastes; Physical and Chemical Characterization of the Pyrolytic Product; Bioresource Technology, 90(3), 241-247.

Van Soest PJ (1967) Use of detergents in the analysis of fibrous feeds. IV. Determination of plant cell-wall constituents. Journal of Association Officials of Animal Chemistry, (50), 50–55.

Zulkali, M. M. D., Ahmad, A. L., & Norulakmal, N. H. (2006). Oryza sativa L. husk as heavy metal adsorbent: optimization with lead as model solution. Bioresource technology, 97(1), 21-25.

5 ARTIGO II

A combination of chemical and physical pretreatments in the saccharification of malt bagasse I: the effects of ultrasonication in diluted acid medium

Abstract

Malt bagasse is a lignocellulosic byproduct of the brewery industry and is rich in fibers and proteins. It is produced in abundance and can be reused as a substrate to obtain fermentable sugars. However, to obtain an efficient enzymatic saccharification, pretreatments must be used. The objective of this work was to evaluate the combination of ultrasonication in diluted acid medium as a pretreatment of lignocellulosic biomass to obtain fermentable sugars and a residual solid fraction that is more susceptible to enzymatic hydrolysis. Malt bagasse was submitted to different pH values (3, 4 and 5), ultrasonication times (10, 35 and 60 min) and biomass contents (6, 8 and 10 %, w/v). In general, the pretreated samples demonstrated a higher crystallinity index and thermal stability than raw malt bagasse. Considering the experimental conditions used in this study, time was the most important variable; more time resulted in higher sugar release and greater changes in the residual solid fraction recovered after pretreatment. The sample processed at pH 5 for 60 min with a biomass concentration of 8 % resulted in the highest cellulose content, lowest lignin content, and greatest removal of other components, such as proteins and lipids, indicating the potential of malt bagasse to be used as raw material to obtain fermentable sugars.

Keywords: Fermentable sugars. Ultrasound. Lignocellulosic material. Biorefinery.

Introduction

Agroindustrial residues include lignocellulosic materials, composed mainly of cellulose, hemicellulose and lignin, which form an intricate structure recalcitrant to decomposition and can be used to obtain fermentable sugars to be employed as substrates in fermentation processes (Alvira et al. 2010; Gao et al. 2018). The valorization of these residues is within the scope of biorefinery, which aims to develop a sustainable economy using renewable resources to obtain biobased products (Bhowmick et al. 2018).

Cellulose and hemicellulose can be selectively saccharified by enzymes; however, for efficient enzymatic saccharification, pretreatment of the lignocellulosic materials is necessary. Several pretreatment processes have been studied, including treatments that can alter the structural composition of lignocellulosic materials to increase cellulose digestibility by cleaving the reticulated matrix of hemicellulose and lignin and increasing the porosity and surface area of the fibers for subsequent enzymatic hydrolysis (Suriyachai et al. 2018).

Malt bagasse represents 85 % of all byproducts generated by the brewing industry. It is considered a lignocellulosic material, containing approximately 14 % proteins and 74 % carbohydrates, and is composed of 62 % insoluble fibers, which include 12 % cellulose, 26 % lignin and 23 % hemicellulose (Mello and Mali, 2014). Therefore, the potential of malt bagasse as a substrate to obtain fermentable sugars, such as xylose, which can be converted to xylitol, is a product of great importance for the food and pharmaceutical industries (Dasgupta et al. 2017).

Ultrasonication is an emerging technology for the pretreatment of lignocellulosic biomass (Hassan et al., 2018). It is a physical process that has demonstrated satisfactory results in studies of hemicellulose extraction, lignin removal and disruption of cellulose crystallinity in recent years, promoting an acceleration of lignocellulosic biomass saccharification (Bundhoo and Mohee 2018; Sindhu et al 2017; Subhedar et al. 2018; Sun et al. 2004; Velmurugan and Muthukumar 2012; Wu et al. 2017; Yachmenev et al. 2009). The mechanism of ultrasonic pretreatment is attributed to cavitation. The impact produced by the collapse of cavitation bubbles provides an important benefit of access to the surface of lignocellulosic materials, resulting in the alteration of the biomass surface structure and the production of oxidizing radicals that chemically attack the lignocellulosic matrix

The most frequently used chemical pretreatments of lignocellulosic residues are based on the use of acidic or alkaline reagents. An acid pretreatment, such as the use of sulfuric and hydrochloric acids, breaks down the heterocyclic ether bonds between the sugar monomers in the polymer chains of hemicellulose and cellulose resulting in their depolymerization (Velmurugan and Muthukumar, 2011). Mussatto and Roberto (2005), Mussatto et al. (2008) and Ravindran et al. (2018) reported the use of a diluted acid medium on malt bagasse to obtain xylose from hemicellulose hydrolysis. Several investigations also reported the use of a diluted acid medium as a pretreatment of lignocellulosic residues employing sulfuric acid at concentrations ranging from 0.5 to 6 % (w/v) at temperatures ranging from 100 to 160 °C (Jung et al. 2013; Mussatto et al. 2008; Rajan and Carrier 2014; Ravindran et al. 2018; Saha et al. 2005).

The heterogeneity and structural complexity of lignocellulosic materials makes it challenging and difficult to generalize pretreatments and protocols for its saccharification. The combination of physical, physico-chemical, chemical and biological pretreatments have been described in the literature as being more effective than the use of a single pretreatment (Sindhu et al. 2016). The combination of ultrasound may potentiate the efficiency of lignocellulose saccharification by acid hydrolysis (Velmurugan and Muthukumar 2011). Some investigators have recently reported the combination of ultrasonication and an alkaline medium as a pretreatment of lignocellulosic

materials, such as oil palm empty fruit bunches (Addullah et al. 2016), chili postharvest residue (Sidhu et al. 2017), rice straw (Wu et al. 2017), groundnut shells, coconut coir and pistachio shells (Subdehar et al. 2018). Sindhu et al. (2013) reported the surfactant-assisted ultrasound pretreatment of sugarcane tops.

The combination of ultrasonication and an acid medium has not been reported in the literature; Velmurugan and Muthukumar (2011) reported the use of an alkaline pretreatment combined with ultrasonication followed by an acid treatment (0.5-3.0 % sulfuric acid) combined with ultrasonication to obtain fermentable sugars from sugarcane bagasse. In this work, we intended to combine ultrasonication and acid hydrolysis using mild acid hydrolysis conditions and considering the sulfuric acid concentration and temperature, which resulted in a simple and cost effective approach, devoid of corrosive materials and minimal effluents containing acids. The objective of this work was to evaluate the combination of ultrasonication in diluted acid medium as a pretreatment of lignocellulosic biomass to obtain fermentable sugars and a residual solid fraction that is more accessible to enzymatic hydrolysis.

Materials and methods

Malt bagasse

Malt bagasse was provided by Microcervejaria Fábrica 1 (Londrina-Paraná, Brazil), dried (60 °C) in an air-circulating oven (Marconi MA 035 – São Paulo, Brazil) for 24 h and milled to yield particles < 0.30 mm in size. The chemical composition of the residue (proteins, lipids, moisture and ash) was determined by the Association of Official Analytical Chemists (AOAC) method (2003), and the total amount of carbohydrates was determined by calculating the difference. All samples were run in triplicate. Total dietary fiber and soluble and insoluble fractions were determined according to the American Association of Cereal Chemists method (AACC method 32-07, 1990).

Experimental design: ultrasonication in acid medium pretreatments

To evaluate the efficiency of the combination of ultrasonication in diluted acid medium on malt bagasse, a Box and Behnken (1960) experimental design was chosen, consisting of an incomplete factorial design with three independent variables at three levels of variation and 15 experimental runs of which three are replicates at the center point (Table 1). The independent variables were pH (3, 4 and 5), time (10, 35 and 60 min) and biomass content (6, 8 and 10 %), and the levels of each variable were denoted as -1, 0 and +1 for statistical analysis. The variables and their levels were established based on preliminary experiments (data not shown). During this process, the temperature was controlled (± 25 °C) using a water bath.

All samples were submitted to ultrasonication using a Fisher Scientific Sonicator model 505, 50/60HZ (Pittsburgh, PA – USA), coupled with a probe with a tip diameter of 1.27 cm (Fisher Scientific model FB 4219, Pittsburgh, PA – USA). The ultrasonic treatments were carried out with an amplitude of 40 %. Acid solutions (200 mL) of each sample were prepared according to the experimental design (Table 1) employing sulfuric acid 0.1 – 1.0 mol/L solution . The samples submitted to ultrasonication in acid medium were vacuum filtered, and the liquid hydrolysate was recovered and neutralized with 0.1 mol/L NaOH solution until a pH range of 6.0-7.0 was achieved,

and the sugar content was quantified. The residual solid fractions were washed with water to neutrality and dried at 40 °C in an air-circulating oven (Tecnal – São Paulo-Brazil) for further analysis.

Table 1 Box-Behnken experimental design and the results obtained for reducing sugars (RS), xylose and glucose contents on liquid hydrolysate of malt bagasse samples submitted to ultrasonication in diluted acid medium

	Independent variables Coded values (real values)			Response variables		
Run	X_1 pH	X_2 Time (min)	X_3 Biomass (%)	RS (g/100 g bagasse)	Xylose (g/100 g bagasse)	Glucose (g/100 g bagasse)
1	-1 (3)	-1 (10)	0 (8)	2.90	0.48	0.03
2	+1 (5)	-1 (10)	0 (8)	4.30	0.81	0.08
3	-1 (3)	+1 (60)	0 (8)	4.63	1.05	0.14
4	+1 (5)	+1 (60)	0 (8)	3.34	0.69	0.08
5	-1 (3)	0 (35)	-1 (6)	3.18	0.77	0.04
6	+1 (5)	0 (35)	-1 (6)	3.93	1.07	0.07
7	-1 (3)	0 (35)	+1 (10)	2.90	0.91	0.04
8	+1 (5)	0 (35)	+1 (10)	4.26	1,04	0.09
9	0 (4)	-1 (10)	-1 (6)	3.52	0.65	0.04
10	0 (4)	+1 (60)	-1 (6)	3.77	0.57	0.12
11	0 (4)	-1 (10)	+1 (10)	3.72	0.54	0.11
12	0 (4)	+1 (60)	+1 (10)	4.66	0.80	0.08
13	0 (4)	0 (35)	0 (8)	3.16	0.54	0.04
14	0 (4)	0 (35)	0 (8)	3.01	0.55	0.05
15	0 (4)	0 (35)	0 (8)	3.24	0.56	0.05

Determination of fermentable sugars on liquid hydrolysate

Reducing sugars (RS) were determined by the di-nitrosalicylic acid (DNS) method (Miller 1959), and the method of xylose determination was adapted from Pham et al. (2011). The glucose content was determined using a Sigma-Aldrich glucose assay kit (GAGO20, Missouri, USA).

Characterization of raw malt bagasse and the residual solid fraction resulted from pretreatments

Cellulose, hemicellulose and lignin contents

Cellulose and hemicellulose contents were determined by the Van Soest method (1967) and lignin content was determined by the Technical Association of the Pulp and Paper Industry method (TAPPI T222 om-88 method, 1999).

X-ray diffraction (XRD)

The crystallinity of each sample was investigated using XRD. The samples were finely ground to a powder (particles < 0.18 mm in size), and the diffraction analysis was performed with a PANalytical X'Pert PRO MPD diffractometer (Netherlands) using copper Kα radiation (λ = 1.5418 Å), a voltage of 40 kV and a 30 mA current. Analysis was performed between 2θ = 5° and 2θ = 50°. All assays were performed with ramping at 1°/min. The crystallinity index (CI) was calculated using Equation 1 (Segal et al. 1959) as follows:

$$CI\ (\%) = ((I_{002} - I_{am})/I_{002})*100, \text{ Equation 1}$$

where I_{am} is the intensity of diffraction at 2θ = 18° (amorphous portion) and I_{002} is the maximum intensity of 002 lattice diffraction (approximately 2θ = 22°).

Thermogravimetric analysis (TGA)

Thermogravimetric analysis (TGA 50, Shimadzu, Japan) was conducted under a nitrogen atmosphere (50 mL min^{-1}), and the samples were heated from 25 to 600 °C at a heating rate of 10 °C/min. The weight loss (%) was evaluated by measuring the residual weight at 600 °C.

Fourier transform-infrared spectroscopy (FT-IR)

For this procedure, the samples were ground to a fine powder (particles < 0.18 mm in size), mixed with potassium bromide and compressed into tablets. FT-IR analysis was conducted with a Shimadzu FT-IR-8300 (Japan), which has a spectral resolution of 4 cm^{-1} and a spectral range of 4000-500 cm^{-1}.

Scanning electron microscopy (SEM)

SEM analysis was performed with an FEI Quanta 200 microscope (Oregon, USA). Dried samples were mounted for visualization on bronze stages using double-sided tape. The surfaces were then coated with a thin gold layer (40-50 nm thickness). All samples were examined using an accelerating voltage of 30 kV.

Statistical analysis

Experimental data were analyzed to fit second order polynomial equations to response variables, which included reducing sugars (RS), xylose, glucose and cellulose. Surface plots were generated from complete models and the hemicellulose and lignin (models not significant) were verified from Tukey test using Statistica (Statsoft, Oklahoma, U.S.A.) computer software.

Results and discussion

Chemical composition of malt bagasse

The raw malt bagasse used in this study consisted of the following composition: 20.60 ± 0.84 % proteins, 9.10 ± 0.35 % lipids, 4.11 ± 0.18 % ash, 4.04 ± 0.49 % moisture, 1.34 ± 0.34 % carbohydrates and 60.80 ± 0.32 % total

dietary fiber, with a cellulose content of 8.66 ± 1.02 %, hemicellulose content of 26.76 ± 1.23 % and lignin content of 25.38 ± 1.89 %. These results are similar to the results reported by Mello and Mali (2014), who determined a composition of 12.29 % cellulose, 23.41 % hemicellulose and 26.41 % lignin. Mussato and Roberto (2005) reported that malt bagasse contains approximately 16.8 % cellulose, 28.4 % hemicellulose, 27.8 % lignin, 15.0 % proteins and 4.6 % ash, and these values were in accordance with our results, except for cellulose, which was lower in our study. According to Santos et al. (2003), the variation in the composition of malt bagasse is due to the variety, harvest time, conditions for malting barley and the quality and type of adjuncts added during the fermentation process, which is unique to each brewery.

Effects of pretreatment on fermentable sugar production

The results of RS, xylose and glucose content are presented in Table 1. These results were statistically analyzed, and the regression coefficients of the second order equations and the analysis of variance (ANOVA) of these samples are shown in Table 2.

Table 2 Regression coefficients and ANOVA of mathematical models obtained for RS, xylose, glucose and cellulose [a]

Coefficient	RS	Xylose	Glucose	Cellulose
β_0	3.14	0.55	0.045	7.57
β_1	0.28*	0.05	0.008	0.34
β_2	0.24*	0.08*	0.020*	1.45*
β_3	0.14	0.03	0.007	0.02
β_{11}	0.15	0.26**	0.004	2.90**
β_{22}	0.50*	-0.05	0.031*	1.30
β_{33}	0.28*	0.13*	0.010	-2.55*
β_{12}	-0.67**	-0.17**	-0.026*	1.24
β_{13}	0.15	-0.04	0.005	-0.42
β_{23}	0.17	0.08	-0.027*	-0.52
R^2	0.87	0.93	0.90	0.90
Model (p)	0.0850	0.0146	0.0462	0.0428

[a] – β_1 = pH; β_2 = time; β_3 = biomass and *$p \leq 0.05$; **$p \leq 0.01$

For all models, the coefficients of determination (R^2) were considered satisfactory (> 0.87), which indicates that 87, 93 and 90 % of the total variation around the average could be explained by the models obtained for RS, xylose and glucose, respectively (Table 2). The models obtained for xylose and glucose were significant ($p \leq 0.05$), and the model obtained for RS ($p = 0.0850$) was not significant ($p > 0.05$); however, this model was employed to study the trends of this response after the pretreatment of malt bagasse. The lack of fit of the RS model was not significant, and for xylose and glucose, the lack of fit was significant, which can be explained according to Ribeiro et al. (2008) regarding the good repetition of the tests of the central points, which resulted in a high calculated F-value for the lack of fit.

Among the independent variables investigated in this study, the linear effect of time (X_2) presented a positive and significant ($p \leq 0.05$) effect for all responses (Table 2), indicating that increased sugar yields were obtained with increased processing time (60 min), which is shown in Fig. 1. Laopaiboon et al. (2010) reported that a higher efficiency of acid hydrolysis of sugarcane bagasse was observed at a reaction time of 5 h at 100 °C. In this study, the use of acid hydrolysis combined with ultrasonication decreased the time required for the maximum hydrolysis efficiency. Velmurugan and Muthukumar (2011) reported that a synergistic effect of ultrasound and acid-catalyzed reactions decreased the time required for acid hydrolysis, and they also reported that the production of fermentation inhibitors was significantly reduced in ultrasound-assisted acid hydrolysis.

The results (Table 1) indicate that glucose yields were lower than xylose yields for all conditions investigated in the experimental design, which is an interesting observation because the objective of the pretreatment conditions was to remove hemicellulose and lignin, allowing cellulose to be accessible for enzymatic reactions after pretreatment. According to Taherzadeh and Karimi (2007), glucose yields after acid pretreatment were minimal, which is less important than xylose yields because it is the degradation of xylose that produces inhibitors that severely limit cell growth and enzymatic reactions during fermentation. The hemicellulose content of malt bagasse (26.76 %) was greater than cellulose (8.66 %), and according to Mussato and Roberto (2005), hemicellulose from malt bagasse mainly consists of a xylan backbone (approximately 70 %), while the remaining 30 % is an arabinan structure, which explains the higher xylose yields compared to glucose (Table 1).

The linear effect of variable X_1 (pH) was significant ($p \leq 0.05$) only for RS yields. Higher pH values resulted in greater RS yields, and the other responses (xylose and glucose) were not affected by this variable. Jung et al. (2013) reported that a variation of sulfuric acid concentration from 0.5 % to 2.0 % (w/v) did not affect the reduction of sugar yields of oil palm empty fruit bunches submitted to acid hydrolysis.

Fig. 1 Contour plots of reducing sugars (A), xylose (B) and glucose (C) on liquid hydrolysate and cellulose (D) on a residual solid fraction from malt bagasse samples submitted to ultrasonication in diluted acid medium

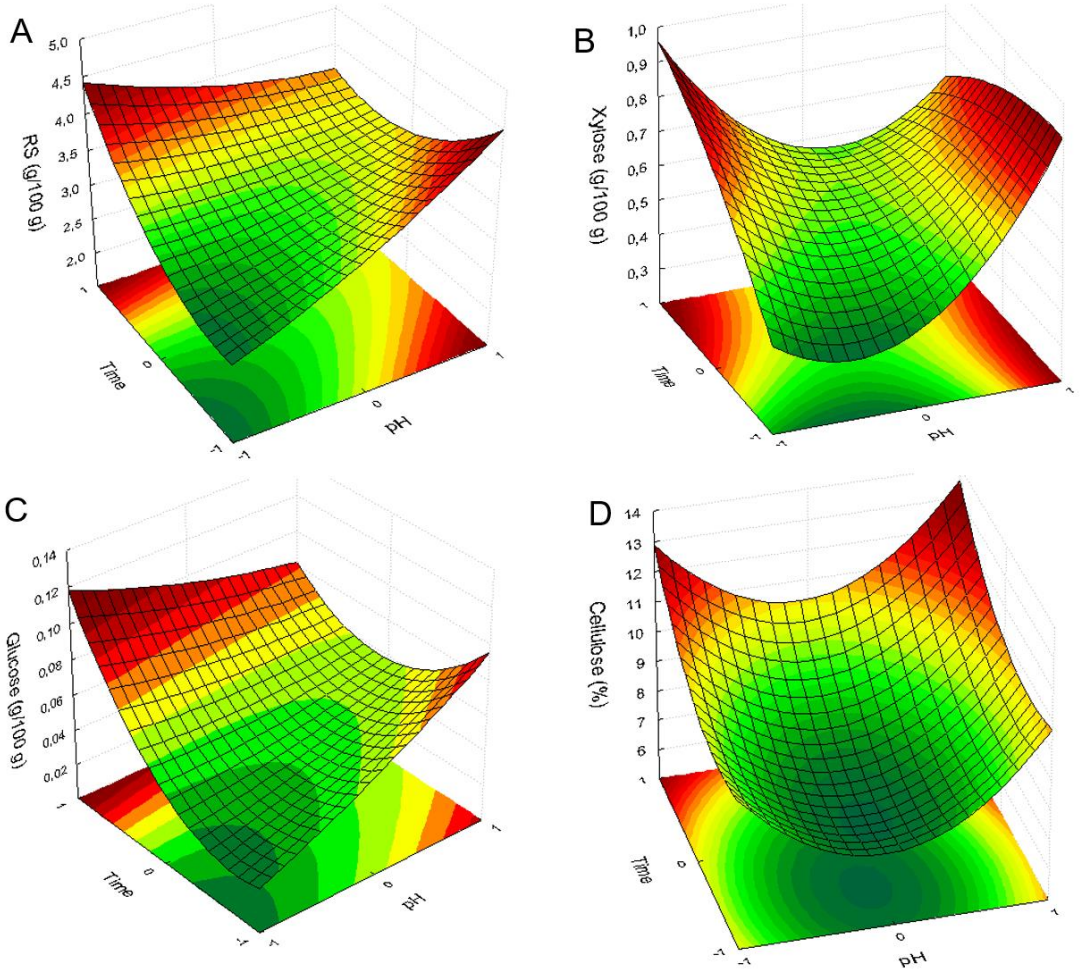

Effects of pretreatment in the residual solid fraction recovered after malt bagasse was submitted to ultrasonication in diluted acid medium

Cellulose, hemicellulose and lignin contents

The cellulose, hemicellulose and lignin contents of the residual solid fraction recovered after malt bagasse was submitted to ultrasonication in diluted acid medium are presented in Table 3. A significant ($p \leq 0.05$) mathematical model ($R^2 = 0.90$) was obtained for cellulose content (Table 2), and the linear (X_2) and quadratic (X_{22}) coefficients of time demonstrated positive and significant ($p \leq 0.05$) effects for cellulose content (Table 2), indicating that greater cellulose recovery was obtained at a longer processing time (60 min), which is shown in Fig. 1d. The samples that had a higher cellulose content corresponded to experiments 3 and 4, which were processed over 60 min using a biomass content of 8 % (Table 1), with pH values of 3 and 5, respectively. The cellulose content of these samples (12.45 % for experiment 3, 16.12 % for experiment 4) (Table 3) was significantly ($p \leq 0.05$) greater than the cellulose content of raw malt bagasse (8.66 %).

Table 3 Composition and crystallinity index (CI) of solid fraction of malt bagasse recovered after ultrasonication in diluted acid medium[a]

Run	Cellulose (%)	Hemicellulose (%)	Lignin (%)	Insoluble dietary fibers (%)	Others[b] (%)	CI (%)
1	9.93^{c}	39.94^{c}	22.12^{bc}	71.99^{d}	28.01^{cd}	32
2	8.62^{d}	41.63^{c}	24.20^{a}	74.45^{cd}	25.55^{de}	31
3	12.45^{b}	39.7^{cd}	25.30^{a}	77.54^{c}	22.46^{e}	27
4	16.12^{a}	48.94^{b}	20.09^{b}	85.15^{a}	14.85^{g}	32
5	7.58^{d}	50.54^{b}	23.57^{a}	81.69^{b}	18.31^{f}	19
6	8.59^{d}	53.09^{a}	19.98^{c}	81.65^{b}	18.35^{f}	30
7	8.09^{d}	44.19^{d}	20.51^{c}	72.80^{d}	27.20^{d}	16
8	7.44^{d}	47.87^{b}	21.21^{bc}	76.52^{c}	23.48^{de}	32
9	5.21^{f}	28.81^{f}	24.82^{a}	58.85^{f}	41.15^{a}	21
10	7.02^{de}	40.46^{c}	25.41^{a}	72.90^{d}	27.10^{d}	30
11	6.66^{de}	30.35^{f}	23.82^{a}	60.82^{f}	39.18^{a}	30
12	6.40^{de}	34.91^{e}	24.13^{a}	65.44^{e}	34.56^{b}	30
13	7.68^{d}	35.98^{e}	25.26^{a}	68.92^{e}	31.08^{c}	35
14	7.75^{d}	38.15^{cd}	24.46^{a}	70.36^{d}	29.64^{c}	33
15	7.29^{d}	35.88^{e}	25.06^{a}	68.23^{e}	31.77^{c}	38
Raw malt bagasse	8.66^{d}	26.76^{g}	25.38^{a}	60.80^{f}	39.20^{a}	15

[a-] Different small letters in the same column indicate significant differences between means (Tukey test, $p \leq 0.05$).

[b-] Ash, proteins, lipids and other minor components

The hemicellulose content of the residual solid fraction recovered after malt bagasse was submitted to ultrasonication in diluted acid medium ranged from 28.81 to 53.09 % (Table 3), which was significantly ($p \leq 0.05$) greater than the hemicellulose content of raw malt bagasse, which indicated that the insoluble dietary fiber content significantly increased for all pretreated samples, resulting in samples with greater proportions of hemicellulose compared to the raw material.

The lignin content of the residual solid fraction ranged from 19.98 to 25.41 % (Table 3), and only samples corresponding to experiments 1 (22.12 %), 4 (20.09 %), 6 (19.98 %), 7 (20.51 %) and 8 (21.21 %) (Table 2) had significantly lower ($p \leq 0.05$) lignin content when compared to raw malt bagasse (25.38 %), and demonstrated lignin mass losses of 12.84, 20.84, 21.29, 19.17 and 16.42 %, respectively. Mussato et al. (2008) reported that the lignin mass loss of raw malt bagasse after being submitted to acid hydrolysis (1.25 % H_2SO_4 solution for 17 min at 120 °C) was 14 %; they also reported that it is not necessary to promote the complete removal of lignin and hemicellulose to achieve a high cellulose conversion ratio during the enzymatic hydrolysis of cellulose from malt bagasse.

For all samples, except for the samples from experiments 9 and 11, that were processed for a shorter amount of time (10 min) at an intermediary pH (4), the insoluble fiber content was significantly greater than raw

malt bagasse (Table 3), indicating that other components such as lipids, proteins and ash were removed from malt bagasse.

X-ray diffraction (XRD)

The components in lignocellulosic biomass can be crystalline or amorphous, and crystallinity is attributed to cellulose, while hemicellulose and lignin are amorphous, thus the increase in crystallinity is an indication of increase of cellulose content and in effectiveness of the pretreatment (Ravindran et al. 2018). The crystallinity index (CI) was calculated for all pretreated samples and raw malt bagasse using the results from XRD (Table 3), and in Fig. 2, the diffractograms of the samples that had greater (experiments 3 and 4) and lower (experiments 9, 11 and 12) cellulose content in comparison to raw malt bagasse are shown.

The malt bagasse diffractogram (Fig. 2) is typical of an amorphous material, with a CI of 15.00 %, and only a discrete peak near $2\theta = 22°$ appeared, which is attributed to the structure of the native cellulose. Malt bagasse had high protein (20.60 %), lipid (9.10 %), hemicellulose (26.76 %) and lignin (25.38 %) contents, all of which contributed to the amorphous fraction of malt bagasse. The cellulose content of malt bagasse was 8.66 %, and according to Velmurugan and Muthukumar (2012), the CI of a lignocellulosic material is influenced by its composition; as lignin and hemicellulose are amorphous fractions, cellulose content corresponds to their crystalline fractions.

Malt bagasse samples submitted to ultrasonication in diluted acid medium demonstrated similar crystalline patterns as raw malt bagasse, with a single, defined peak at $2\theta = 22°$ (Fig. 2). The CI of raw malt bagasse (15 %) increased for all pretreated samples, which had CIs ranging from 16 to 38 %. The samples that had the lower CI values were from experiments 5 and 7 (Table 1), and these samples had a cellulose content of 7.58 and 8.09 %, respectively. These samples were prepared using a combination of lower pH and intermediary processing time, and the use of these conditions could have resulted in these lower CI values.

Fig. 2 XRD diffractograms obtained of raw malt bagasse and malt bagasse samples submitted to ultrasonication in diluted acid medium: (Experiments 3, 4, 9 , 11 and 12)

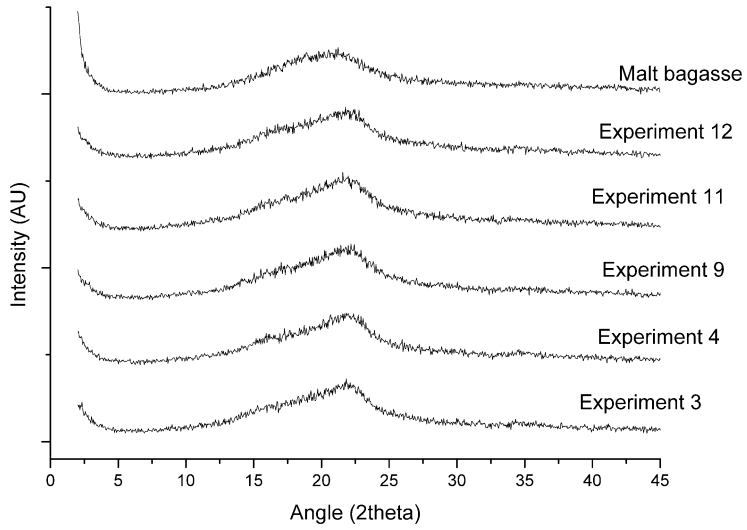

Thermogravimetric analysis (TGA)

TGA is a valuable analytical method to study the thermal properties of macromolecules such as cellulose and hemicellulose. The mass change of a sample was measured as a function of time or temperature and plotted as a TGA curve, which conveys information regarding the thermal behavior of a sample. The curves (not shown) obtained from the TGA analysis were used to examine the changes caused by ultrasonication in diluted acid medium on T_{max} (temperature corresponding to the maximum rate of mass loss), T_{10} (temperature corresponding to 10 % mass loss), T_{50} (temperature corresponding to 50 % mass loss) and M_{600} (mass loss at 600 °C) (Table 4).

Table 4 TGA parameters of malt bagasse samples submitted to ultrasonication in diluted acid medium

	TGA parameters				
Run	T_{max1} (°C)	T_{max2} (°C)	T_{10} (°C)	T_{50} (°C)	M_{600} (%)
1	309	368	253	353	79
2	311	356	263	354	79
3	312	366	256	348	78
4	312	365	270	356	79
5	300	356	268	350	79
6	303	362	269	355	79
7	314	355	260	349	78
8	314	365	264	354	79
9	311	362	265	351	78
10	317	365	265	353	79
11	305	362	266	353	78
12	311	362	265	348	78
13	311	365	266	353	79
14	310	365	268	352	79
15	314	359	264	352	79
Raw malt bagasse	310	354	217	346	77

T_{max} = temperature corresponding to the maximum rate of mass loss, T_{10} = temperature corresponding to 10 % mass loss, T_{50} = temperature corresponding to 50 % mass loss and M_{600} = mass loss at 600 °C

The thermograms showed three-stage decomposition weight loss. The first stage, a small weight loss (< 10 %) was found in the range from 50 to 125 °C for all samples, and according to Ibrahim et al. (2010), the first stage (temperature below 200 °C) corresponds to the evaporation of water or low molecular weight compounds present in the lignocellulosic residues, which results in mass losses < 10 %.

A second degradation stage showed a double-peak distribution at 300-317 °C and 355-368 °C (curves not shown) for all samples, with the first set of peaks likely corresponding to hemicellulose decomposition and the second set of peaks corresponding to cellulose decomposition. Abdullah et al. (2010) and Ibrahim et al. (2010)

reported that between 200 to 500 °C, weight loss corresponded to the liberation of volatile hydrocarbons from rapid thermal decomposition of hemicellulose, cellulose and some components of lignin. Abdullah et al. (2010) also reported that the thermograms of lignocellulosic materials showed a double-peak distribution in the second degradation stage, with hemicellulose decomposition detected at approximately 334 °C and cellulose decomposition at 365 °C, which are values similar to those observed in this study. For all samples, a third-stage degradation was observed in thermograms at temperatures above 450-500 °C (curves not shown), and it could be associated with lignin. In this stage, the decomposition rate occurred at a lower rate compared to stage-two.

Compared to the raw malt bagasse, all samples submitted to ultrasonication in diluted acid medium presented greater thermal stability (Table 4), which was demonstrated by the greater T_{10} and T_{50} values for all pretreated samples. These results are in agreement with the results reported by Ibrahim et al. (2010), where an increase in crystallinity resulted in increased thermal stability; in our study, all pretreated samples had higher CIs than raw malt bagasse, except for the sample from experiment 7 (Table 3).

The sample that presented the greatest T_{10} and T_{50} values (Table 4) was the sample from experiment 4, which also yielded greater cellulose content (Table 3). According to Yang et al. (2007), hemicellulose decomposition begins easily, with weight loss primarily occurring between 220-315 °C, and cellulose decomposition occurs at a higher temperature range (315-400 °C); therefore, greater cellulose content results in higher thermal stability.

The mass loss at 600 °C (M_{600}) was 77 % for raw malt bagasse (Table 4), and for the pretreated samples, the values slightly increased, ranging from 78-79 %. The lignin content of raw malt bagasse and pretreated samples ranged from 19.98 and 25.38 %, which explains the residual solid fraction at approximately 20 % at 600°C. Abdullah et al. (2010) and Yang et al. (2007) reported that lignin decomposition occurred slowly over a large temperature range from ambient conditions to 900 °C.

Fourier transform-infrared spectroscopy (FT-IR)

As shown in Fig. 3, the spectra generated for malt bagasse and samples pretreated by ultrasonication in diluted acid medium were similar, indicating similarities in their chemical groups. All spectra showed wide absorption bands in the 3400-3500 cm^{-1} region corresponding to stretching vibrations of hydroxyl groups, which indicates H-bonding interactions in these materials.

The bands observed at 2900 cm^{-1} correspond to -C-H stretching; and H-C-H- and -C-O-H-conjugated bending vibrations were observed in all sample spectra (Fig. 3). A shoulder peak at 2850 cm^{-1}, which is characteristic of $-OCH_3$, was observed in raw malt bagasse and was weakened in the pretreated samples, which is attributed to the depolymerization of lignin during the pretreatment process (Adel et al. 2010).

In the malt bagasse spectrum, several bands were observed in the region between 1800-1100 cm^{-1} (Fig. 3), and these bands correspond to cellulose, hemicellulose and lignin (Bordîlau et al. 2009). In the pretreated samples, the bands at 1750 cm^{-1} (C=O stretching in carbonyl groups from lignin and hemicellulose) and 1650 cm^{-1} (C=C alkene from lignin) appeared more defined, possibly because other components were removed from these samples, which resulted in materials with higher insoluble dietary fiber contents (Table 3). Bands at 1450 and 1380 cm^{-1} also appeared more defined in pretreated samples, and according to Ibrahim et al. (2010), this could be attributed to cellulose.

Fig. 3 FTIR spectra obtained of raw malt bagasse and malt bagasse samples submitted to ultrasonication in diluted acid medium: (Experiments 3, 4, 9, 11 and 12)

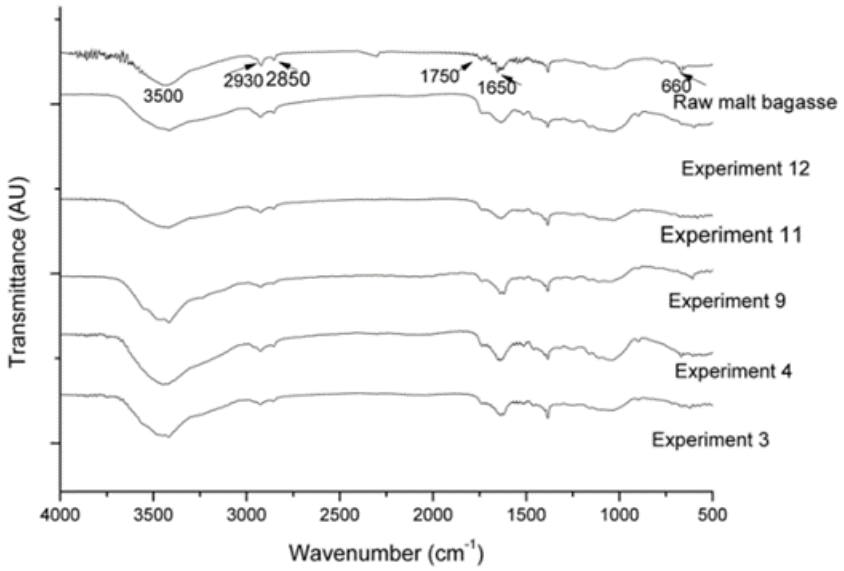

Scanning electron microscopy (SEM)

Fig. 4 shows SEM micrographs of the raw malt bagasse (Fig. 4a) in comparison with samples from experiments 3 (Fig. 4b) and 4 (Fig. 4c), which were the samples with higher cellulose content. Samples from experiments 11 (Fig. 4d) and 12 (Fig. 4e) were the samples with lower cellulose content.

Raw malt bagasse showed a typical morphology of lignocellulosic materials, with the original fibers bundled with the nonfibrous components (hemicellulose and lignin), which formed a compact structure (Fig. 4a), and an outer layer covering the material surface was also observed. According to Fung et al. (2010), lignocellulosic materials in their native state contain waxes and other encrusting substances such as hemicellulose, lignin, and pectin that form a thick and smooth outer layer.

The morphology of the samples after pretreatment changed, with a notable increase in the surface porosity of the fibers, especially for samples from experiments 3 (Fig. 4b) and 4 (Fig. 4c), where a more visible removal of the outer layer covering the material surface (arrows) was observed. In the samples from experiments 11 (Fig. 4 d) and 12 (Fig. 4e), the outer layers were fractured but remained preserved.

Subhedar et al. (2018) reported morphological changes of lignocellulosic materials submitted to ultrasonic treatment based on the opening of the biomass structural configuration, resulting in the exposure of cellulose and hemicellulose, which may facilitate the access of enzymes, such as cellulases, in the process of complete saccharification of these materials.

Fig. 4 Scanning electron microscopy micrographs of raw malt bagasse (a) and malt bagasse samples submitted to ultrasonication in diluted acid medium: (b) Experiment 3 (pH 3, 60 min, 8 % biomass), (c) experiment 4 (pH 5, 60 min, 8 % biomass), (d) experiment 11 (pH 4, 10 min, 10 % biomass) and (e) experiment 12 (pH 4, 60 min, 10 % biomass).

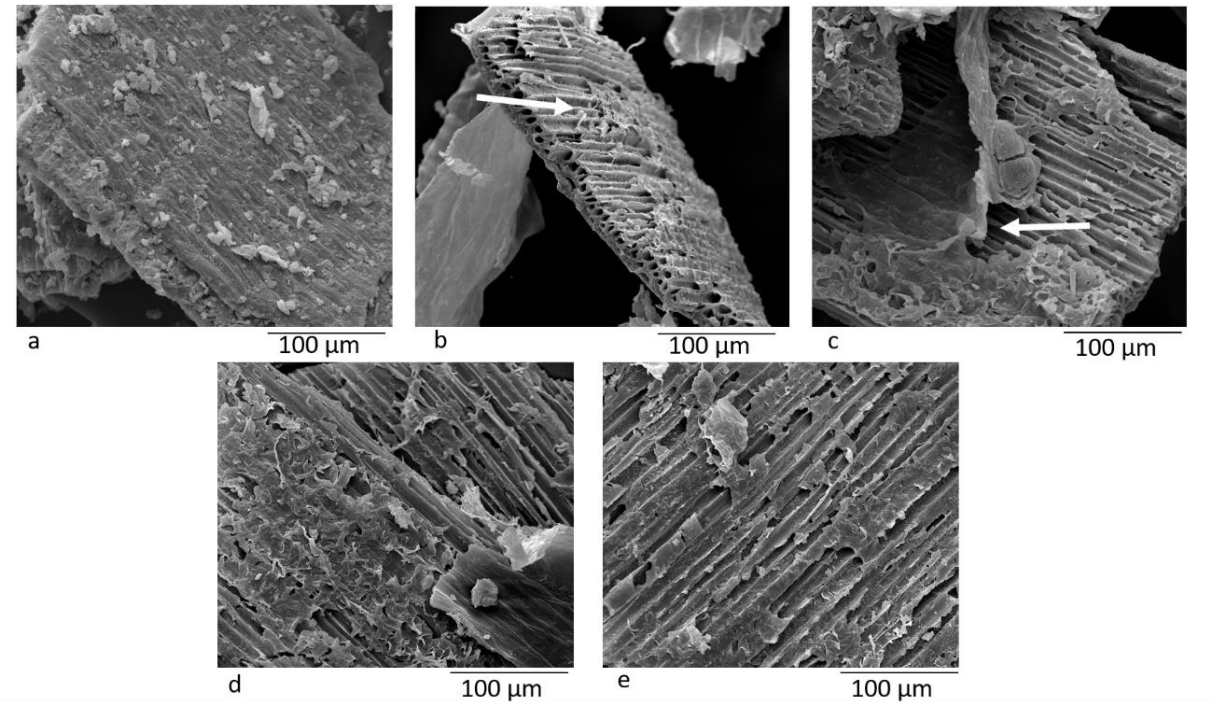

Conclusion

Ultrasonication in diluted acid medium can be used as an alternative method for the pretreatment of malt bagasse. Overall, the pretreated samples had a higher crystallinity index and thermal stability than raw malt bagasse, and changes in the surface morphology of the fibers were observed, with an increase in surface porosity.

Considering the experimental conditions employed in this study, pretreatment time was the most important variable, which resulted in greater sugar release and greater changes in the residual solid fraction recovered after pretreatment. The sample from experiment 4 (processed at pH 5 for 60 min with a biomass concentration of 8 %) resulted in greater cellulose content and lower lignin content, and this condition was also effective in the removal of other components, such as ash, lipids and proteins, which resulted in greater insoluble dietary fiber content, indicating the potential of malt bagasse to be used as raw material to obtain fermentable sugars.

Acknowledgments

The authors thank the Laboratory of Microscopy and Microanalysis (LMEM) and the Laboratory of X-ray Diffraction (LDRX) at the State University of Londrina for the analysis, Fundação Araucária for financial support and CAPES for the doctoral grant of Léa Rita P.F. Mello.

Compliance with ethical standards

Conflict of interest - The authors declare that there is no conflict of interest.

Authors Contributions

Léa Rita P. F. Mello performed all the laboratory activities related to this study, she elaborated the figures and tables from the experimental results and discussed the results.

Suzana Mali supervised the entire execution of the experimental part of this study and assisted in supervising the whole process of writing the manuscript.

References

AACC - American Association of Cereal Chemists (1990) Approved methods of the American association of cereal chemists. St Paul MN: AACC.

Abdullah SS, Yusup S, Ahmad MM, Ramli A, Ismail L (2010) Thermogravimetry study on pyrolysis of various lignocellulosic biomass for potential hydrogen production. International journal of chemical and biological engineering. Int J Chem Biol Eng 3:137–141

Adel AM, El–Wahab ZHA, Ibrahim AA, Al–Shemy MT (2010) Characterization of microcrystalline cellulose prepared from lignocellulosic materials. Part I. Acid catalyzed hydrolysis. Bioresour Technol 101: 4446–4455

Alvira P, Tomás-Pejó E, Ballesteros M, Negro MJ (2010) Pretreatment technologies for an efficient bioethanol production process based on enzymatic hydrolysis: a review. Bioresour Technol 101:4851–4861

AOAC – Official Methods of Analysis, 14th ed. Ass Off (2003) Analytical Chem Washington. USA

Bhowmick GD, Sarmah, AK, Sen R. (2018) Lignocellulosic biorefinery as a model for sustainable development of biofuels and value added products. Bioresour Technol 247:1144–1154

Bhutto AW, Qureshi K, Harijan K, Abro R, Abbas T, Bazmi AA, Yu G (2017) Insight into progress in pre-treatment of lignocellulosic biomass. Energy 122:724–745

Bundhoo ZM and Mohee R (2018) Ultrasound-assisted biological conversion of biomass and waste materials to biofuels: A review. Ultrason Sonochem 40:298–313

Dasgupta D, Bandhu S, Adhikari DK and Ghosh D (2017) Challenges and prospects of xylitol production with whole cell bio-catalysis: a review. Microbiol Res 197:9–21

Fung WY, Yuen KH, Liong MT (2010) Characterization of fibrous residues from agrowastes and the production of nanofibers. J Agr Food Chem 58:8077–8084

Gao J, Zheng C, Tan T, Liu S, Li H (2018) Enhanced saccharification of rice straw using combined ultra-high pressure and ionic liquid microemulsion pretreatments. 3 Biotech 8:208

Hassan SS, Williams GA, Jaiswal AK (2018) Emerging Technologies for the Pretreatment of Lignocellulosic Biomass. Bioresour Technol 262:310–318

Ibrahim MM, Agblevor FA and El-Zawawy WK (2010) Isolation and characterization of cellulose and lignin from steam-exploded lignocellulosic biomass. BioResources 5:397–418

Jung YH, Kim IJ, Kim HK, Kim KH (2013) Dilute acid pretreatment of lignocellulose for whole slurry ethanol fermentation. Bioresour Technol 132:109–114

Laopaiboon P, Thani A, Leelavatcharamas, V, Laopaiboon L (2010) Acid hydrolysis of sugarcane bagasse for lactic acid production. Bioresour Technol 101:1036–1043

Mello LRPF, Mali S (2014) Use of malt bagasse to produce biodegradable baked foams made from cassava starch. Ind Crop Prod 55:187–193

Miller G (1959) Use of dintrosalicilic acid reagent for determination of reducing sugars. Anal Chem 31:426 – 428, 1959

Mussatto SI and Roberto IC (2005) Acid hydrolysis and fermentation of brewer's spent grain to produce xylitol. J Sci Food Agr 85:2453–2460

Mussatto SI, Fernandes M, Milagres AM, Roberto IC (2008) Effect of hemicellulose and lignin on enzymatic hydrolysis of cellulose from brewer's spent grain. Enzyme Microb Technol 43:124–129

Pham PJ, Hernandez R, French WT, Estill FB, Mondala AHA (2011) Spectrophotometric method for quantitative determination of xylose in fermentation médium. Biomass Bioenerg 35:2814–2821

Rajan K and Carrier DJ (2014) Effect of dilute acid pretreatment conditions and washing on the production of inhibitors and on recovery of sugars during wheat straw enzymatic hydrolysis. Biomass Bioenerg 62:222–227

Ravindran R, Jaiswal S, Abu-Ghannam N, Jaiswal AK (2018) A comparative analysis of pretreatment strategies on the properties and hydrolysis of brewers' spent grain. Bioresour Technol 248:272-279

Ribeiro SDCA, Park KJ, Ribeiro CDFA, Tobinaga S, Araujo EAF, Hubinger MD (2008) Optimization of the osmotic dehydration of mapará (Hypophthalmus edentatus) fillets by response surface methodology. Food Sci Technol 28:485–492

Saha BC, Iten LB, Cotta, MA, Wu YV (2005) Dilute acid pretreatment, enzymatic saccharification and fermentation of wheat straw to ethanol. Process Biochem 40:3693–3700

Santos M, Jiménez JJ, Bartolomé B, Gómez-Cordovéz C, Del Nozal MJ, (2003) Variability of brewers' spent grain within a brewery. Food Chem 80:17–21

Segal L, Creely JJ, Martin AE Jr, Conrad CM (1959) An empirical method for estimating the degree of crystallinity of native cellulose using the X-ray diffractometer. Text Res J 29:786–794

Sindhu R, Silviya N, Binod P, Pandey A (2013) Pentose-rich hydrolysate from acid pretreated rice straw as a carbon source for the production of poly-3-hydroxybutyrate. Biochem Eng J 78:67-72

Sindhu R, Binod P, Pandey A (2016) A novel sono-assisted acid pretreatment of chili post harvest residue for bioethanol production. Bioresour Technol 213:58–63.

Sindhu R, Binod P, Mathew K, Abraham A, Gnansounou E, Ummalyma, SB, Pandey A (2017) Development of a novel ultrasound-assisted alkali pretreatment strategy for the production of bioethanol and xylanases from chili post harvest residue. Bioresour Technol 242:146–151

Subhedar PB, Ray P and Gogate PR (2018) Intensification of delignification and subsequent hydrolysis for the fermentable sugar production from lignocellulosic biomass using ultrasonic irradiation. Ultrason Sonochem 40:140–150

Sun JX, Sun XF, Zhao H and Sun RC (2004) Isolation and characterization of cellulose from sugarcane bagasse. Polym Degrad Stabil 84:331–339

Suriyachai N, Champreda V, Kraikul N, Techanan W, Laosiripojana N (2018) Fractionation of lignocellulosic biopolymers from sugarcane bagasse using formic acid-catalyzed organosolv process. 3Biotech 8: 221

Taherzadeh MJ and Karimi K (2007) Enzymatic-based hydrolysis processes for ethanol from lignocellulosic materials: A review. BioResources 2:707–738

TAPPI Test Methods T 222 om-88 (1999) Acid insoluble lignin wood and pulp. Atlanta

Van Soest PJ (1967) Use of detergents in the analysis of fibrous feeds. IV. Determination of plant cell-wall constituents. Journal of Association Officials of Animal Chemistry 50:50–55

Velmurugan R and Muthukumar K (2011) Utilization of sugarcane bagasse for bioethanol production: sono-assisted acid hydrolysis approach. Bioresour Technol 102:7119–7123

Velmurugan R and Muthukumar K (2012) Ultrasound-assisted alkaline pretreatment of sugarcane bagasse for fermentable sugar production: optimization through response surface methodology. Bioresour Technol 112:293–299

Wu H, Dai X, Zhou S, GanY, Xiong Z, Qin Y, Ma J, Yang L, Wu Z, Wang T, Wang W, Wang C (2017) Ultrasound-assisted alkaline pretreatment for enhancing the enzymatic hydrolysis of rice straw by using the heat energy dissipated from ultrasonication. Bioresour Technol 241: 70–74

Yachmenev V, Condon B, Klasson T, Lambert A (2009) Acceleration of the enzymatic hydrolysis of corn stover and sugar cane bagasse celluloses by low intensity uniform ultrasound. Biobased Mater Bio 3: 25–31

Yang H, Yan R, Chen H, Lee DH, Zheng C (2007) Characteristics of hemicellulose, cellulose and lignin pyrolysis. Fuel 86:1781–1788

6 ARTIGO III

A combination of chemical and physical pretreatments in the saccharification of malt bagasse II: the effects of ultrasonication in alkaline medium

Abstract

Brazil is an important agroindustrial residue generator, as malt bagasse, which is a byproduct of the brewery industry rich in fibers and proteins. Lignocellulosic residues can be reused as substrates for fermentation in fermentative processes, however, in order to improve the enzymatic access of these recalcitrant structures, pretreatments should be used. The objective of this study was to investigate the combination of ultrasonication in alkaline medium as pretreatment to enhance rupture of lignocellulosic matrix and to facilitate saccharification of malt bagasse. A factorial experimental design 3^2 was employed to evaluate the effects of pH (9, 10 and 11) and time of ultrasonication (10, 35 and 60 min) on malt bagasse. The pretreated samples had higher crystallinity indexes and thermal stability than raw malt bagasse. The time was the most important variable, higher times resulted in higher sugars release and greater changes in the residual solid fraction recovered after pretreatment. The condition that resulted in the sample with the highest cellulose content and lignin content removal was that employing pH 9 for 60 min. Ultrasonication in alkaline medium can be considered a promising pretreatment method to break the recalcitrance of malt bagasse, resulting in a more susceptible material to be submitted to an enzymatic hydrolysis in a saccharification process.

Keywords: Ultrasound. Lignocellulosic material. Alkaline. Saccharification. Biorefinery.

Introduction

Malt bagasse is a byproduct obtained from brewing industry, it is considered a lignocellulosic material that is rich in proteins (14 %) and carbohydrates (74%), being composed of 62 % insoluble fibers, which include 12 % cellulose, 26 % lignin and 23 % hemicellulose (Mello and Mali, 2014). Thus, this raw material presents high potential of application as substrate to obtain fermentable sugars, such as glucose and xylose.

In the last decades, several energy research programs have been directed towards the discovery of new sustainable energy sources, with the purpose of reducing dependence on fossil fuels and use of natural non-renewable resources. In this context, the biorefinery is proposed to achieve sustainable development by conversion of abundant, available and renewable lignocellulosic biomass into energy, fuels, chemicals and new materials (Bhowmick et al. 2018, Hassan et al. 2018).

Ultrasonication is a physical process that can be used as pretreatment in lignocellulosic materials and residues and has demonstrated satisfactory results in studies of hemicellulose extraction, lignin removal and disruption of cellulose crystallinity, promoting an acceleration of saccharification in lignocellulosic biomass. The effect of ultrasound on the lignocellulosic biomass can be explained due to the mechanical impacts produced by the collapse of the cavitation bubbles (Bundhoo and Mohee 2018; Wu et al. 2017).

Alkaline pretreatments are effective for lignin solubilization, exhibiting minor cellulose and hemicellulose solubilization than acid processes (Carvalheiro et al. 2008). Alkaline pretreatments can be performed at room temperature, and also produce less sugar degradation than acid pretreatment (Kumar et al. 2009, Zhang et al. 2016). NaOH causes swelling, increasing the internal surface of cellulose and decreasing the degree of polymerization and crystallinity, which provokes lignin structure disruption (Taherzadeh and Karimi, 2008).

Current research reported the combination of ultrasonication and an alkaline medium as a pretreatment of lignocellulosic materials. Subhedar et al. (2018) investigated the ultrasound-assisted delignification and enzymatic hydrolysis of three biomass types (groundnut shells, pistachio shell and coconut coir) and reported an approximate 80–100 % increase in delignification over conventional alkali treatments. Wang et al. (2017) studied the saccharification of grass clipping and reported that the solubilization of hemicellulose and lignin increased after ultrasound-alkaline pretreatment. In the last few years, several other authors studied the combination of ultrasonication and an alkaline medium as pretreatment of lignocellulosic materials, such as sugarcane bagasse (Velmurugan and Muthukumar 2012), newspaper (Subhedar and Gogate 2014), rice straw (Wu et al. 2017), chili post-harvest residue (Sidhu et al. 2017) and wood (Wang et al. 2019). The combination of ultrasonication and an alkaline medium was not reported in the literature for malt bagasse.

In this study, the combination of ultrasonication and alkaline medium was employed as pretreatment of malt bagasse to obtain fermentable sugars and a residual solid fraction that is more accessible to enzymatic hydrolysis.

Materials and methods

Malt bagasse

Malt bagasse was provided by Microcervejaria Fábrica 1 (Londrina-Paraná, Brazil), dried (60 °C) in an air-circulating oven (Marconi MA 035 – São Paulo, Brazil) for 24 h and milled to yield particles < 0.30 mm in size.

The chemical composition of the residue (proteins, lipids, moisture and ash) was determined by the Association of Official Analytical Chemists (AOAC) method (2003), and the total amount of carbohydrates was determined by calculating the difference. All samples were run in triplicate. Total dietary fiber and soluble and insoluble fractions were determined according to the American Association of Cereal Chemists method (AACC method 32-07, 1990).

Experimental design: ultrasonication in alkaline medium pretreatments

To evaluate the efficiency of the combination of ultrasonication in alkaline medium on malt bagasse, a complete factorial experimental design was chosen, consisting two independent variables at three levels of variation, resulting in 9 experimental runs (Table 1). The independent variables were pH (9, 10 and 11) and time (10, 35 and 60 min) and the levels of each variable were denoted as -1, 0 and +1 for statistical analysis. For all samples was employed biomass content 10 %. The variables and their levels were established based on preliminary experiments (data not shown). During this process, the temperature was controlled (± 25 °C) using a water bath.

All samples were submitted to ultrasonication using a Fisher Scientific Sonicator model 505, 50/60HZ, coupled with a probe with a tip diameter of 1.27 cm (Fisher Scientific model FB 4219, Pittsburgh, PA – USA). The ultrasonic treatments were carried out with an amplitude of 40 %. Alkaline solutions (200 mL) of each sample were prepared according to the experimental design (Table 1) employing NaOH 0.1 – 1.0 mol/L to adjust the pH. The samples submitted to ultrasonication in alkaline medium were vacuum filtered, and the liquid hydrolysate was recovered and neutralized with 0.1 mol/L H_2SO_4 solution until a pH range of 6.0-7.0 was achieved, and the sugar content was quantified. The residual solid fractions were washed with water to neutrality and dried at 40 °C in an air-circulating oven (Tecnal – São Paulo-Brazil) for further analysis.

Table 1 Factorial experimental design (3^2) and the results obtained for reducing sugars (RS), xylose and glucose contents of malt bagasse on liquid hydrolysates of samples submitted to ultrasonication in alkaline medium

Run	Independent variables Coded values (real values)		Response variables		
	X_1 Time (min)	X_2 pH	RS (g/100 g bagasse)	Xylose (g/100 g bagasse)	Glucose (g/100 g bagasse)
1	-1 (10)	-1 (9)	8.77	1.04	0.58
2	-1 (10)	0 (10)	9.17	0.98	0.57
3	-1 (10)	1 (11)	9.52	1.00	0.51
4	0 (35)	-1 (9)	7.74	1.08	0.42
5	0 (35)	0 (10)	8.29	1.12	0.42
6	0 (35)	1 (11)	8.62	1.10	0.32
7	1 (60)	-1 (9)	8.77	0.98	0.44
8	1 (60)	0 (10)	9.95	1.30	0.59
9	1 (60)	1 (11)	9.58	1.27	0.45

Determination of fermentable sugars on liquid hydrolysate

Reducing sugars (RS) were determined by the di-nitrosalicylic acid (DNS) method (Miller 1959), and the method of xylose determination was adapted from Pham et al. (2011). The glucose content was determined using a Sigma-Aldrich glucose assay kit (GAGO20, Missouri, USA).

Characterization of raw malt bagasse and the residual solid fraction resulted from pretreatments

Cellulose, hemicellulose and lignin contents

Cellulose and hemicellulose contents were determined by the Van Soest method (1967) and lignin content was determined by the Technical Association of the Pulp and Paper Industry method (TAPPI T222 om-88 method, 1999).

X-ray diffraction (XRD)

The samples were finely ground to a powder (particles < 0.18 mm in size), and the diffraction analysis was performed with a PANalytical X'Pert PRO MPD diffractometer (Netherlands) using copper Kα radiation (λ = 1.5418 Å), a voltage of 40 kV and a 30 mA current. Analysis was performed between 2θ = 5° and 2θ = 50°. All assays were performed with ramping at 1°/min. The crystallinity index (CI) was calculated using Equation 1 (Segal et al. 1959) as follows:

$$CI\ (\%) = ((I_{002} - I_{am})/I_{002})*100, \text{ Equation 1}$$

where I_{am} is the intensity of diffraction at 2θ = 18° (amorphous portion) and I_{002} is the maximum intensity of 002 lattice diffraction (approximately 2θ = 22°).

Thermogravimetric analysis (TGA)

Thermogravimetric analysis (TGA 50, Shimadzu, Japan) was conducted under a nitrogen atmosphere (50 mL min^{-1}), and the samples were heated from 25 to 600 °C at a heating rate of 10 °C/min. The weight loss (%) was evaluated by measuring the residual weight at 600 °C.

Fourier transform-infrared spectroscopy (FT-IR)

Samples were ground (particles < 0.18 mm in size), mixed with potassium bromide and compressed into tablets. FT-IR analysis was conducted with a Shimadzu FT-IR-8300 (Japan), which has a spectral resolution of 4 cm^{-1} and a spectral range of 4000-500 cm^{-1}.

Scanning electron microscopy (SEM)

SEM analysis was performed with an FEI Quanta 200 microscope (Oregon, USA). Dried samples were mounted for visualization on bronze stages using double-sided tape. The surfaces were then coated with a thin gold layer (40-50 nm thickness). All samples were examined using an accelerating voltage of 30 kV.

Statistical analysis

Experimental data were analyzed to fit second order polynomial equations to response variables, which included reducing sugars (RS), xylose and glucose. Surface plots were generated from complete models using Statistica (Statsoft, Oklahoma, U.S.A.) computer software.

Results and discussion

Chemical composition of malt bagasse

The chemical composition of raw malt bagasse used in this study consisted of the following composition: 20.60 ± 0.84 % proteins, 9.10 ± 0.35 % lipids, 4.11 ± 0.18 % ash, 4.04 ± 0.49 % moisture, 1.34 ± 0.34 % carbohydrates and 60.80 ± 0.32 % total dietary fiber, with a cellulose content of 8.66 ± 1.02 %, hemicellulose content of 26.76 ± 1.23 % and lignin content of 25.38 ± 1.89 %. Ravindran et al. (2018) reported values for hemicellulose (26.94 %) and lignin (30.48 %) contents close to our values, and a higher cellulose content (19.21 %). Similarly, Mussato et al. (2008) reported hemicellulose (28.4 %) and lignin (27.8 %) contents very close to our values and also a higher cellulose content (16.8 %). These differences can be related to the barley variety, harvest time or mashing conditions (Forssell et al. 2008).

Effects of pretreatment on fermentable sugar production

The Table 1 shows the results of RS, xylose and glucose content. These results were statistically analyzed, and the regression coefficients of the second order equations (models) and the analysis of variance (ANOVA) of these mathematical models are shown in Table 2.

Table 2 Regression coefficients and ANOVA of mathematical models obtained for RS, xylose and glucose [a]

Coefficient	RS	Xylose	Glucose
β_0	8.42	1.09	0.44
β_1	0.14	0.09*	-0.03
β_2	0.40*	0.04	-0.02
β_{11}	1.07*	-	0.14*
β_{22}	-0.30	-	-0.07
β_{12}	0.01	0.08	0.02
R^2	0.94	0.76	0.90
Model (p)	0.0467	0.2296	0.1090

[a] – β_1 = time; β_2 = pH and *$p \leq 0.05$

The coefficients of determination (R^2) were considered satisfactory for RS and glucose models (≥ 0.90), for xylose the R^2 was low and the model was employed to study only the tendency of the response and it was not employed to predict or to optimize the process. The model obtained for RS ($p = 0.0467$) were significant at 5% of significance ($p \leq 0.05$), whereas, for xylose (0.2296) and glucose (0.1090) were not significant ($p > 0.05$) at this significance level (Table 2).

For RS response (Table2), linear effect of pH (X_2) and quadratic effect of time (X_{11}) were positive and significant ($p \leq 0.05$), while for xylose and glucose responses, the linear (X_1) and quadratic (X_{11}) effects of time were positive and significant ($p \leq 0.05$), respectively (Table 2). In Figure 1 it can be observed the effects of time and pH on RS, xylose and glucose responses.

Maximum RS values were obtained when malt bagasse was submitted to longer ultrasonication times combined to higher pH values (Fig. 1A and Table 1). Wang et al. (2017) reported that compared with alkaline pretreatment, the combination of ultrasound and alkaline pretreatment was more effective in release RS from lignocellulosic materials. Zhang et al. (2008) also found that the decomposition rate of corn stover pretreated by ultrason-alkaline was higher than that of single alkaline pretreatment. Subhedar and Gogate (2014) reported that the combination of ultrasonication and an alkaline medium can overcome the one important limitation associated to the alkaline pretreatment of lignocellulosic biomass that is relatively the use of longer pretreatment times. It is important to point out that in this study we employed ultrasonication times ranging from 10 to 60 min, which are similar to processing times employed by Velmurugan and Muthukumar (2012) and Wu et al. (2017), which studied the ultrasound-assisted alkaline pretreatment of sugarcane bagasse (5–50 min) and rice straw (60 min), respectively, while Wang et al. (2017) reported processing times ranging from 1 to 80 h for the study of ultrasound-assisted alkali ne pretreatment of grass clipping and Subhedar et al. (2018) reported processing times from 1 to 7 h.

The longer processing time (60 min) resulted in higher xylose (Fig. 1B) and glucose releasing from malt bagasse, which is associated to the combined effect of shear forces and shock waves from ultrasonication and the reactive hydroxyl radicals generated by cavitation that can attack the lignocellulosic constituents, resulting in disruption of the lignocellulose matrix (Wu et al. 2017). It can be observed the higher xylose release in all conditions compared to glucose (Table 1), and it is related to the composition of malt bagasse hemicellulose, which consists of a xylan backbone (approximately 70 %), while the remaining 30 % is an arabinan structure (Mussato and Roberto 2005). According to Wang et al. (2018), ultrasound-alkaline pretreatment was more efficient on removing hemicellulose and lignin from grass clipping than only the alkaline pretreatment and considering that hemicellulose and lignin are the main components of cellulose-hemicellulose-lignin network, after lignin removal and hemicellulose degradation, certainly a further saccharification process by enzymatic hydrolysis will be enhanced.

Fig. 1 Contour plots of reducing sugars (A), xylose (B) and glucose (C) on liquid hydrolysate from malt bagasse samples submitted to ultrasonication in alkaline medium

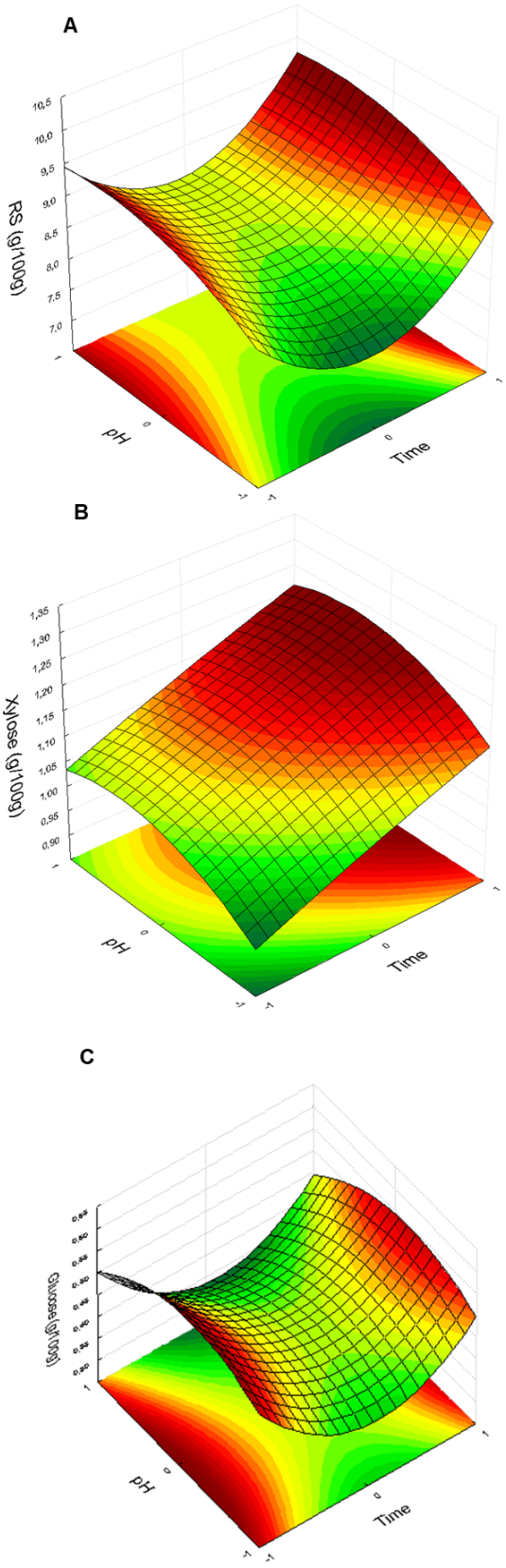

Effects of pretreatment in the residual solid fraction recovered after malt bagasse was submitted to ultrasonication in alkaline medium

Cellulose, hemicellulose and lignin contents

In the residual solid fraction recovered after malt bagasse has been submitted to ultrasonication in alkaline medium were quantified cellulose, hemicellulose and lignin contents. The cellulose contents ranged from 7.51 to 17.95 % (Table 3) and the samples 1 (8.75 %), 3 (7.51 %) and 4 (7.99 %) had the lower cellulose values, which were not statistically different from raw malt bagasse (8.66 %). The higher cellulose values were obtained for samples submitted to the experiments 9, 6 and 5, with 17.95, 16.29 and 15.99 % cellulose, respectively, in these samples the cellulose content increased about twice after the pretreatment compared to raw malt bagasse.

The hemicellulose contents ranged from 30.27 to 55.43 % (Table 3), and all pretreated samples presented significantly ($p \leq 0.05$) higher hemicellulose contents than raw malt bagasse (26.76 % hemicellulose), except the sample submitted to experiment 1, which consisted of low time and low pH condition. The samples submitted to experiments 8 and 9 had hemicellulose contents 1.98 and 2.07 times higher than raw malt bagasse, respectively, and both were submitted to the highest time of ultrasonication (60 min).

The lignin content of the residual solid fraction ranged from 17.56 to 33.72 % (Table 3), the majority of experiments presented significantly lower ($p \leq 0.05$) lignin content when compared to raw malt bagasse (25.38 %), demonstrating the lignin removal after employed pretreatment.

For all pretreated samples, the insoluble fiber content (sum of cellulose, hemicellulose and lignin) was significantly greater than raw malt bagasse (Table 3), indicating that other components such as lipids, proteins and ash were removed from malt bagasse.

The residual solid fraction resulted from raw malt bagasse submitted to the experiment 9 presented the best combination of results, consisting of 97.31 % insoluble dietary fibers, 17.95 % cellulose, 55.43 % hemicellulose and 23.93 % lignin. These results demonstrate the impacts of ultrasonication in alkaline medium on disruption of lignocellulosic matrix of the malt bagasse. Several studies have reported the effects of pretreatments that combine ultrasonication and alkaline medium on lignocellulosic materials. Subhedar and Gogate (2014) and Wang et al. (2017) reported that the use of alkaline pretreatment can be improved by application of combined ultrasound, they stressed that the turbulence generated by cavitation results in increased delignification extent. According to Velmurugan and Muthukumar (2012), the delignification occurs because the oxidation of lignin matrix by hydroxyl radicals formed during sonication. Subhedar et al. (2018) reported that alkaline pretreatment results in lignin decomposition due to the rupture of aryl ether linkages in the lignin catalyzed by hydroxyl ions. Soontornchaiboon et al. (2016) obtained reduced lignin contents and increased cellulose concentrations using ultrasound-assisted alkali pretreatment on several agricultural wastes, and Subhedar et al. (2018) demonstrated the satisfactory effects of ultrasound-assisted alkaline pretreatment on lignocellulosic materials as groundnut shells, coconut coir and pistachio shells.

Table 3 Composition and crystallinity index (CI) of solid fraction of malt bagasse recovered after ultrasonication in alkaline medium[a]

Run	Cellulose (%)	Hemicellulose (%)	Lignin (%)	Insoluble dietary fibers (%)	Others[b] (%)	CI (%)
1	8.75^{c}	30.27^{c,d}	33.72^{a}	72.73^{c}	27.70^{c}	42.6
2	12.38^{b}	41.20^{b}	28.76^{a,b}	82.34^{b}	17.66^{d}	39.5
3	7.51^{c}	32.59^{c}	22.05^{c}	62.16^{d}	37.84^{a}	11.1
4	7.99^{c}	32.31^{c}	21.24^{c}	61.53^{d}	38.47^{a}	36.0
5	15.99^{a}	44.26^{b}	20.63^{c}	80.87^{b}	19.13^{d}	37.8
6	16.29^{a}	35.52^{c}	17.56^{d}	69.38^{c,d}	30.62^{b,c}	20.0
7	13.07^{b}	31.70^{c}	21.95^{c}	66.72^{c,d}	33.28^{b}	32.3
8	11.42^{b}	53.21^{a}	33.01^{a}	97.63^{a}	2.37^{e}	34.1
9	17.95^{a}	55.43^{a}	23.93^{b,c}	97.31^{a}	2.69^{e}	38.3
Raw malt bagasse	8.66^{c}	26.76^{d}	25.38^{b}	60.80^{d}	39.20^{a}	15.0

[a-] Different small letters in the same column indicate significant differences between means (Tukey test, $p \leq 0.05$)

[b-] Ash, proteins, lipids

X-ray diffraction (XRD)

The diffractograms of the samples that had higher (experiments 5, 6 and 9) and lower (experiments 3 and 4) cellulose contents in comparison to raw malt bagasse are shown in Fig. Malt bagasse samples submitted to ultrasonication in alkaline medium demonstrated similar crystalline patterns that raw malt bagasse, with a single, defined peak at $2\theta = 22°$, attributed to the structure of the native cellulose (Nishino et al. 2014), while the amorphous region was obtained at around at $2\theta = 18°$ (Fig. 2).

The CI of pretreated samples ranged from 11 to 38 % and the CI of malt bagasse was 15 % (Table 3), which can be attributed to its high protein (20.60 %), lipid (9.10 %), hemicellulose (26.76 %) and lignin (25.38 %) contents, all of these contributing to the amorphous fraction of malt bagasse.

All pretreated sample presented higher CI values when compared to raw malt bagasse (Table 3), except the sample submitted to the experiment 3 (10 min, pH 11) that presented a CI of 11 %; this sample presented the lower cellulose content (7.51 %). In general, the ultrasonication combined to the alkaline pretreatment resulted in more crystalline materials, and this could be explained by the increase in cellulose content of pretreated samples, and also by the removal of amorphous lignin and other amorphous components from raw malt bagasse, such as lipids and proteins.

Fig. 2 XRD diffractograms obtained of raw malt bagasse and malt bagasse samples submitted to ultrasonication in alkaline medium: Experiment 3 (pH 11, 10 min), experiment 4 (pH 9, 35 min), experiment 5 (pH 10, 35 min), experiment 6 (pH 11, 35 min) and experiment 9 (pH 11, 60 min)

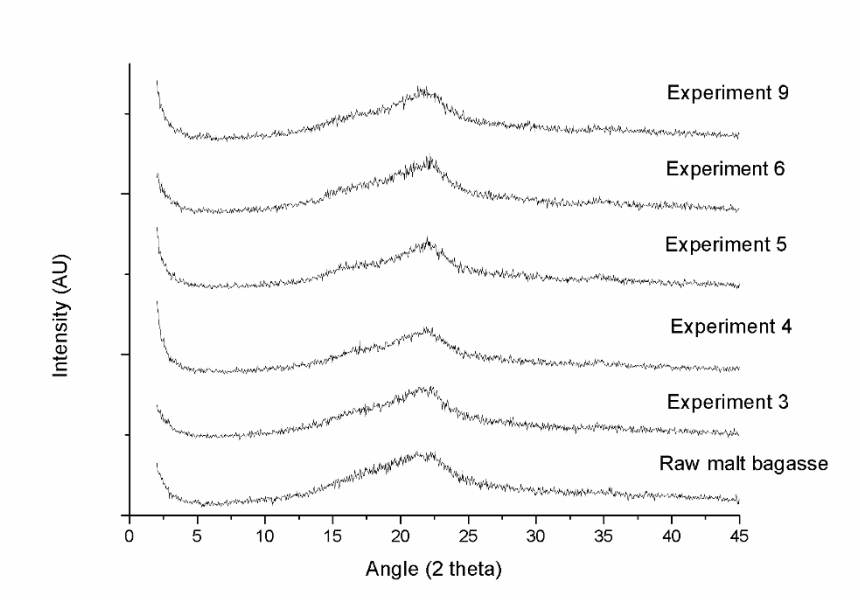

Thermogravimetric analysis (TGA)

The curves obtained from the TGA analysis (not shown) were used to examine the changes caused by ultrasonication in alkaline medium on T_{max} (temperature corresponding to the maximum rate of mass loss), T_{10} (temperature corresponding to 10 % mass loss), T_{50} (temperature corresponding to 50 % mass loss) and M_{600} (mass loss at 600 °C) (Table 4).

The thermograms of the samples that had higher (experiments 5 and 9) and lower (experiments 3 and 4) cellulose contents in comparison to raw malt bagasse. It was observed a three-stage decrease in weight (figure not shown) for all samples. Subhedar et al. (2018) and Subhedar and Gogate (2014) also observed a three-stage weight for lignocellulosic materials analyzed by TGA.

In the first stage (50 – 125 ºC), a small weight loss (< 10 %) was found for all samples corresponding to the residual moisture losses and also to the evaporation of other low molecular weight compounds present in the lignocellulosic residues (Ibrahim et al. 2010; Subhedar et al. 2018).

A second degradation stage was observed for all samples from the great slope of the TGA curves (not shown), which showed a double-peak distribution at 300-321 °C and 354-380 °C (Table 4), with the first group of peaks corresponding to hemicellulose decomposition and the second group corresponding to cellulose decomposition. Subhedar et al. (2018) also attributed this second stage to hemicellulose and cellulose degradation, which occurs between 200 and 400 ºC.

A third-stage degradation was observed in all samples in the thermograms at temperatures above 450-500 °C (figure not shown), and it could be associated with lignin. According to Subhedar and Gogate (2014), the thermal decomposition of lignin is very complex and depends on its origin, it occurs over a broad temperature interval (120 – 600 º C), because various oxygen functional groups from lignin have different thermal stabilities and their scission occurs at different temperatures.

All samples submitted to ultrasonication in alkaline medium presented higher thermal stability than raw malt bagasse (Table 4), which was demonstrated by the greater T_{10} and T_{50} values for all pretreated samples. The mass loss at 600 °C (M_{600}) was 77 % for raw malt bagasse (Table 4), and for the pretreated samples it ranged ranging from 74 to77 %.

Table 4 TGA parameters of malt bagasse samples submitted to ultrasonication in alkaline medium

	TGA parameters				
Run	T_{max1} (ºC)	T_{max2} (ºC)	T_{10} (ºC)	T_{50} (ºC)	M_{600} (%)
1	307	380	267	372	77
2	313	377	277	370	76
3	321	366	267	365	74
4	311	376	276	373	75
5	319	371	282	366	75
7	300	376	264	369	76
8	312	356	258	351	77
9	307	355	244	351	76
Raw malt bagasse	310	354	217	346	77

T_{max} = temperature corresponding to the maximum rate of mass loss, T_{10} = temperature corresponding to 10 % mass loss, T_{50} = temperature corresponding to 50 % mass loss and M_{600} = mass loss at 600 ºC

Fourier transform-infrared spectroscopy (FT-IR)

The FT-IR spectra of pretreated were very close to each other (Fig. 3), indicating that the samples had similarities in their chemical groups before and after the pretreatment. In all samples can be observed a wide absorption band centered at 3500 cm^{-1}, which was attributed to the stretching of aliphatic and phenolic OH bands from cellulose, hemicellulose and lignin (Wu et al. 2017).

In all FT-IR spectra it was observed bands observed at 2900 cm^{-1} corresponding to -C-H stretching, H-C-H- and -C-O-H-conjugated bending vibrations (Fig. 3). In raw malt bagasse a shoulder peak was observed at 2850 cm^{1}, which is characteristic of $-OCH_3$ from lignin (Adel et al., 2010) and this band was weakened in all pretreated samples, which is attributed to the depolymerization of lignin during the pretreatment process).

It was also found a reduction in band intensities corresponding to aromatic ring stretch (1635 cm^{-1}) attributed to the removal of lignin in the experiments 9, 6 and 5, which presented higher cellulose and lower lignin contents. Our study is according to Singh et al. (2014) who reported that the reduction in this band intensity corresponds to lignin removal after treatment of the biomass with ultrasound in alkaline medium.

The main differences in the spectra between the pretreated samples and raw malt were observed in the region between 1750-900 cm^{-1} (Fig. 3). Samples submitted to experiments 9, 6 and 5 presented weakened bands in this region, probably due to changes in sample composition after pretreatment. In these samples, the band at 1750 cm^{-1} that corresponds to C=O stretching in carbonyl groups from lignin and hemicellulose (Wu et al. 2017) appeared more defined than in the malt bagasse spectrum, possibly because other components (lipids, proteins,

ashes) were removed from these samples, resulting in materials with higher insoluble dietary fiber contents (Table 3).

Fig. 3 FTIR spectra obtained of raw malt bagasse and malt bagasse samples submitted to ultrasonication in diluted acid medium: (Experiments 3, 4, 5, 6 and 9)

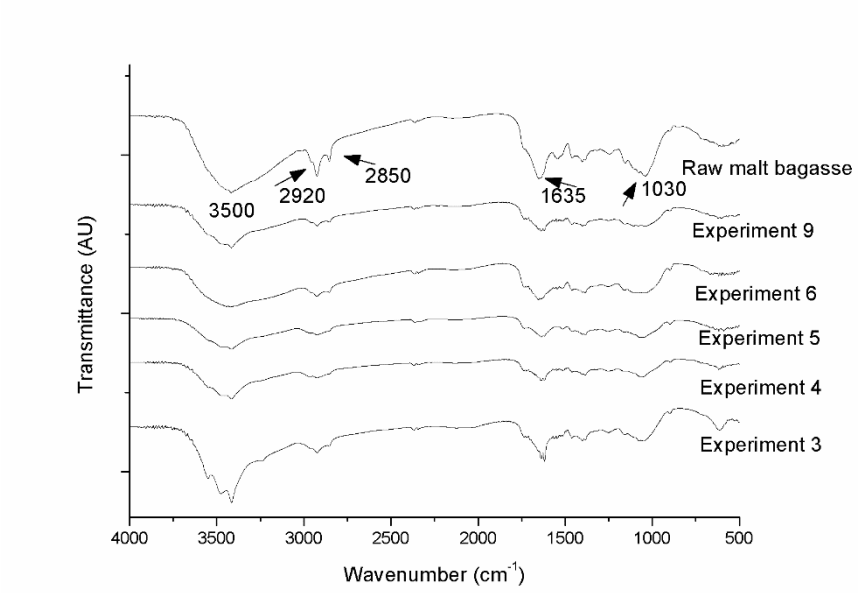

Scanning electron microscopy (SEM)

The morphological changes observed on malt bagasse surface resulted from pretreatment were examined by SEM. Samples from experiments 3 (Fig. 4b) and 4 (Fig. 4c) were the samples with lower cellulose contents and samples from experiments 5 (Fig. 4d), experiments 7 (Fig. 4e), experiments 8 (Fig. 4f) and 9 (Fig. 4g) were the samples with higher cellulose contents.

Raw malt bagasse (Fig. 4a) presented a compact structure, which is typical of lignocellulosic materials, with lignin and hemicellulose deposited between the cellulosic microfibrils forming an interrupted lamellar structure. The compact structure of lignocellulosic materials is associated with the presence of H-bonding, covalent O-H bond and Van der Waal's interactions between cellulose, hemicellulose and lignin (Subhedar and Gogate, 2014).

The employed pretreatment changed the surface of all samples in different degrees, samples with lower cellulose contents from experiments 3 (Fig. 4b) and 4 (Fig. 4c) were affected in a lower degree, and some pores and cracks were observed in these samples surfaces. Samples obtained from experiments 5 (Fig. 4d), experiments 7 (Fig. 4e), experiments 8 (Fig. 4f) and 9 (Fig. 4g) were the samples with higher cellulose contents, and these samples appeared to be affected in a higher extension, with several and large pores, exposing their internal content. According to Wu et al. (2017), the formed cracks and voids can be attributed to the combined effect of ultrasound and an alkaline medium, which can acts degrading ester bonds and cleaving glycosidic linkages in the lignocellulosic matrix, resulting in the alteration of the structure of lignin, the reduction of the lignin-hemicellulose complex, and the increased porosity and surface area of lignocellulosic materials. Soontornchaiboon et al. (2016)

and Wang et al. (2017) reported fracture and roughness of the surface of lignocellulosic biomass treated with ultrasound, and these structural changes can improve the enzymatic accessibility to cellulose and hemicellulose.

Fig. 4 SEM micrographs of raw malt bagasse (a) and malt bagasse samples submitted to ultrasonication in alkaline medium: (b) Experiment 3 (pH 11, 10 min), (c) experiment 4 (pH 9, 35 min), (d) experiment 5 (pH 10, 35 min), (e) experiment 7 (pH 9, 60 min), (f) experiment 8 (pH 10, 60 min) and experiment 9 (pH 11, 60 min)

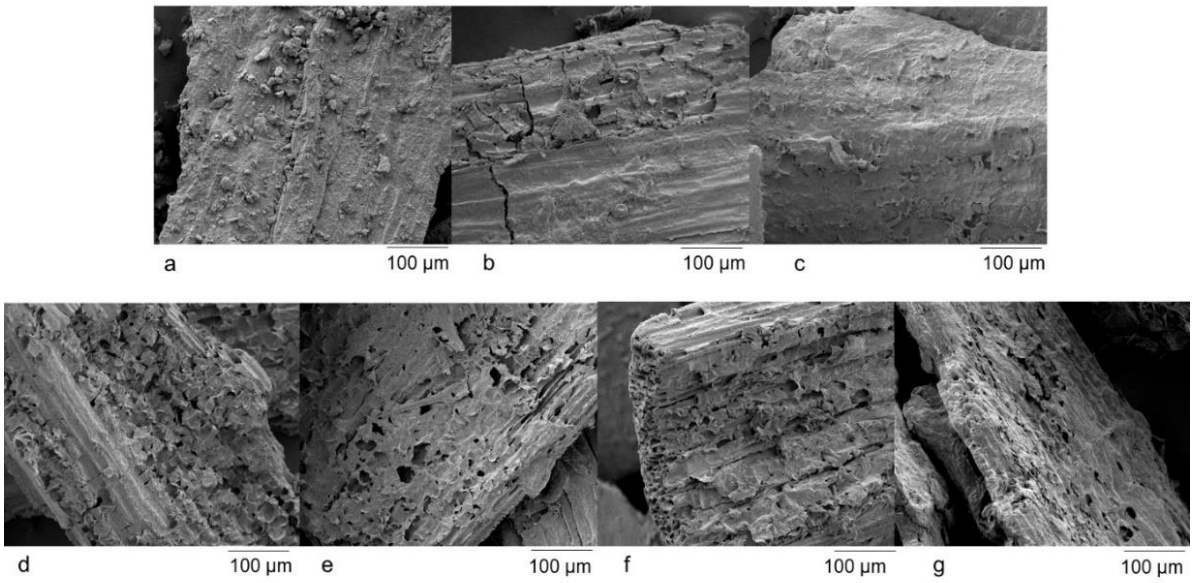

Conclusion

The ultrasonication combined with alkaline medium demonstrated be effective when employed as pretreatment of malt bagasse, indicating great potential to obtain fermentable sugars.

In the experimental conditions employed in this study, the time was the most important variable, which resulted in higher sugars release and greater changes in the residual solid fraction recovered after pretreatment. The sample processed at pH 11 for 60 min resulted in higher cellulose content and lignin removal compared to raw malt bagasse, and this condition was also effective in the removal of other components, such as ash, lipids and proteins, which resulted in higher insoluble dietary fiber content.

The effectiveness of ultrasonication combined to an alkaline medium in the deconstruction of lignocellulosic matrix was confirmed by the increase in cellulose and decrease in lignin contents, and also by increase in crystallinity index and thermal stability of the pretreated samples. In addition, increasing the porosity at the surface of the fiber improves the access of enzymes to the enzymatic hydrolysis.

Acknowledgments

The authors thank the Laboratory of Microscopy and Microanalysis (LMEM) and the Laboratory of X-ray Diffraction (LDRX) at the State University of Londrina for the analysis, Fundação Araucária for financial support and CAPES for the doctoral grant of Léa Rita P.F. Mello.

Compliance with ethical standards

Conflict of interest - The authors declare that there is no conflict of interest.

Authors Contributions

Léa Rita P. F. Mello performed all the laboratory activities related to this study, she elaborated the figures and tables from the experimental results and discussed the results.

Suzana Mali supervised the entire execution of the experimental part of this study and assisted in supervising the whole process of writing the manuscript.

References

AACC - American Association of Cereal Chemists (1990) Approved methods of the American association of cereal chemists. St Paul MN: AACC.

Abdullah SS, Yusup S, Ahmad MM, Ramli A, Ismail L (2010) Thermogravimetry study on pyrolysis of various lignocellulosic biomass for potential hydrogen production. International journal of chemical and biological engineering. Int J Chem Biol Eng 3:137–141

Adel AM, El–Wahab ZHA, Ibrahim AA, Al–Shemy MT (2010) Characterization of microcrystalline cellulose prepared from lignocellulosic materials. Part I. Acid catalyzed hydrolysis. Bioresour Technol 101: 4446–4455

AOAC – Official Methods of Analysis, 14th ed. Ass Off (2003) Analytical Chem Washington. USA

Bhowmick GD, Sarmah, AK, Sen R. (2018) Lignocellulosic biorefinery as a model for sustainable development of biofuels and value added products. Bioresour Technol 247:1144–1154

Bundhoo ZM and Mohee R (2018) Ultrasound-assisted biological conversion of biomass and waste materials to biofuels: A review. Ultrason Sonochem 40:298–313

Carvalheiro F, Duarte LC, Gírio FM (2008) Hemicellulose biorefineries: a review on biomass pretreatments. J Sci Ind Res 67:849-864

Forssell P, Kontkanen H, Schols HA, Hinz S, Eijsink VGH, Treimo J, Robertson JA, Waldron KW, Faulds CB, Buchert J (2008) Hydrolysis of brewers' spent grain by carbohydrate degrading enzymes. J Inst Brew114:306–314

Hassan SS, Williams GA, Jaiswal AK (2018) Emerging Technologies for the Pretreatment of Lignocellulosic Biomass. Bioresour Technol 262:310–318

Hay JX W, Wu TY, Juan JC, Jahim JM (2015). Improved biohydrogen production and treatment of pulp and paper mill effluent through ultrasonication pretreatment of wastewater. Energy Convers Manag 106:576-583

Ibrahim MM, Agblevor FA and El-Zawawy WK (2010) Isolation and characterization of cellulose and lignin from steam-exploded lignocellulosic biomass. BioResources 5:397–418

Kumar P, Barrett DM, Delwiche MJ, Stroeve P (2009) Methods for pretreatment of lignocellulosic biomass for efficient hydrolysis and biofuel production. Ind Eng Chem Res 48: 3713–3729

Mello LRPF, Mali S (2014) Use of malt bagasse to produce biodegradable baked foams made from cassava starch. Ind Crop Prod 55:187–193

Miller G (1959) Use of dintrosalicilic acid reagent for determination of reducing sugars. Anal Chem 31:426 – 428, 1959

Mussatto SI and Roberto IC (2005) Acid hydrolysis and fermentation of brewer's spent grain to produce xylitol. J Sci Food Agr 85:2453–2460

Mussatto SI, Fernandes M, Milagres AM, Roberto IC (2008) Effect of hemicellulose and lignin on enzymatic hydrolysis of cellulose from brewer's spent grain. Enzyme Microb Technol 43:124–129

Nishino T, Matsuda I, Hirao K (2004) All-cellulose composite. Macromolecules 7:7683–7687

Pham PJ, Hernandez R, French WT, Estill FB, Mondala AHA (2011) Spectrophotometric method for quantitative determination of xylose in fermentation médium. Biomass Bioenerg 35:2814–2821

Ravindran R, Jaiswal S, Abu-Ghannam N, Jaiswal AK (2018) A comparative analysis of pretreatment strategies on the properties and hydrolysis of brewers' spent grain. Bioresour Technol 248:272-279

Segal L, Creely JJ, Martin AE Jr, Conrad CM (1959) An empirical method for estimating the degree of crystallinity of native cellulose using the X-ray diffractometer. Text Res J 29:786–794

Singh S, Bharadwaja STP, Yadav PK, Moholkar VS (2014) Mechnistic investigation in ultrasound-assisted (Alkaline) delignification of Parthenium hysterophorus biomass. Ind Eng Chem Res 53:14241-14252.

Sindhu R, Binod P, Mathew K, Abraham A, Gnansounou E, Ummalyma, SB, Pandey A (2017) Development of a novel ultrasound-assisted alkali pretreatment strategy for the production of bioethanol and xylanases from chili post harvest residue. Bioresour Technol 242:146–151

Soontornchaiboon W, Kim SM, Pawongrat R (2016) Effects of alkaline combined with ultrasonic pretreatment and enzymatic hydrolysis of agricultural wastes for high reducing sugar production. Sains Malaysiana 45:955–962.

Subhedar PB, Gogate PR (2014) Alkaline and ultrasound assisted alkaline pretreatment for intensification of delignification process from sustainable raw-material. Ultrason Sonochem 21:216– 225

Subhedar PB, Ray P and Gogate PR (2018) Intensification of delignification and subsequent hydrolysis for the fermentable sugar production from lignocellulosic biomass using ultrasonic irradiation. Ultrason Sonochem 40:140–150

Taherzadeh MJ and Karimi K (2008) Pretreatment of lignocellulosic wastes to improve ethanol and biogas production: a review. Int J Mol Sci 9:1621–1651

TAPPI Test Methods T 222 om-88 (1999) Acid insoluble lignin wood and pulp. Atlanta

Van Soest PJ (1967) Use of detergents in the analysis of fibrous feeds. IV. Determination of plant cell-wall constituents. Journal of Association Officials of Animal Chemistry 50:50–55

Velmurugan R and Muthukumar K (2012) Ultrasound-assisted alkaline pretreatment of sugarcane bagasse for fermentable sugar production: optimization through response surface methodology. Bioresour Technol 112:293–299

Wang S, Li F, Zhang P, Jin S, Tao X, Tang X, Wang H (2017). Ultrasound assisted alkaline pretreatment to enhance enzymatic saccharification of grass clipping. Energ Convers Manage149:409-415

Wang Z, Qu L, Qian J, He Z, Yi S (2019). Effects of the ultrasound-assisted pretreatments using borax and sodium hydroxide on the physicochemical properties of Chinese fir. Ultrason Sonochem 50: 200-207.

Wu H, Dai X, Zhou S, GanY, Xiong Z, Qin Y, Ma J, Yang L, Wu Z, Wang T, Wang W, Wang C (2017) Ultrasound-assisted alkaline pretreatment for enhancing the enzymatic hydrolysis of rice straw by using the heat energy dissipated from ultrasonication. Bioresour Technol 241:70–74

Zhang Y, Fu E, Liang J. (2008) Effect of ultrasonic waves on the saccharification processes of lignocellulose. Chem Eng Technol. 31:1510–5.

Zhang Z, Xie Y, He X, Li X, Hu J, Ruan Z, Zhao S, Peng N, Liang Y (2016) Comparison of high-titer lactic acid fermentation from NaOH- and NH_3-H_2O_2-pretreated corncob by Bacillus coagulans using simultaneous saccharification and fermentation. Sci. Rep 6:37245

7 CONSIDERAÇÕES FINAIS

Os resíduos lignocelulósicos são um potente recurso na geração de novos produtos, possibilitando o desenvolvimento sustentável e preservação do meio ambiente. Este trabalho estudou a aplicação do bagaço de malte como bioadsorvente e a combinação de pré-tratamentos para a obtenção de açúcares fermentescíveis, com o propósito de reaproveitamento e valorização do bagaço de malte.

O comportamento sortivo do bagaço de malte foi estudado para avaliar o seu potencial de aplicação como um bioadsorvente de chumbo em soluções aquosas. A rápida e elevada eficiência na sorção de íons de chumbo demonstrou que este resíduo é um material com potencial de aplicação como bioadsorvente na remoção de chumbo em águas contaminadas.

O pré-tratamento de ultrassonicação em meio ácido mostrou-se eficaz para a obtenção de açúcares e aumento da porosidade superficial da fibra do bagaço de malte, que é importante no processo de hidrólise enzimática subsequente. Os maiores teores de celulose foram obtidos com o maior tempo de tratamento, não sendo influenciado pelo pH, no entanto, a remoção de lignina foi pouco efetiva.

A ultrassonicação combinada ao meio alcalino obteve melhores resultados na liberação de açúcares comparado ao pré-tratamento com meio ácido, demostrando ser mais efetivo na desconstrução da matriz lignocelulósica. Neste tratamento, o teor de celulose também foi maior com o tempo de tratamento mais longo. Além disso, o efeito do tempo de tratamento promoveu maiores alterações na fração sólida residual. No geral, a combinação de ultrassonicação com meio alcalino demonstrou maior eficiência no pré-tratamento do bagaço de malte.

REFERÊNCIAS

ABDOLALI, A.; NGO, H. H.; GUO, W.; LU, S.; CHEN, S. S.; NGUYEN, N. C.; WU, Y. A breakthrough biosorbent in removing heavy metals: Equilibrium, kinetic, thermodynamic and mechanism analyses in a lab-scale study. **Science of the Total Environment**, v. 542, p. 603-611, 2016.

AGRARIA - Disponível em: http://www.agraria.com.br/maltes.php. Acesso em janeiro de 2019.

AKUNWA, N. K.; MUHAMMAD, M. N.; AKUNNA, J. C. Treatment of metal-contaminated wastewater: A comparison of low-cost biosorbents. **Journal of environmental management**, v. 146, p. 517-523, 2014.

ANVISA - Agência Nacional de Vigilância Sanitária. Resolução - CNNPA nº 12, de 1978. D.O. de 24/07/1978.

ASCHERI, D. P.; BURGER, M. C. DE M.; MALHEIROS, L. V.; OLIVEIRA, V. N. Curvas de secagem e caracterização de hidrolisados de bagaço de cevada. **47º CBQ – Congresso Brasileiro de Química**- Natal- RN. 2007. http://www.abq.org.br/cbq/2007/. Acesso em novembro de 2018.

ALVIRA P.; TOMAS-PEJO, E.; BALLESTEROS, M.; NEGRO, M. J. Pretreatment technologies for an efficient bioethanol production process based on enzymatic hydrolysis: A review. **Bioresource Technology**, v. 101, p. 4851–4861, 2010.

ANNADURAI, G.; JUANG, R. S.; LEE, D. J. Adsorption of heavy metals from water using banana and orange peels. **Water Science and Technology**, v. 47, p.185-190, 2003.

BASU, M.; GUHA, A. K.; RAY, L. Adsorption of lead on cucumber peel. **Journal of cleaner production**, v. 151, p. 603-615,2017.

BENVINDO DA LUZ, A.; et al.; **Tratamento de minérios,** 3ra edição rev. e ampliada. Rio de Janeiro: CETEM/MCT, 2002.

BETANCUR, G. J. V., PEREIRA JUNIOR, N. Sugarcane bagasse as feedstock for second generation ethanol production. Part 1: diluted acid pretreatment optimization. **Electronic Journal of Biotechnology***,* v. 1, p. 1–9, 2010.

BHOWMICK, G. D.; SARMAH, A. K.; SEN R. Lignocellulosic biorefinery as a model for sustainable development of biofuels and value added products. **Bioresource Technology**, v. 247, p. 1144–1154, 2018.

BON, E. P. S.; FERRARA, M. A.; CORVO, M. L. **Enzimas em Biotecnologia: produção, aplicações e mercado.** Rio de Janeiro: Interciência, p.506, 2008.

BROCHIER, M. A.; CARVALHO, S. Environmental, productive and economic aspects of use of brewery residue as food of lamb feedlots in finishing phase. **Ciências Agrotécnicas**, Lavras, v. 33, n. 5, p. 1392-1399, 2009.

BUNDHOO, Z. M. A.; MOHEE. Ultrasound-assisted biological conversion of biomass and waste materials to biofuels: A review. **Ultrasonics Sonochemistry**, v. 40, p. 298-313, 2018.

CANILHA, L.; MILAGRES, A. M. F.; SILVA, S. S.; SILVA, J. B. A.; FELIPE, M. G. A.; ROCHA, G. J. M.; FERRAZ, A.; CARVALHO, W. Sacarificação da Biomassa Lignocelulósica Através de Pré-hidrólise Ácida Seguida Por Hidrólise Enzimática: Uma Estratégia de "Desconstrução" da Fibra Vegetal. **Revista Analytica**, n. 44, dezembro 2009/janeiro, 2010.

CANILHA, L.; CHANDEL, A. K.; MILESSI, S. S. T.; ANTUNES, F. A. F.; FREITAS, W. L. C.; FELIPE, M. G. A.; SILVA, S. S. Bioconversion of sugarcane biomass into ethanol: an overview about composition, pretreatment methods, detoxification of hydrolysates, enzymatic saccharification, and ethanol fermentation. **BioMed Research International**, 2012.

CARVALHEIRO, F.; DUARTE, L. C.; GÍRIO, F. M. Hemicellulose biorefineries: a review on biomass pretreatments. **Journal of Scientific & Industrial Research**, v. 67, p. 849-864, 2008.

CASTRO, A. M.; PEREIRA JR. N. Produção, Propriedades e Aplicação de Celulases na Hidrólise de Resíduos Agroindustriais. **Química Nova**, vol. 33, No. 1, p. 181-188, 2010.

CHOI, S. B.; YUN, Y. S.; Biosorption of cadmium by various types of dried sludge an equilibrium study and investigation of mechanisms. **Journal of Hazardous Materials**. B138, P. 378–383, 2006.

CONRAD, K.; HANSEN, H. C. B. Sorption of zinc and lead on coir. **Bioresource Technology**, v. 98, n. 1, p. 89-97, 2007.

CORREIA, I. K.S.; SANTOS, P. F.; SANTANA, C. S.; NERIS, J. B; LUZARDO, F. H.; VELASCO, F. G. Application of coconut shell, banana peel, spent coffee grounds, eucalyptus bark, piassava (*Attalea funifera*) and water hyacinth (*Eichornia crassipes*) in the adsorption of Pb2+ and Ni2+ ions in water. **Journal of Environmental Chemical Engineering**, v. 6, p. 2319-2334, 2018.

DĄBROWSKI, A. Adsorption—from theory to practice. **Advances in colloid and interface science**, v. 93, n. 1-3, p. 135-224, 2001.

DASGUPTA, D.; BANDHU, S.; ADHIKARI, D. K.; GHOSH, D. **Challenges and prospects of xylitol production with whole cell bio-catalysis: a review.** Microbiological research, v. 197, p. 9-21, 2017.

DEMIRBAS, A. Heavy metal adsorption onto agro-based waste materials: a review. **Journal of Hazardous Materials**, v. 157, n. 2-3, p. 220-229, 2008.

DUQUE A.; MANZANARES, P.; BALLESTEROS, I.; NEGRO, M. J.; OLIVA, J.M.; GONZÁLEZ, A.; BALLESTEROS, M. Sugar production from barley straw biomass pretreated by combined alkali and enzymatic extrusion. **Bioresource Technology**, v.158, p. 262–268, 2014.

DUTTA, A.; DIAO, Y.; JAIN, R.; RENE, E. R.; DUTTA, S. Adsorption of cadmium from aqueous solutions onto coffee grounds and wheat straw: equilibrium and kinetic study. **Journal of Environmental Engineering**, v. 142, p. C4015014, 2015.

EBRINGEROVA, A.; HROMADKOVA, Z.; HEINZE, T. Hemicellulose. **Advances in Polymer Science**, v. 186, 1-67, 2005.

FERNANDES, H. M. Heavy metal distribution in sediments and ecological risk assessment: the role of genetic processes in reducing metal toxicity in bottom sediments. **Environmental Pollution**, v. 97, 317-325, 1997.

FILLAUDEAU, L.; BLANPAIN-AVET, P.; DAUFIN, G. Water, wastewater and waste management in brewing industries. **Journal of cleaner production**, v. 14, p. 463-471, 2006.

FLOREA, A. M.; BÜSSELBERG, D. Toxic effects of metals: modulation of intracellular calcium homeostasis. **Materialwissenschaft und Werkstofftechnik**, v. 36, p. 757-760, 2005.

FLOREA, A. M.; BÜSSELBERG, D. Occurrence, use and potential toxic effects of metals and metal compounds. **Biometals**, v. 19, p. 419–427, 2006.

FREUNDLICH, H. Over the adsorption in solution. **Journal Physical Chemical.** v. 57, p. 385-471, 1906.

GALUNIN, E.; FERRETI, J.; ZAPELINI, I. V.; TARLEY, C. R.T.; ABRÃO, T.; SANTOS, M. J. Cadmium mobility in sediments and soils from a coal mining area on Tibagi River watershed: Environmental risk assessment. **Journal of Hazardous Materials**. v. 265, p. 280-287, 2014.

GILES, C.H.; MAcEWAN, T.H.; NAKHWA, S.N. “Studies in adsorption. Part XI. A system of classification of solution adsorption isotherms, and its use in diagnosis of adsorption mechanisms and in meadurement of specific surface areas of solids”. **Journal of the Chemical Society**, p. 3973-3993, 1960.

GILES, C. H.; SMITH, D.; HUITSON, A. A general treatment and classification of the solute adsorption isotherm. I. Theoretical. **Journal of colloid and interface science**, v. 47, n. 3, p. 755-765, 1974.

GHASEMI, M.; NAUSHAD, M.; GHASEMI, N.; KHOSRAVI-FARD, Y. Adsorption of Pb(II) from aqueous solution using new adsorbents prepared from agricultural waste: adsorption isotherm and kinetic studies. **Journal of Industrial and Engineering Chemistry**, v. 20, p. 2193-2199, 201.

GíRIO, F. M.; FONSECA. C.; CARVALHEIRO, F.; DUARTE, L. C.; MARQUES, S.; BOGEL-LUKASIK, R. Hemicelluloses for fuel ethanol: A review. **Bioresource Technology**, v. 101, p. 4775–4800, 2010.

GOGATE, P. R.; KABADI, A. M. A review of applications of cavitation in biochemical engineering/biotechnology. **Biochemical Engineering Journal**, v. 44, n. 1, p. 60-72, 2009.

GORELOV, B. M.; DYAKIN, V. V.; KASHIN, G. N.; MAKHNJUK, V. I.; MOROZOVSKAYA, D. V.; SIDORCHUK, V. A. Effect of physical and chemical adsorption of water molecules on YBa2Cu3O7− δ surface composition. **Journal of Electron Spectroscopy and Related Phenomena**, v. 70, n. 2, p. 161-165, 1994.

HASSAN, S. S.; WILLIAMS, G. A.; JAISWAL, A. K.; Emerging Technologies for the Pretreatment of Lignocellulosic Biomass. **Bioresource Technology**, v. 262, p. 310–318, 2018.

HINZ, C. Description of sorption data with isotherm equations. **Geoderma**, v. 99, n. 3-4, p. 225-243, 2001.

IBGE - Instituto Brasileiro de Geografia e Estatística. Disponível em: https://agenciadenoticias.ibge.gov.br/agencia-noticias/2012-agencia-de-noticias/noticias/21413-alternativa-ao-trigo-cevada-ganha-espaco-no-sul-e-projeta-producao-recorde. Acesso em janeiro de 2019.

IQBAL, M.; SAEED, A.; KALIM, I. Characterization of adsorptive capacity and investigation of mechanism of Cu2+, Ni2+ and Zn2+ adsorption on mango peel waste from constituted metal solution and genuine electroplating effluent. **Separation Science and Technology**, v. 44, n. 15, p. 3770-3791, 2009.

JAIN, M.; GARG, V. K.; KADIRVELU, K.; SILLANPÄÄ, M. Adsorption of heavy metals from multi-metal aqueous solution by sunflower plant biomass-based carbons. **International journal of environmental science and technology**, v. 13, p. 493-500, 2016.

KADIRVELU, K.; THAMARAISELVI, K.; NAMASIVAYAM, C. Removal of heavy metals from industrial wastewaters by adsorption onto activated carbon prepared from an agricultural solid waste**. Bioresource Technology**, v. 76, n. 1, p. 63-65, 2001.

KAMM, B.; KAMM, M.; GRUBER, P. R.; KROMUS, S**.** Biorefinery systems - An overview, in Biorefineries, chapter 1, P. 3-40, 2006- Industrial Processes and Products. **Status Quo and Future Directions.**

KARIMI, M.; JENKINS, B.; STROEVE, P. Ultrasound irradiation in the production of ethanol from biomass. **Renewable and Sustainable Energy Reviews**, v. 40, p. 400-421, 2014.

KUMAR, J.; BALOMAJUMDER, C.; MONDAL, P. Application of Agro-Based Biomasses for Zinc Removal from Wastewater–A Review. **Clean–Soil, Air, Water**, v. 39, n. 7, p. 641-652, 2011.

KUNZE, W.; in: Mieth, H.O. (Ed.), Technology Brewing and Malting International Edition. VLB, Berlin. 726 p. 1996.

Langmuir I. The constitution and fundamental properties of solids and liquids. J Am Chem Soc. 1916; 38(11):2221-2295.

LANGMUIR I. The constitution and fundamental properties of solids and liquids. **Journal of the American Chemical Society.** v. 38, p. 2221-2295,1916.

LESMANA, S.O.; FEBRIANA, N.; SOETAREDJO, F. E.; SUNARSO, J.; ISMADJI,S. Studies on potential applications of biomass for the separation of heavy metals from water and wastewater. **Biochemical Engineering Journal**. v. 44, p.19–41, 2009.

LI, Q. Z.; CHAI, L. Y.; JING, Z. H. A. O.; YANG, Z. H.; WANG, Q. W. Lead desorption from modified spent grain. **Transactions of Nonferrous Metals Society of China**, v. 19 p. 1371-1376, 2009a.

LI, Q.; CHAI, L.; YANG, Z.; WANG, Q. Kinetics and thermodynamics of Pb(II) adsorption onto modified spent grain from aqueous solutions. **Applied surface science**, v. 255, p. 4298-4303, 2009b.

LI, Q.; CHAI, L.; QIN, W. Cadmium (II) adsorption on esterified spent grain: equilibrium modeling and possible mechanisms. **Chemical engineering journal**, v. 197, p. 173-180, 2012.

LIMOUSIN, G.; GAUDET, J. P.; CHARLET, L.; SZENKNECT, S.; BARTHÈS, V.; KRIMISSA, M. Sorption isotherms: A review on physical bases, modeling and measurement. **Applied Geochemistry**, v. 22, p. 249-275, 2007.

LIYAKATHALI, N. A. M.; MULEY, P. D.; AITA, G.; BOLDOR, D. Effect of frequency and reaction time in focused ultrasonic pretreatment of energy cane bagasse for bioethanol production. **Bioresource Technology**, v. 200, p. 262-271, 2016.

LUFT, L.; CONFORTIN, T. C.; TODERO, I.; SILVA, J. R.; TOVAR, L. P.; KUHN, R. C.; JAHAN, S. L.; TREICHEL, H.; MAZUTTI, M. A. Ultrasound Technology Applied to Enhance Enzymatic Hydrolysis of Brewer's Spent Grain and its Potential for Production of Fermentable Sugars. **Waste and Biomass Valorization**, 1-8, 2018.

LUO, J.; FANG, Z.; SMITH, JR; Richard, L. Ultrasound-enhanced conversion of biomass to biofuels. **Progress in Energy and Combustion Science**, v. 41, p. 56-93, 2014.

MAPA - Ministério da Agricultura, Pecuária e Abastecimento. **Plano Agrícola e Pecuário, 2015/2016**. Disponível em: http://www.agricultura.gov.br/assuntos/politica-agricola/todas-publicacoes-de-politica-agricola/plano-agricola-pecuario. Acesso em novembro de 2018.

MASON, T.J.; LORIMER, J.P. Applied Sonochemistry**. The Uses of Power Ultrasound in Chemistry and Processing,** Wiley-VCH, 2002.

McCABE, W.L.; SMITH, J.C.; HARRIOTT, P., 1993, **Unit operations of chemical engineering.** New York. 5° Edition. McGraw-Hill International E ditions. 1130pp.

MENON, V.; RAO, M. Trends in bioconversion of lignocellulose: biofuels, platform chemicals & biorefinery concept. **Progress in energy and combustion science**, v. 38, n. 4, p. 522-550, 2012.

MELLO, L. R. P. F.; MALI, S. Use of malt bagasse to produce biodegradable baked foams made from cassava starch. **Industrial Crops and Products**, v. 55, p.187-193, 2014.

MONTANHER, S. F.; OLIVEIRA, E. A.; ROLLEMBERG, M. C. Removal of metal ions from aqueous solutions by sorption onto rice bran. **Journal of Hazardous Materials**, v. 117, p. 207-211, 2005.

MOOD, S. H.; GOLFESHAN, A. H.; TABATABAEI, M.; JOUZANI, G. S.; NAJAFI, G. H.; GHOLAMI, M.; ARDJMAND, A. Lignocellulosic biomass to bioethanol, a comprehensive review with a focus on pretreatment. **Renewable and Sustainable Energy Reviews**, v. 27, p.77–93, 2013.

MOSIER, N.; WYMAN, C.; DALE, B.; ELANDER, R.; LEE, Y. Y.; HOLTZAPPLE, M.; LADISCH, M. Features of promising technologies for pretreatment of lignocellulosic biomass. **Bioresource Technology**, v. 96, p.673–686, 2005.

MUSSATTO, S. I e ROBERTO, I. C. Acid hydrolysis and fermentation of brewer's spent grain to produce xylitol. **Journal of the Science of Food and Agriculture**. v. 85, p. 2453–2460, 2005.

MUSSATTO, S. I.; DRAGONE, G.; ROBERTO, I. C. Brewers'spent grains: generation, Characteristics and potencies' applications. **Journal of Central Science**. v. 4, p. 1-14, 2006.

NAIYA, T. K.; CHOWDHURY, P.; BHATTACHARYA, A. K.; DAS, S. K. Saw dust and neem bark as low-cost natural biosorbent for adsorptive removal of Zn (II) and Cd (II) ions from aqueous solutions. **Chemical Engineering Journal**, v. 148, n. 1, p. 68-79, 2009.

NASCIMENTO, R. F. DO; LIMA, A. C. A. DE; VIDAL, C. B.; MELO, D. Q.; RAULINO, G. S. C. Adsorção: aspectos teóricos e aplicações ambientais. **Biblioteca de Ciências e Tecnologia**, 2014.

NGUYEN, T. A. H.; NGO, H. H.; GUO, W. S.; ZHANG, J.; LIANG, S.; YUE, Q. Y.; LI, Q.; NGUYEN, T. V. Applicability of agricultural waste and by-products for adsorptive removal of heavy metals from wastewater. **Bioresource Technology**, v. 148, p. 574–585, 2013.

OFOMAJA, A. E.; HO, Y. Effect of pH on cadmium biosorption by coconut copra Meal. **Journal of Hazardous Materials**, B 139, p. 356–362, 2007.

OLAJIRE, A. A. The brewing industry and environmental challenges. **Journal of Cleaner Production**, 2012.

OGEDA, T. L.; PETRI, D. F. S; Hidrólise Enzimática de Biomassa. **Química Nova**, v. 33, n. 7, p. 1549-1588, 2010.

OLIVEIRA, W. E.; FRANCA, A. S.; OLIVEIRA, L. S.; ROCHA, S. D. Untreated coffee husks as biosorbents for the removal of heavy metals from aqueous solutions. **Journal of Hazardous Materials**, v. 152, n. 3, p. 1073-1081, 2008.

PEHLIVAN, E.; ALTUN, T.; CETIN, S.; BHANGER, M. I. Lead sorption by waste biomass of hazelnut and almond shell. **Journal of hazardous materials**, v. 167, p.1203-1208, 2009a.

PEHLIVAN, E.; ALTUN, T.; PARLAYICI, S. Utilization of barley straws as biosorbents for Cu2+ and Pb2+ ions. **Journal of hazardous materials**, v. 164, p. 982-986, 2009b,

PENG, F.; PENG, P.; XU, F.; SUN, R-C. Fractional purification and bioconversion of hemicelluloses. **Biotechnology Advances**, v. 30, p. 879–903, 2012.

PILLI, S.; BHUNIA, P.; YAN, S.; LEBLANC, R. J.; TYAGI, R. D.; SURAMPALLI, R. Y. Ultrasonic pretreatment of sludge: a review. **Ultrasonics Sonochemistry**, v. 18, p. 1-18, 2011.

PINO, G. H.; MESQUITA, L. M. S.; TOREM, M. L.; PINTO, G. A. S.; "Biosorption of heavy metals by powder of green coconut shell, **Separation Science and Technology**, vol. 41, n. 14, p. 3141–3153, 2006.

PORTUGAL-PEREIRA, J. ; SORIA, R.;RATHMANN, R.; SCHAEFFER, R.; SZKLO, A. Agricultural and agro-industrial residues-to-energy: Technoeconomic and environmental assessment in Brazil. **Biomass and Bioenergy**, v. 81, 521-533, 2015.

PETRELLA, A.; SPASIANO, D.; ACQUAFREDDA, P.; DE VIETRO, N.; RANIERI, E.; COSMA, P.; PETRUZZELLI, D. Heavy metals retention (Pb (II), Cd (II), Ni (II)) from single and multimetal solutions by natural biosorbents from the olive oil milling operations. **Process Safety and Environmental Protection**, v. 114, p.79-90, 2008.

REHMAN, M. S. U.; KIM, I.; CHISTI, Y.; HAN, J. I. Use of ultrasound in the production of bioethanol from lignocellulosic biomass. **Energy Education Science and Technology Part A: Energy Science and Research**, v. 30, n. 2, p. 1391-1410, 2013.

SAEED, A.; IQBAL, M.; AKHTAR, M. W. Removal and recovery of lead (II) from single and multimetal (Cd, Cu, Ni, Zn) solutions by crop milling waste (black gram husk). **Journal of Hazardous Materials**, v. 117, p. 65-73, 2005.

SAMPAIO, L. R.; MEDEIROS, E. P.; CONRADO, L. S. Produção de Bioadsorventes Obtidos da Torta de Mamona para Remoção de Íons Cobre em Soluções Aquosas. In: **IV CONGRESSO BRASILEIRO DE MAMONA E I SIMPÓSIO INTERNACIONAL DE OLEAGINOSAS ENERGÉTICAS***,* 2010, João Pessoa - PB.

SANTOS, H. F. Análise Conformacional de Modelos de Lignina. **Química Nova**, v. 24, nº. 4, p. 480-490, 2001.

SANTOS, F. A.; QUEIRÓZ J. H.; COLODETTE J. L.; FERNANDES S. A.; GUIMARÃES, V. M.; REZENDE S.T. Potencial da palha de cana-de-açúcar para produção de etanol. **Química Nova**, 35:1004-1010, 2012.

SANTOS, M. S.; RIBEIRO, F. M. **Cervejas e refrigerantes**. São Paulo: CETESB, 58p. 2005.

SILVA, R.; HARAGUCHI, S. K.; MUNIZ, E. C.; RUBIRA, A. Aplicações de fibras lignocelulósicas na química de polímeros e em compósitos. **Química Nova**, v. 32, n. 3, p. 661-671, 2009.

SEMERJIAN, L. Removal of heavy metals (Cu, Pb) from aqueous solutions using pine (*Pinus halepensis*) sawdust: Equilibrium, kinetic, and thermodynamic studies. **Environmental Technology & Innovation**, v. 12, p. 103, 2018.

SING, K. Reporting physisorption data for gas/solid systems with special reference to the determination of surface area and porosity (Recommendations 1984**). Pure and applied chemistry**, v. 57, n. 4, p. 603-619, 1985.

SINDHU, R.; BINOD, P.; PANDEY, A. A novel sono-assisted acid pretreatment of chili post harvest residue for bioethanol production. **Bioresource Technology**, v. 213, p. 58–63, 2016.

SINDHU, R.; BINOD, P.; MATHEW, .; ABRAHAM, A.; GNANSOUNOU, E.; UMMALYMA, S. B.; PANDEY, A. Development of a novel ultrasound-assisted alkali pretreatment strategy for the production of bioethanol and xylanases from chili post harvest residue. **Bioresource Technology,** v. 242 p.146–151, 2017.

SINGH, S.; BHARADWAJA, S.T . P.; YADAV, P. K.; MOHOLKAR, V. S. Mechnistic investigation in ultrasound-assisted (Alkaline) delignification of Parthenium hysterophorus biomass. **Industrial & Engineering Chemistry Research**, v. 53, n. 37, p. 14241-14252, 2014.

SIPS R. On the structure of a catalyst surface. **The Journal of Chemical Physics**, v.16, p. 490-495, 1950.

SOONTORNCHAIBOON, W. KIM, S. M.; PAWONGRAT, R. Effects of alkaline combined with ultrasonic pretreatment and enzymatic hydrolysis of agricultural wastes for high reducing sugar production. **Sains Malaysiana**, v. 45, p. 955–962, 2016.

SUBHEDAR P. B.; GOGATE, P. R. Alkaline and ultrasound assisted alkaline pretreatment for intensification of delignification process from sustainable raw-material. **Ultrasonics Sonochemistry**, v. 21, p. 216– 225, 2014.

SUBHEDAR, P. B.; GOGATE, P. R. Intensification of delignification and subsequent hydrolysis for the fermentable sugar production from lignocellulosic biomass using ultrasonic irradiation. **Ultrasonics Sonochemistry**, v.40, p. 140-150, 2018.

SUD, D.; MAHAJAN, G.; KAUR, M.P. Agricultural waste material as potential adsorbent for sequestering heavy metal ions from aqueous solutions – A review. **Bioresource Technology**, v. 99, p. 6017–6027, 2008.

SUN, Y., CHENG, J. Hydrolysis of lignocellulosic materials for ethanol production: A review. **Bioresource Technology**, v 83, (1), p. 1-11, 2002.

SUN, R.C.; TOMKINSON, R.C. 2002. Characterization of hemicelluloses obtained by classical and ultrasonically assisted extractions from wheat straw. **Carbohydrate Polymers**, v. 50 (3), p. 263–271, 2002.

STICKLEN, M. B. Plant genetic engineering for biofuel production: towards affordable cellulosic ethanol. **Nature Reviews Genetics**, v. 9, p. 433-443, 2008.

TAHERZADEH, M.J. and KARIMI K. Enzymatic-based hydrolysis processes for ethanol from lignocellulosic materials: A review. **BioResources**, v. 2, p. 707-738, 2007.

VELMURUGAN, R.; MUTHUKUMAR, K.; Utilization of sugarcane bagasse for bioethanol production: sono-assisted acid hydrolysis approach. **Bioresource Technology**,102:7119e23, 2011.

VELMURUGAN, R.; MUTHUKUMAR, K. Ultrasound-assisted alkaline pretreatment of sugarcane bagasse for fermentable sugar production: optimization through response surface methodology. . **Bioresource Technology,** 112, p. 293–299, 2012.

VINATORU, M. An overview of the ultrasonically assisted extraction of bioactive principles from herbs. **Ultrasonics Sonochemistry**, v. 8, p. 303–13, 2001.

VOLESKY, B. Detoxification of metal-bearing effluents: biosorption for the next century, **Hydrometallurgy**, v. 59, p. 203 -216, 2001.

VOLESKY, B. Biosorption process simulation tools, **Hydrometallurgy**, v.71, p. 179-190, 2003.

VOLESKY, B. **Sorption and Biosorption**. 2004, BV Sorbex, Canada.

WADANAMBI, L.; DUBEY, B.; TOWNSEND, T. The leaching of lead from lead-based paint in landfill environments. **Journal of Hazardous Materials**, v. 157, n. 1, p. 194-200, 2008.

WANG, X. S.; QIN, Y.; LI, Z. F.; Biosorption of zinc from aqueous solutions by rice bran: kinetics and equilibrium studies. Separation science and technology, v. 41, n. 4, p. 747-756, 2006.

WANG, Z.; HOU, X.; SUN, J.; LI, M.; CHEN, Z.; GAO, Z. Comparison of ultrasound-assisted ionic liquid and alkaline pretreatment of Eucalyptus for enhancing enzymatic saccharification. **Bioresource Technology**, v. 254, p. 145-150, 2018.

WANG, Z; QU, L.; QIAN, J.; HE, Z.; YI, S. Effects of the ultrasound-assisted pretreatments using borax and sodium hydroxide on the physicochemical properties of Chinese fir. **Ultrasonics Sonochemistry**, v. 50, p. 200-207, 2019.

WU, H.; DAI, X.; ZHOU, S.; GAN, Y.; XIONG, Z.; QIN, Y.; MA, J.; YANG, L.; WU, Z.; WANG, T.; WANG, W.; WANG, C. Ultrasound-assisted alkaline pretreatment for enhancing the enzymatic hydrolysis of rice straw by using the heat energy dissipated from ultrasonication. **Bioresource Technology**, v. 241, p. 70–74, 2017.

YACHMENEV, V.; CONDON, B.; KLASSON, T.; LAMBERT, A. Acceleration of the enzymatic hydrolysis of corn stover and sugar cane bagasse celluloses by low intensity uniform ultrasound. **Journal of Biobased Materials and Bioenergy**, v.3, p. 25–31, 2009.

ZULKALI, M. M. D.; AHMAD, A. L.; NORULAKMAL, N. H. Oryza sativa L. husk as heavy metal adsorbent: optimization with lead as model solution. **Bioresource technology**, v. 97, p. 21-25, 2006.